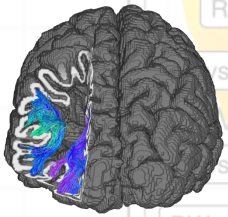

ABSTRACT

The ventral occipito-temporal (vOT) association cortex makes a significant contribution to our ability to recognize different types of visual patterns. It is widely accepted that a subset of this circuitry, including the visual word form area (VWFA), can be trained to perform the task of rapidly identifying word forms. An important open question is the computational role of this circuitry: To what extent is it part of the bottom-up hierarchical processing of information related to visual word recognition and/or involved in processing top-down signals from higher-level language regions? This doctoral dissertation thesis aims to characterize vOT reading circuitry using behavioral, functional, structural and quantitative MRI indexes, and to link vOT computations to the other two important regions within the language network: the posterior parietal cortex (pPC) and the inferior frontal gyrus (IFG). The results have revealed that two distinct word-responsive areas can be distinguished in the vOT: one is responsible for visual feature extraction and is connected to the intraparietal sulcus via the vertical occipital fasciculus; the second is responsible for semantic processing and is connected to the angular gyrus via the posterior arcuate fasciculus, and to the IFG via the anterior arcuate fasciculus. Importantly, reading behavior was predicted by functional activation in regions identified along the vOT, pPC and IFG trajectory, as well as by the structural properties of the white matter fiber tracts linking them. The present work constitutes a critical step in the creation of a highly detailed characterization of the early stages of reading at the individual-subject level and establishes a baseline model as well as parameter ranges that should help to clarify and identify functional and structural differences between typical, poor and atypical readers.

BASQUE CENTER
ON COGNITION, BRAIN
AND LANGUAGE

Multimodal characterization of visual word recognition

GARIKOITZ LERMA-USABIAGA

2017

eman ta zabal zazu

Universidad del País Vasco

Euskal Herriko Unibertsitatea

Multimodal MRI characterization of visual word recognition: an integrative view

Doctoral dissertation by:
Garikoitz Lerma-Usabiaga

Supervised by:
Dr. Pedro M. Paz-Alonso
Dr. Manuel Carreiras

2017

Multimodal MRI characterization of visual word recognition: an integrative view

Garikoitz Lerma-Usabiaga

BCBL Basque Center on Cognition, Brain and Language

Paseo Mikeletegi, 69,

Donostia-San Sebastián, Spain

April, 2017

BASQUE CENTER
ON COGNITION, BRAIN
AND LANGUAGE

Universidad
del País Vasco

Euskal Herriko
Unibertsitatea

Multimodal MRI characterization of visual word recognition: an integrative view.

Doctoral dissertation by:

Garikoitz Lerma-Usabiaga

To obtain the grade of doctor by the University of the Basque Country

Supervised by:

Dr. Pedro M. Paz-Alonso and Dr. Manuel Carreiras

Donostia – San Sebastián, 2017

Brain research at BCBL
Jon Lerma Mendizabal, 2016

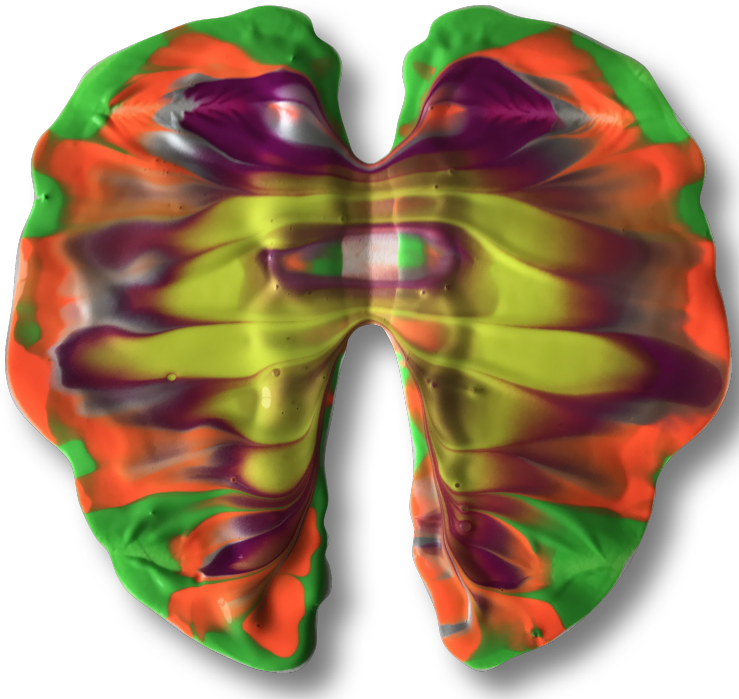

Butterfly brain
Ane Lerma Mendizabal, 2017

Acknowledgements

To Abene: I could write another thesis just about you. Thanks for everything.

To Jon and Ane: this is what I was doing. Thank you so much for understanding and loving me.

To the rest of my direct and extended family: without your support this work would never have happened. Thank you for being there.

To Kepa: it all started with your initial bet on me. Many thanks for this great scientific and learning journey. It will take me years to fully internalize the kind of help and support you have provided. This work is as much yours as it is mine.

To Manolo: thanks for your work co-directing this doctoral dissertation, for your support and, especially, for so thoroughly designing and sustaining an incredibly great institution such as the BCBL. Thanks to your motivation, hard work, openness to discussion and quest for continuous improvement, I could not think of a better research center to have worked on my doctoral dissertation.

To all BCBLians: a fantastic group of people, past, present and, I am sure, future. Thanks to all the researchers with whom I interacted (scientifically and not scientifically). Thanks to everyone in the BCBL administration, IT and lab departments. Without your daily work and support, science at the BCBL would not happen.

To the rest of my new scientific colleagues/friends worldwide: thanks for all the interesting conversations; there are more to come.

To all my Asteasu, Glasgow, Barcelona, Mundaka and Bilbao friends: thanks for all the great moments, we will have more now that I am submitting this.

Contents

List of Figures

List of Tables

List of Acronyms

aAF = anterior arcuate fasciculus

AFD = Apparent Fiber Density

ANCOVA = Analysis of Covariance

ANOVA = Analysis of Variance

BOLD = Blood Oxygen Level-Dependent

CB = Chequerboard

CS = Consonant String

CSD = constrained spherical deconvolution

CSF = Cerebrospinal fluid

CT = cortical thickness

dMRI = diffusion MRI

DTI = diffusion tensor imaging

DWI = diffusion weighted imaging

EEG = Electroencephalography

FA = Fractional Anisotropy

FDR = False Discovery Rate

FEF = Frontal eye fields

FF = False Font

FFA = Fusiform Face Area

fMRI = functional MRI

FoV = Field of View

FWE = Family Wise Error

GMax = Global Maxima

HMOA = Hindrance Modulated Orientational Anisotropy

HRF = Hemodynamic Response Function

IFG = inferior-frontal gyrus

IFOF = inferior fronto-occipital fasciculus

ILF = inferior longitudinal fasciculus

IPS = intra-parietal sulcus

LGN = Lateral geniculate nucleus

MEG = Magnetoencephalography

MRI = Magnetic Resonance Imaging

MTV = Macromolecular Tissue Volume

pAF = posterior arcuate fasciculus

PET = positron emission tomography

pPC = posterior parietal cortex

PS = Phase-Scrambled word

PW = Pseudo-Word

qMRI = quantitative MRI

ROI = Region of Interest

RW = Real Word

SD = Scrambled Word

TE = Echo Time

TR = Repetition Time

vOF = vertical occipital fasciculus

vOT = ventro-occipital-temporal cortex

VWFA = visual word-form area

WM = White Matter

1 Resumen en castellano

La capacidad de (escribir y) leer es una de las tecnologías de la comunicación más exitosas jamás inventadas por el ser humano. Su importancia e influencia en la educación, cultura, negocios y en la comunicación interpersonal es extraordinaria. Después de un periodo en la historia del ser humano en el que sólo las élites podían acceder a la lectura, su democratización junto con la industrialización acompañaron el mayor periodo de creación de riqueza y bienestar que haya conocido el ser humano. Hoy en día, gracias al desarrollo de las nuevas tecnologías de telecomunicación, el poder de la lectura no ha hecho más que expandirse. En la comunicación interpersonal, los sistemas de correo electrónico o mensajería instantánea permiten tanto la comunicación en tiempo real como en diferido. La mayor revolución probablemente se haya dado en el ámbito de la educación, donde el acceso universal de los materiales educativos ha democratizado la educación haciéndola accesible a todos los niveles socio-económicos y muchos rincones del planeta.

La importancia y la ubicuidad de los sistemas escritos es tan importante que prácticamente se da por contado con la capacidad lectora de la población, olvidando a veces que es una parte importante de la evolución de la sociedad. Un considerable parte del tiempo de los primeros años formativos es dedicado a la adquisición de la lectura y escritura. En este momento, es importante reseñar que existe una parte importante de la población que tiene algún trastorno en el proceso de adquisición de la lectura (por ejemplo, dislexia), que si no es tratado adecuadamente, pueden afectarle negativamente tanto en el proceso educativo como en la

integración satisfactoria en la sociedad. Lamentablemente, la ciencia actual todavía no es capaz de explicar satisfactoriamente ni el proceso de lectura normal, ni las diferencias en aquellos que no pueden leer de una manera típica.

El estudio científico de la lectura se puede abordar desde muy variadas aproximaciones científicas, y una de las más completas actualmente consiste en poder observar y medir la conducta lectora, caracterizarla, y examinar sus bases neurológicas. En este sentido, se ha demostrado que la corteza ventro-occipito-temporal (vOT) tiene un papel relevante a la hora de reconocer diferentes tipos de patrones visuales. Una subregión de esta área, llamada el área de la forma visual de las palabras (VWFA, en sus siglas en inglés), es ampliamente reconocida por la comunidad científica como un área entrenada para el reconocimiento visual rápido de las palabras. De todas maneras, existe todavía una importante discusión teórica sobre el rol computacional de la VWFA: ¿En qué medida es parte de un proceso jerárquico que va de abajo arriba en el procesamiento de palabras, o/y además toma parte en el procesamiento de señales provenientes de las áreas superiores del lenguaje?

El objetivo de esta tesis doctoral es caracterizar los circuitos de lectura de la vOT utilizando medidas conductuales combinadas con índices funcionales, estructurales y cuantitativos obtenidos con la técnica de la resonancia magnética, y enlazando sus computaciones con otras áreas relevantes en las redes de la lectura y el lenguaje como son la corteza parietal posterior (pPC) y el giro frontal inferior (IFG).

Los resultados de este trabajo mostraron una clara segregación en dos áreas dentro de la vOT: una responsable de la extracción de los aspectos visuales de las palabras conectada con el sulco intraparietal a través del fascículo occipital vertical, y una segunda área responsable del procesamiento semántico que está conectada al giro angular a través del fascículo arqueado posterior, y al IFG a través del fascículo arqueado anterior. Este segregación en dos regiones de la vOT fue observada a través de distintos análisis.

En primer lugar, se llevó a cabo una caracterización exhaustiva de la activación de estas dos regiones dentro de la vOT dependiendo de diferentes contrastes de activación funcional. Estos análisis mostraron que la activación producida en la vOT para estos contrastes se organizó en función de su naturaleza semántica (incluyendo palabras contra pseudopalabras, consonantes y fuentes falsas) y perceptual (incluyendo palabras contra diseño en forma de damero, palabras revueltas o palabras revueltas en el dominio de fase). En los contrastes funcionales de naturaleza perceptual se resta un tipo u otro de información visual, y lo que permanece son principalmente características léxico-semánticas, fonológicas y ortográficas. Sin embargo, en los contrastes funcionales de naturaleza semántico las pseudopalabras se pueden leer perfectamente y cumplen con las leyes ortográficas, esto significa que en el proceso cognitivo resultante, al restar la señal de fMRI de las pseudopalabras a las palabras, solo nos quedaría las áreas involucradas en algún procesamiento léxico-semántico. Por otra parte, las consonantes no se pueden leer. No tienen ortografía ni fonología. Esto significaría que al restar la señal de las consonantes a las palabras quedarían muchos más componentes de la

palabra que en el caso de restar la señal de las pseudopalabras a las palabras. En relación a las fuentes falsas, en este trabajo empleamos el georgiano, cuyas fuentes son muy parecidas a las tiras de consonantes. Además, al ser un sistema en uso el georgiano mantiene todas las relaciones estadísticas entre sus letras al igual que cualquier lengua. Por lo tanto, en vOT, esta separación entre contrastes semánticos y perceptuales mostró diferencias en el eje anterior/posterior y la segregación funcional de dos regiones en la vOT.

En segundo lugar, otra área importante dentro del circuito de la lectura es el pPC o corteza posterior parietal, en cual se encuentran dos subregiones de interés: una más posterior denominada sulco intraparietal (iPS), y otra más anterior conocida como el giro angular (AG). Nuestros datos mostraron que empezando en el iPS ventral y subiendo el iPS hasta el AG se puede observar un gradiente funcional equivalente al encontrado en el eje anterior posterior del vOT. Por una parte, en paralelo a la parte posterior del vOT, el iPS parece estar relacionado funcionalmente con procesos perceptuales y visuales. Nuestros resultados mostraron que la parte posterior del vOT y el iPS están conectadas estructuralmente por el tracto de haces de fibras de materia blanca denominado fascículo occipital vertical (vOF). Por otro lado, el procesamiento funcional llevado a cabo por el AG, al igual que la parte media del vOT, estaría relacionado con procesos semánticos. Además, nuestros resultados también mostraron que parte media del vOT y el AG están conectados estructuralmente por el tracto de materia blanca conocido como el fascículo arcuado posterior (pAF). Así, nuestros datos sugieren que para el iPS y el vOT posterior la

palabra es una unidad visual, en cambio, para el AG y el vOT medio, la palabra es ya una unidad de lenguaje.

Por último, en el IFG observamos una disociación similar, pero en este caso más selectiva. En esta región, el contraste entre palabras y pseudopalabras fue el único contraste separado del resto y que en consonancia con las teorías principales sobre el rol del IFG en la lectura, se ubicó en el *pars triangularis*, asociado normalmente con el procesamiento léxico-semántico. Al contrario, el resto de contrastes (incluidos los perceptuales) que conllevan tanto aspectos fonológicos como semánticos, se ubicaron topográficamente en zonas más posteriores del IFG, en concreto en el área conocida como *pars opercularis*, y asociada típicamente con procesos fonológicos.

Es además importante mencionar que la lectura fue predicha mediante activaciones funcionales en las tres áreas (vOT, pPC, IFG), y de manera disociada para los contrastes semánticos y perceptuales, así como mediante las propiedades estructurales de los tractos que los unen estas regiones entre sí.

En resumen, los hallazgos de la presente tesis doctoral proporcionan evidencia del rol crucial de la selección de contrastes funcionales en los diseños experimentales de fMRI, y la necesidad de ajustar estos a las hipótesis científicas que se quieran someter a prueba en el experimento en cuestión. Hasta ahora no existía ningún estudio que hubiera afrontado esta comparación de manera sistemática con el objetivo de discernir las diferencias computacionales en el vOT y relacionarlas funcional y

estructuralmente. Con este estudio proponemos que al menos, existen dos áreas en el sulco lateral occipito-temporal. Una más anterior y de carácter más semántico, y otra más posterior y de carácter más perceptual, que se dedican a procesar información diferente en el proceso de reconocimiento visual de las palabras.

Además, el presente trabajo ha conseguido relacionar la involucración de estas áreas con otras áreas críticas dentro de la red de lectura, como son el pPC y el IFG. Hasta ahora ningún estudio ha investigado el papel conjunto de estos factores de forma sistemática, ni ha conseguido explicar de este modo los resultados en la conducta individual. Es importante resaltar también que en el presente trabajo se emplea un método multimodal mediante la combinación de las técnicas más innovadoras de neuroimagen. Esto permite añadir un factor novedoso e importante para lograr avances científicos.

La presente tesis doctoral proporciona nuevos conocimientos sobre la neurobiología de la lectura, tiene implicaciones para las teorías y debates actuales en el campo de la neurociencia cognitiva del lenguaje y lectura, y proporciona nuevos conocimientos sobre cómo trabajan las distintas áreas cerebrales en consonancia para producir la conducta lectora. Por último, consideramos que las contribuciones de este trabajo constituyen un paso crítico en la creación de una caracterización altamente detallada de los estadios iniciales de la lectura a nivel del sujeto lector individual, y para la creación de un modelo de base parametrizable, que en el futuro pueda servir para clarificar las diferencias funcionales y estructurales entre los

lectores con distintos grados de destreza, así como entre aquellos que sufren de dislexia o trastorno específico del lenguaje.

2 ABSTRACT

The ventral occipito-temporal (vOT) association cortex makes a significant contribution to our ability to recognize different types of visual patterns. It is widely accepted that a subset of this circuitry, including the visual word form area (VWFA), can be trained to perform the task of rapidly identifying word forms. An important open question is the computational role of this circuitry: To what extent is it part of the bottom-up hierarchical processing of information related to visual word recognition and/or involved in processing top-down signals from higher-level language regions? This doctoral dissertation thesis aims to characterize vOT reading circuitry using behavioral, functional, structural and quantitative MRI indexes, and to link vOT computations to the other two important regions within the language network: the posterior parietal cortex (pPC) and the inferior frontal gyrus (IFG). The results have revealed that two distinct word-responsive areas can be distinguished in the vOT: one is responsible for visual feature extraction and is connected to the intraparietal sulcus via the vertical occipital fasciculus; the second is responsible for semantic processing and is connected to the angular gyrus via the posterior arcuate fasciculus, and to the IFG via the anterior arcuate fasciculus. Importantly, reading behavior was predicted by functional activation in regions identified along the vOT, pPC and IFG trajectory, as well as by the structural properties of the white matter fiber tracts linking them. The present work constitutes a critical step in the creation of a highly detailed characterization of the early stages of reading at the individual-subject level and establishes a baseline model as well as parameter ranges that

should help to clarify and identify functional and structural differences between typical, poor and atypical readers.

3 LANGUAGE AND READING

Language is the quintessential human cognitive ability, and has served as the main medium of communication for humans for thousands of years. On the other hand, writing and reading are arguably one of the most important communication technologies ever invented, and essential to functioning in modern societies, since they allow for offline communication across time (we can read texts written in the past) and space (we can read texts written in other parts of the world).

In this chapter, I first introduce the history of language and reading. Then, I sketch different historical scientific approaches to language and human cognition research. Finally, the chapter presents an overview of classical and modern models of language and reading, as well as the main brain regions that support these capacities.

3.1 History

Some researchers estimate that humans have been talking to each other for about 50,000 years. Before modern humans arrived in Europe about 45,000-42,000 years ago, the Neanderthals were already present. It is not clear how *homo sapiens* outpaced the Neanderthals, but some scholars believe that a crucial factor was their capacity for speech and the social advantages it confers. Although some of the recent fossil and genetic evidence (Rutherford, 2016) suggests that Neanderthals had the necessary infrastructure for speech, some of the fossil evidence, including skull differences in the basicranial line, nasopharynx and upper vocal cavity

(Donald, 1991) support the claim that *homo sapiens* benefitted from a speech advantage.

Writing technology and the ability to read were developed much later in history, approximately 5,000-4,000 years ago. Sumerian cuneiform and other early accounting methods and writing systems used mainly in commerce were developed around 4,000 and 3,000 B.C., while Egyptian hieroglyphics date from 2,000 to 1,500 B.C. Although used for the same objectives, these codes differ from our western writing systems in that they were not phonetically related to speech; the first phonetic written systems were developed around 1,700 BC (see *Figure 1* for early writing systems examples).

Figure 1. Examples of early writing systems

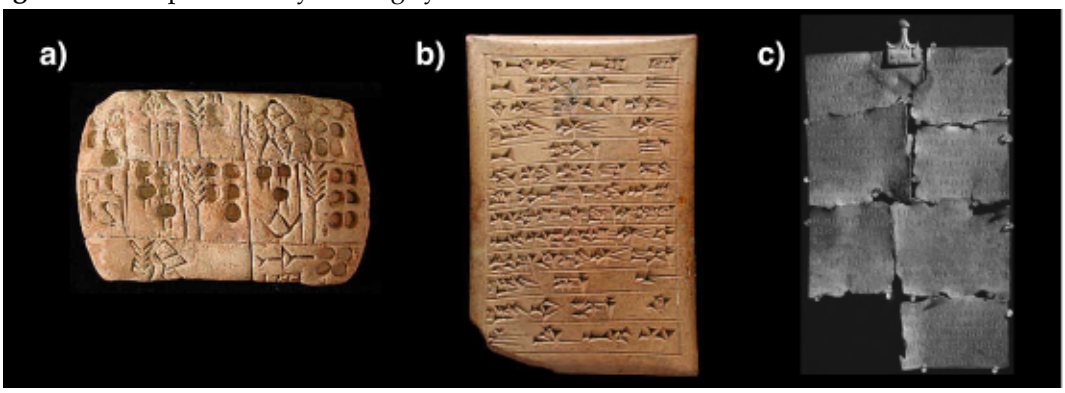

a) Pictogram used to communicate basic information about crops and taxes (around 3100 B.C.); b) clay tablet written in cuneiform; and, c) Tabula Cortonensis written in Etruscan (based on the Greek alphabet and read from right to left, 3rd or 2nd century BC) (Robinson, 2009)

Writing systems evolved in accordance with social expectations and beliefs about reading (Finkelstein and McCleery, 2013). For centuries, writing and reading constituted expert tools whose use was restricted to educated elites, and granted them important life advantages. Over the years, the usefulness of these tools and societal evolution, led to their use by a larger public. However, evolutionarily speaking, it is only in recent

years that the human species has broadly adopted writing and reading (see Figure 2). Therefore, it is reasonable to believe that our biology has not been altered due to the practice of reading and that the brain was not specifically "designed" or did not evolve for reading. But the opposite might be true, that is, the characteristics of writing and reading may have emerged from and been shaped by existing cognitive capabilities (Changizi et al., 2006; Changizi and Shimojo, 2005; Schoenemann, 2009).

Figure 2. Evolution of world literacy rates

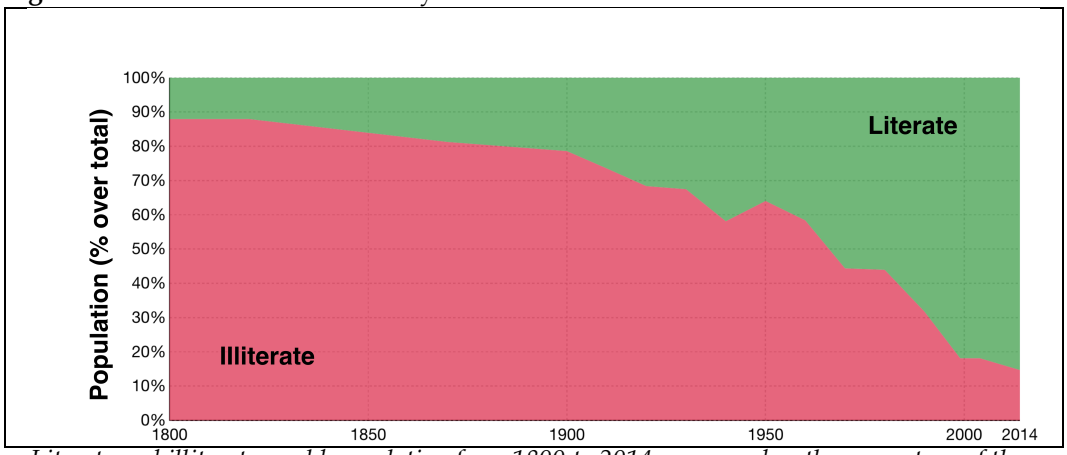

Literate and illiterate world population from 1800 to 2014, expressed as the percentage of the total population (adapted from https://ourworldindata.org/literacy/)

The spread of literacy has been very successful. In our modern societies, with omnipresent internet connected screens, reading and writing have become one of the most common tools for communication between humans. Nevertheless, learning how to write and read properly is an arduous process. Human children spend a significant amount of time during their formative years dedicated to this endeavor, and if this task is undertaken later in life, it becomes even more demanding. Reading requires the visual recognition of a word and associating this letter string (i.e., orthography) to the corresponding units of speech (i.e., phonology). First, the reader has to represent the links between the components of

printed words and the components of spoken words, and second s/he will access the meaning of the word (i.e., semantics), making the process of reading a multilevel interactive process involving visual, orthographic, phonologic and semantic language systems.

The scientific fields that attempt to understand language are complex, varied and address multiple levels, ranging from Linguistics and Behavioral Psychology to Molecular Biology, which examines the neuronal synaptic connections in the brain. In this doctoral dissertation I am interested in understanding how language, and specifically reading, as human cognitive processes, are implemented in the brain. In the next section, I briefly sketch the history of the science of human cognition and, then, present some of the main neurocognitive models of language and reading.

3.2 Science and theory

The history of language research was itself an interesting journey. The study of language is at the core of a number of disparate fields ranging from philosophy and psychology to computer science and Artificial Intelligence, as well as linguistics and anthropology. All of these fields have made important contributions to our knowledge of language, but to shed light on how the brain implements language we need to understand how the brain works.

Even when restricted to the study of language, human cognition can be approached from different perspectives and methodological approaches. These approaches have evolved as a consequence of the accumulation of

scientific knowledge and the development of new research techniques. In a review paper, Kriegeskorte (2015) outlined the main steps taken in different scientific approaches to understanding how the brain works (see Table 1). Classical behaviorism (developed by pioneers such as Edward Thorndike, John B. Watson, Ivan Pavlov and B. F. Skinner since the late 1800s) was the first to undertake a systematic approach to understanding human and animal behavior, and had the objective of making predictions that could be tested experimentally. In the mid-20th century, researchers in the new field of cognitive psychology began to address not only behavior but also the mental processes that occur between stimulus and response, such as attention, memory, and language, among others. Cognitive psychology emphasized the importance of information processing, but lacked fully explicit computational models. Those computational models came later in the 1980s, proposed by cognitive scientists empowered by increasingly powerful and sophisticated computers. During the 1950s, cognitive scientists joined the debate as part of a movement called the cognitive revolution, led among others by the linguist Noam Chomsky. Cognitive science emerged with contributions from psychology, philosophy, linguistics, anthropology, neuroscience and artificial intelligence, and its main objective was the interdisciplinary scientific study of the mind and its processes. It wasn't until the 1980s that cognitive scientists produced the first successful models for language and reading. Nevertheless, at that time computing technology was not sufficiently advanced and models of cognition in cognitive science were restricted to toy problems.

Table 1. Historical progress toward understanding how the brain works (Kriegeskorte, 2015)

Elements required for understanding how the brain works		Behaviorism	Cognitive psychology	Cognitive science	Cognitive neuroscience	Classical computational neuroscience	Future cognitive computational neuroscience
Data	Behavioral	✓	✓	✓	✓	✓	✓
	Neurophysiological				✓	✓	✓
Theory	Cognitive		✓	✓	✓		✓
	Fully computationally explicit			✓		✓	✓
	Neurally plausible			✓		✓	✓
Explanation of real-world tasks requiring rich knowledge and complex computations			✓		✓		✓
Explanation of how high-level neuronal populations represent and compute							✓

Subsequently, in the late 1980s, and enabled by important advances in neuroimaging techniques, the field of cognitive neuroscience brought neurophysiological data into the equation. For the first time in history, it was possible to look at the living brain while it was performing cognitive tasks. Nevertheless, the drawback was that due to the vast amount of data, its complexity, and the development of new neuroimaging methods and techniques, enormous effort went into analyzing the information itself at the expense of theoretical sophistication, which was often reduced to the box and arrow models from cognitive psychology. At last, and somehow in parallel to the development of cognitive neuroscience, computational neuroscience was introduced. Computational neuroscience is another interdisciplinary field, combining neuroscience, cognitive science, psychology, electrical engineering, computer engineering, mathematics and physics, and it studies brain function in terms of the information processing properties of individual neurons and networks. Models in computational neuroscience use fully explicit and biologically plausible computational information to predict neurophysiological and behavioral data, although, again, due to the complexity of this data, computational neuroscience has not yet been able to tackle high-level

brain representations. Despite the success of recent efforts, radical improvements to computational power will be needed in the years to come to allow computational neuroscience to further contribute to the understanding of high-level brain functions.

As proposed in the last column of Table 1, Cognitive Computational Neuroscience might be a good name for a future integrative scientific discipline that explains brain function. In principle, this discipline could explain high-level cognitive and behavioral processes at the neuronal level using detailed computational models. In this regard, there is currently a strong ongoing debate within the field of psychology (Schwartz et al., 2016a, 2016b; Staats, 2016; Tryon, 2016): some authors believe that the conflict between eliminative reductionism and emergentism should be addressed. Eliminative reductionism is the belief that the neural level of analysis will eventually render the psychological level of analysis superfluous. On the other hand, emergentism assumes that higher-order mental functions are not directly reducible to their underlying neural processes, meaning that neuroscience (cognitive and computational) should contribute to psychology, not 'be' psychology. This would mean integrating neuroscience, computational neuroscience and neural network approaches in a larger methodological and technical approach within the classical psychological account. It seems that in the end, although coming from divergent philosophical substrates, cognitive computational neuroscience and an integrative approach to psychological phenomena are basically similar or pursue the same goal: more integration at all levels.

Thus, to further advance our object of scientific inquiry it is first necessary to solve the double problem of computational power and scale. On the one hand, computational neuroscience addresses problems at a very low, neuronal and synaptic level. Using the latest tools developed in computer science, one of the objectives is to integrate and predict neurobiological data. On the other hand, cognitive neuroscience addresses problems at a higher scale, generating and integrating neurobiological and behavioral data. To integrate these two approaches, at least two things will need to happen: 1) improvements in computational power which allow us to tackle more complex neurocomputational problems than the current ones; and, 2) improvements in the spatial and temporal resolution of neuroimaging techniques used in cognitive neuroscience.

To conclude, it is worth reminding that Cognitive Neuroscience is a relatively young science comprising only about 30 years of research activity (Raichle, 2009). Most importantly, it is based on advanced neuroimaging techniques that keep evolving at an increasing rate, and whose precision keeps improving over time. Neuroimaging as a field evolves in two different ways: via the improvement of existing techniques (better spatial and temporal resolution, better contrast) and via new developments that may yield exponential improvements or even a paradigm change (for example, optogenetics or calcium imaging). To advance our knowledge of the neurobiology of reading, in this doctoral dissertation proposal I used both behavioral and magnetic resonance imaging (MRI) techniques. MRI is one of the main neuroimaging tools used in cognitive neuroscience. More precisely, with functional MRI (fMRI) it is possible to locate the cortical and subcortical grey-matter brain

regions engaged in a certain functional task, and with structural MRI it is possible to observe brain changes in grey and white matter. In the next section, I will briefly introduce the main language models that existed before cognitive neuroscience emerged as a discipline, and the current language models that are being discussed in this field.

3.3 Cognitive neuroscience and reading models

Before the advent of modern neuroimaging techniques, the main source of neurobiological information was neuropsychological research with patients. The most popular neurobiological model of language, proposed first in the 19th century, remained dominant for some two centuries. Known as the Wernicke-Lichteim-Geschwind (WLG) model (see *Figure 3a*), the basic premises of this model include the involvement of Wernicke's area in speech comprehension, Broca's area in speech production, and the arcuate fasciculus as the white-matter fiber tract connecting these regions. In the 1980s, when the main theoretical models in cognitive sciences were proposed (see *Figure 3b*), the WLG model was still widely used. The new theoretical models proposed by cognitive scientists were mainly focused on the new possibilities offered by computers and recent advancements in artificial intelligence, and tried to model the existing behavioral data. At that time, two main models emerged in regard to reading: the Parallel Distributed Processing (PDP) model (see Seidenberg, 2012, for a review; Figure 3*b1*) and the Dual Route Cascaded (DRC) model (Coltheart et al., 2001; Figure 3*b2*). These models were consistent with previous behavioral results, but they lacked the restrictions imposed by biology, thus making it difficult to adjudicate

between models. While the approach of the DRC model was more data-driven, the connectionist approach of the PDP model was more theory-driven, meaning that the PDP model derived from a set of principles concerning neural computation and behavior.

Figure 3. Classical language and reading models

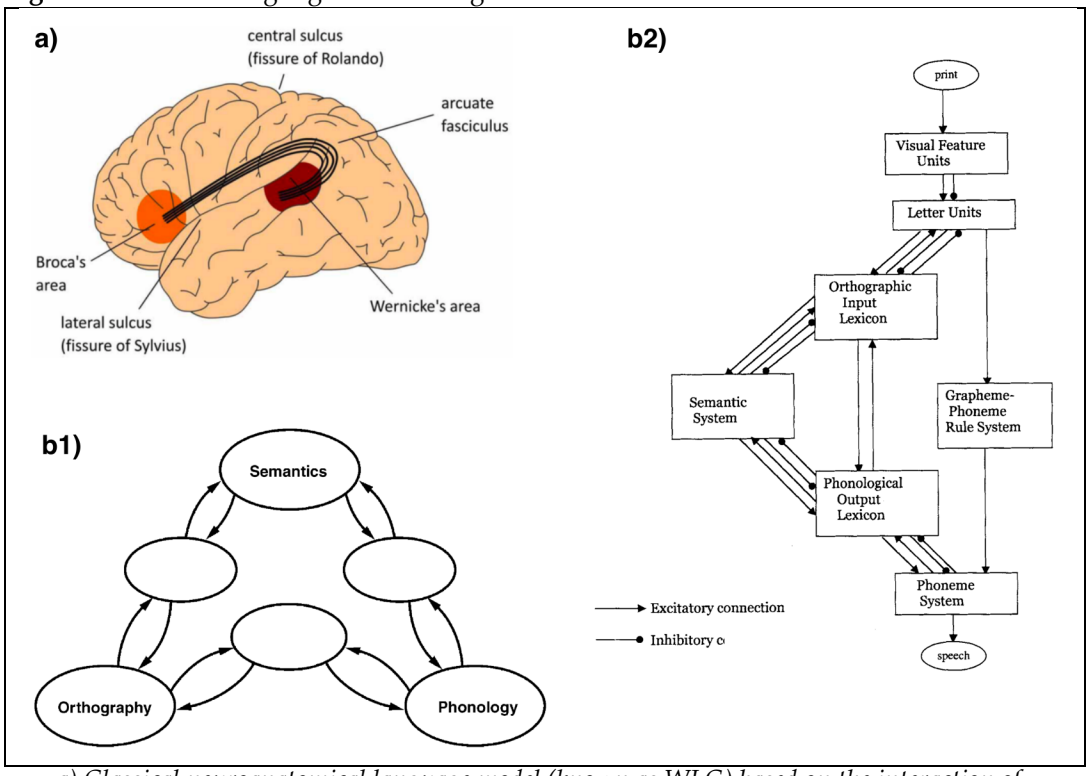

a) Classical neuroanatomical language model (known as WLG) based on the interaction of Wernicke's (language comprehension) and Broca's (language production) areas through the connectivity provided by the arcuate fasciculus. b) Main theoretical reading models in the cognitive sciences, b1) PDP model of reading, and b2) DRC model of reading. Images from Coltheart et al, 2001, Hagoort, 2013, and Seidenberg and Plaut, 2006.

However, for a full understanding of any neurobiological system, it is of crucial importance to constrain models to a biologically plausible substrate. In this vein, the WLG model was still considered neurobiologically valid until recently because there were no new neurophysiological data available. Modern neuroimaging techniques in the late 1980s provided multimodal approaches to the study of language and reading, at much higher spatial and temporal resolutions than had been possible before. However, by integrating information from histology

(Amunts and Zilles, 2012), MEG (Tarkiainen et al., 2002), lesion studies (Caramazza and Zurif, 1976) and MRI (Menenti et al., 2012), enough evidence was gathered to demonstrate that the one-century-old WLG language model was no longer viable (Hagoort, 2013; Poeppel et al., 2012). Although Broca's area, Wernicke's area and adjacent cortex are still considered to be key nodes in the language network, it has been shown that the distribution of labor between these regions is different from that claimed in the WLG model. Adding to the important contribution of new techniques (e.g., MRI) and the availability of quantitatively and qualitatively better data, were new theoretical contributions from close disciplines such as linguistics, cognitive psychology and computational modelling (Poeppel et al., 2012). Language is not monolithic and, consistent with this fact, modern models consider more elements than just speech comprehension and speech production. These related disciplines provided the theoretical background to test new lower level ideas neurobiologically (e.g., phonology versus syntax, or orthographic versus semantic access to words). Therefore, thanks to advancements on many fronts, the WLG model has now been overtaken and new, increasingly detailed, neuroanatomical models have emerged (see Figure 4).

These new models have had the difficult task of integrating all the existing as well as new data from an exponentially growing number of studies. Language, or more specifically the neurobiology of language as a field, is a vast area of knowledge and research. In a review of the last 20 years of PET and MRI studies, Price (2012) divided the Neurobiology of Language research into heard speech, spoken language, and reading. These three big areas were later subdivided into 1) auditory processing of speech and

non-speech, 2) speech selective auditory responses (i.e., phonological processing), 3) speech comprehension, 4) speech production (i.e., word retrieval from semantics), 5) covert articulatory planning, 6) overt articulation during speech production, 7) auditory-motor feedback during speech production, 8) early visual word form processing, and 9) neural pathway dissociation for mapping orthography to phonology. In this vein, neurobiological models with different levels of completeness were proposed: the dorsal and ventral dual-stream model for cortical speech sound and word processing (Hickok and Poeppel, 2007; Figure 4*a*), the cortical model for semantics (Binder and Desai, 2011; Lau et al., 2008), the language processing model (Hagoort, 2013, 2005; Figure 4*b*), the auditory perception and sentence comprehension model, modeling language biology both functionally (Figure 4*c1*) and structurally (Figure 4*c2*) (Friederici, 2012, 2011), and the reading model (Pugh et al., 2001).

Figure 4. Modern functional and structural neuroanatomical models of language

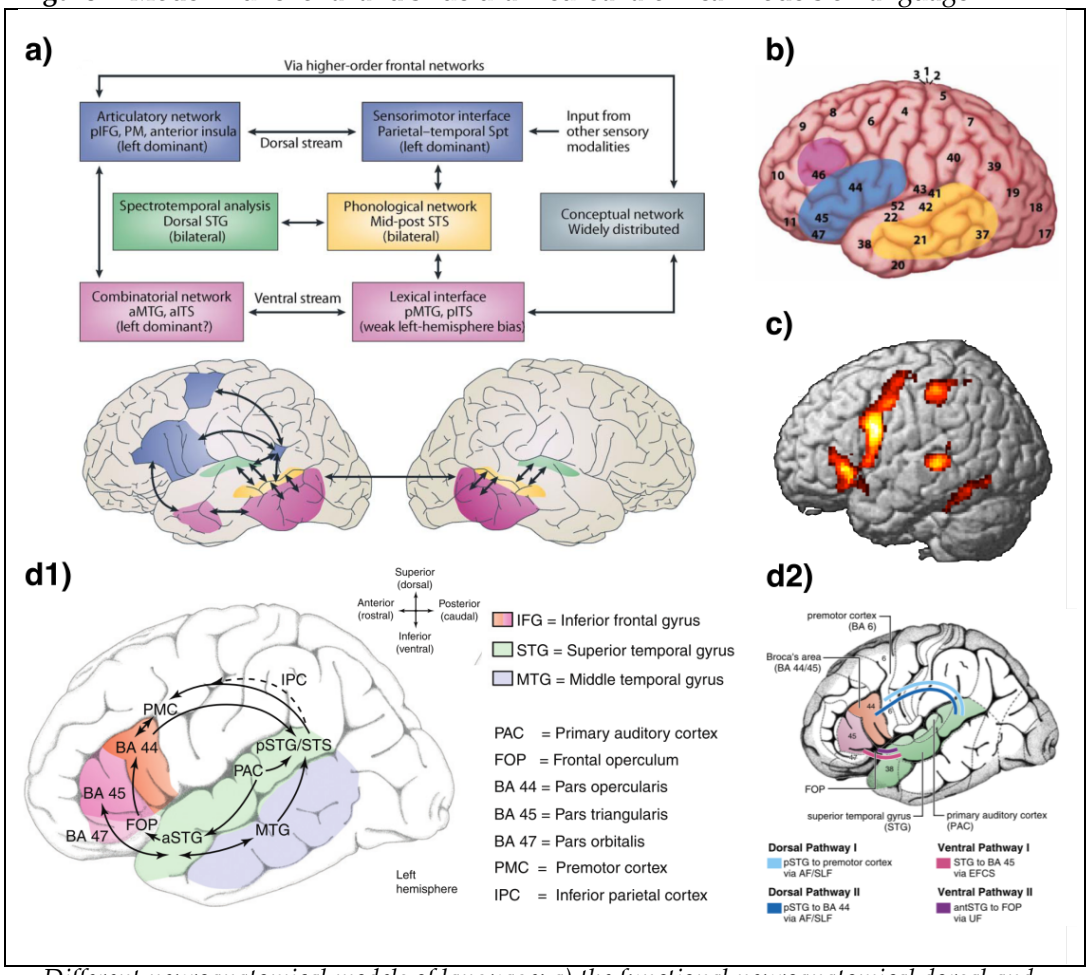

Different neuroanatomical models of language: a) the functional neuroanatomical dorsal and ventral stream model of speech sound and visual word processing (Lau et al., 2008; Poeppel et al., 2012); b) The MUC model of language, with the Memory areas in the temporal cortex (yellow), Unification areas in the IFG (blue), and Control operations areas in the lateral-frontal (pink), numbers indicate Brodmann areas (Hagoort, 2013); c) The reading circuit, involving left fusiform gyrus, posterior temporal cortex, pars opercularis and bilateral insula (Carreiras et al., 2007); and d1) the cortical language circuit, with colored IFG, sTG and mTG, and d2) Structural connectivity between the language cortices: two dorsal and two ventral pathways are shown (Friederici, 2012, 2011). Images from Carreiras et al., 2007, Friederici, 2012, Hagoort, 2013, Poeppel et al., 2012.

It is important to highlight the dual-stream hypothesis of reading because it has been dominant in the field and boasts extensive supporting evidence. Originating from vision research (Goodale and Milner, 1992), the dual-stream hypothesis was adapted for and has been included with more or less detail in all of the above-mentioned models. It proposes a model of reading with a differential involvement of ventral and dorsal routes (Hickok and Poeppel, 2007; Pugh et al., 2001; Schlaggar and McCandliss, 2007). This hypothesis has been supported by functional and

structural neuroimaging studies that have demonstrated differential specialization in regions along the ventral and dorsal streams (Jobard et al., 2003; Saur et al., 2008). The ventral pathway, comprising the vOT and the *pars triangularis* and *orbitalis* regions in the IFG, supports the mapping of orthographic-lexical stimuli onto semantic representations (Sandak et al., 2004). The dorsal pathway, encompassing the posterior IFG *pars opercularis* region, pPC, and the sTG, supports phonological processing. The evidence suggests that learning a new word involves the dorsal stream, while recognizing a word that already pertains to our lexicon is mainly processed by the ventral stream (Pugh et al., 2001). From these models, the most important brain regions for reading, namely pPC (Wernicke's area is partially located here), IFG (Broca's area is located here: *pars opercularis* and *triangularis*), and vOT, will be reviewed in the next chapter.

The vOT was identified by Dejerine (1892) more than a century ago. Its importance and involvement in reading were highlighted and better understood after experiments were performed using modern neuroimaging techniques. Experimental evidence suggests that vOT is the gateway from vision to language, where visual word recognition occurs prior to accessing nonvisual information (Twomey et al., 2011). However, while there is broad agreement that the vOT is involved in the necessary computations for recognizing words, the specific role of the vOT is still under debate. In the next chapter, I describe the main neuroimaging techniques used in the field and in the experiments of the present doctoral dissertation. Following this chapter I review the empirical literature on vOT and, more generally, the neurobiology of reading in more detail.

4 NEUROIMAGING TECHNIQUES

This chapter presents an overview of current neuroimaging methods, highlighting those techniques used in the experiments similar to those conducted for the present doctoral dissertation. Efforts to develop the technological capacity to map activation in the working brain with the objective of associating such activity with typical or atypical behavior has a long history beginning with the pioneering works of Angelo Mosso and his 'human circulation balance' in the early 1900s (Sandrone et al., 2013). Today, several neuroimaging devices are available that allow us to measure brain activation *in vivo*, such as electroencephalography (EEG: measures brain electrical activity by recording voltage differences in the scalp), magnetoencephalography (MEG: measures brain electrical activity by recording magnetic fields in the scalp), positron emission tomography (PET: measurement and reconstruction in an 3D image of gamma-rays emitted by a positron-emitting tracer injected into the subject's blood system), or magnetic resonance imaging (MRI: uses a magnetic field and changes in radiofrequency pulses to create 3D images of the brain).

All of these techniques measure changes related to brain activation. However, only MRI allows us to combine functional and structural neuroimaging. MRI was therefore the technique selected given the goals of the experiments conducted for this doctoral dissertation. In the following subsections, I present a detailed description of the measures used in the present work.

4.1 Functional MRI

Functional MRI (fMRI) allows us to measure many thousands of locations in the brain while subjects perform tasks inside the scanner (Bandettini, 2012). The fMRI technique has a high spatial resolution on the order of 2-3mm (and will get smaller in the future), and is used to locate "where" in the brain cognitive changes occur. These changes may be related to task performance or changes in resting state activity over time.

4.1.1 BOLD signal

BOLD stands for the blood-oxygen-level-dependent response (Ogawa et al., 1990), and is a measurement of the ratio of deoxygenated (deoxyHb) to oxygenated hemoglobin (oxyHb) in the bloodstream. DeoxyHb is paramagnetic and disturbs the homogeneity of the magnetic field, whereas oxyhHb is not, and therefore has no effect on the local magnetic field. Therefore, it is possible to program an MRI sequence to detect changes in the level of deoxygenated and oxygenated hemoglobin molecules present in the blood, based on their different paramagnetic properties. So, if the brain is engaged in a demanding cognitive task, it will require a large blood supply, and this change in blood flow will result in BOLD signal changes. These BOLD signal changes make it possible to map changes in activity associated with cognitive tasks (Raichle, 2009). More concretely, increases in neural activation result in an initial increase in oxygen consumption, and only after a delay of about 2 seconds, a large increase in localized cerebral blood flow is triggered to compensate oxygen consumption. This increased blood flow translates into increased oxygenation and, consequently, also reductions in deoxyHb. This

mechanism explains why it is thought that a higher signal in fMRI images correlates with neural activity. The goal of fMRI experiments is to measure to what extent a given manipulation produces BOLD signal changes.

4.1.2 fMRI designs

There are two major types of experimental designs: block and event-related designs (Buckner et al., 1996; Dale and Buckner, 1997). In a block fMRI design, stimuli are presented continuously for a fixed extended time interval, called a block. In this design, activation blocks are usually followed by rest blocks of an equal duration, and activation blocks for different experimental manipulations or conditions usually alternate. Block designs have superior statistical power (Friston et al., 1999), due to the relatively large BOLD signal change relative to baseline (Buxton et al., 1998), and overall are more robust than event-related designs (Brockway, 2000; Rombouts et al., 1997). Block designs are appropriate if the experimental goal is to detect sustained activation or subtle differences in BOLD signal across different test conditions. In contrast, in event-related designs, discrete and short-duration stimuli conditions are presented in a randomized order. Event-related designs are typically preferred when it is important to reduce expectancy effects (D'Esposito et al., 1999), can better detect transient variations in hemodynamic response, and allow for the analysis of individual responses to trials (Schacter et al., 1997).

4.1.3 Data preprocessing

One of the main issues in analyzing fMRI data is how to compare a group of images in a statistically meaningful way. Before this statistical analysis

can be performed, it is necessary to preprocess the data, usually including these main preprocessing steps: slice timing (temporal interpolation), realignment (spatial interpolation), coregistration (sometimes normalization to a common template), and smoothing (see Figure 5 for a schema of data preprocessing). The slice-timing correction is used to compensate for slice acquisition delays, so that it is equivalent to acquiring a full volume of brain slices at a single time point. Subjects may move in the scanner during data acquisition and consequently the location of voxels may vary between scans; the realignment step to some extent helps to correct these motion artifacts by spatially aligning the acquired functional images.

Figure 5. fMRI data preprocessing and statistical analysis.

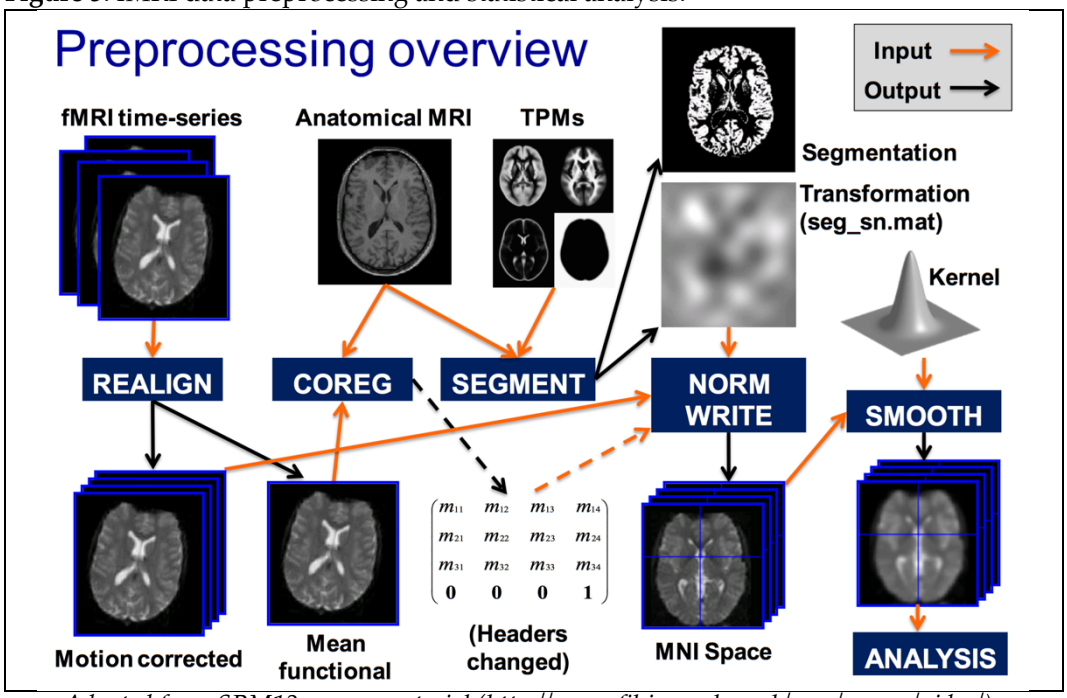

Adapted from SPM12 course material (http://www.fil.ion.ucl.ac.uk/spm/course/video/)

To increase the spatial precision of functional images, they are typically coregistered with a high-resolution T1- or T2-weighted anatomical image from the same subject. In fMRI studies requiring a group analysis another important preprocessing step is normalization, where subjects' brain

images are warped into a standard stereotaxic space. The most common templates are based on the Talairach coordinates, also known as Talairach space, the default for normalization. The Talairach space is a 3-dimension coordinate system or "atlas" of the human brain (Talairach and Tournoux, 1988). Using the same brain space across laboratories and studies allows for results to refer to a standard space, so that the research community can compare and reproduce findings. Furthermore, normalization is used to reduce inter-subject anatomical variability. Finally, during smoothing, voxel values are averaged with those of their closest neighbors. This is done to improve the signal-to-noise ratio: the BOLD response is modulated by blood flow, therefore the rate at which the signal changes in an activated region is limited, and there should not be sharp changes in BOLD signal values.

4.1.4 Statistical analysis

After preprocessing, the functional images are ready for statistical analysis, and usually the most widely used statistical technique to fit and detect variations in BOLD response is the general lineal model (GLM; Friston et al., 1995). Specifically, fMRI analyses are carried out in multiple stages. For example, in a two-sample t-test, the first-level analysis involves modeling the data for each subject separately, and estimating those subject-specific differences due to a particular manipulation. The second-level analysis takes the subject-specific parameter and variance estimates from the first-level model. Within-subject variance is estimated at the first-level and between-subject variance at the second-level. Finally, the model estimates a mean for each group and a contrast of interest to compare between groups (Poldrack, 2011). For an image composed of N voxels,

there are several ways to decide if there are changes in the BOLD response: at the voxel-level, that is, by testing each and every voxel in the brain, and at the cluster-level, by examining specific clusters of activated voxels. Importantly, when comparing multiple voxels one must avoid "multiple testing problems", such as a Type I error, which refers to one or more false positives. Different methods available for avoiding this problem, including the False Discovery Rate (FDR) and the Family-wise error (FWE) rate, which can be applied both at the voxel or cluster level. Deciding what is the most appropriate method to correct for multiple comparisons is still a matter of debate, especially with respect to analysis at the cluster level (Eklund et al., 2016).

4.1.5 Task Analysis

A common objective in fMRI analysis is to localize regions of the brain activated by a certain task or conditions, and determine the brain networks involved in specific cognitive processes. This analysis can be performed at the whole-brain level (i.e., voxel-wise) or focus on specific regions of interest (ROIs). When task analyses are performed at the voxel-level in the whole brain, the statistical sensitivity is usually lower due to the statistical corrections for multiple comparisons. Nevertheless, if a study is focused on particular regions of interest in the brain based on prior evidence and the study hypotheses, it is possible to limit the search for differences in activation to a given number of ROIs (Poldrack, 2007; Saxe et al., 2006). This approach involves the extraction of signal (i.e., parameter estimates) from specific brain regions of interest based on prior evidence suggesting the involvement of these brain regions in a specific cognitive function. There are various reasons to select this type of

analysis. On the one hand, in complex designs, such as factorial designs with multiple levels, it can be difficult to discern the pattern of activity across conditions from an overall voxelwise map; ROI analysis may more clearly illustrate this pattern of activation. On the other hand, by reducing the magnitude of correction needed for a large number of voxels, one can better control for Type I errors by limiting the number of statistical tests to a few ROIs (Poldrack, 2007; Saxe et al., 2006).

4.2 Structural MRI

According to the 'neuron doctrine' (Shepherd, 1991), brain computations are performed by neurons using electrical potentials and synapses. However, it is worth remembering that the almost 100.000 million neurons in an average brain only constitute 15% of the total number of cells in our brains. The rest of the cells are classified as glia (from the Greek 'glue'). After many years of being ignored, these cells have recently become the subject of intensive research (Fields, 2009), and there is evidence showing that the glia may be involved in coding information and cognitive processes (G. Perea et al., 2014).

Neurons are organized within the brain to form grey matter and white matter (WM). On the one hand, the grey matter mainly comprises the neuronal cell bodies that compose the cerebral cortex. On the other hand, WM comprises the long strands of nerve cell extensions (axons) and other support cells (e.g., the above-mentioned glia). These axons carry information from one grey-matter region to the other, and are usually organized into bundles of axons forming the so-called fiber tracts or fascicles.

Although traditionally studied by neuroanatomists and neurologists, the structural properties of grey matter and WM can contribute to a deeper understanding of brain function. Thanks to studies examining the importance of actual changes in grey matter and WM in response to cognitive demands (Draganski et al., 2004), nowadays structural MRI is becoming an important part of the toolbox and measurements used in cognitive neuroscience. Some morphometric features of the brain, such as volumetry, cortical thickness (CT), cortical gyrification or characteristics of the WM tracts can be used as proxies for a related cognitive function. For example: hippocampal volume for memory (Depue and Banich, 2012; Lerma-Usabiaga et al., submitted), CT for intelligence (Shaw et al., 2006), cortical gyrification for Parkinson's disease (Sterling et al., 2016), and WM tracts for cognitive development (Yeatman et al., 2014a).

Thanks to the proliferation of computerized tools, nowadays it is possible to automatically separate the grey matter surface from the WM, to segment the subcortical structures of the brain and to parcel the cortical surface. Previously, this work was done using manual procedures, but this proved highly resource intensive and prone to human error, which affected the variability and reproducibility of the data (Lerma-Usabiaga et al., 2016).

In the experiments presented in this doctoral dissertation, I have used three different structural measurements: DWI to study the micro-structural properties of WM; CT, for examining grey matter properties; and, qMRI, as a proxy for estimating the myelination of WM fibers.

4.2.1 Diffusion-weighted imaging

Water molecules diffuse differently along tissues depending on tissue type, integrity, architecture and the presence of barriers. Diffusion of water molecules in WM tends to be anisotropic (directionally-dependent; i.e., the movement of water molecules is restricted to the longitudinal axis of the axon), whereas in grey matter it is usually less anisotropic and in CSF is unrestricted or isotropic (i.e., water molecules can move freely in any direction; see Figure 6). With diffusion MRI sequences, it is possible to acquire images sensitive to this preferred direction of diffusion. Depending on the level of alignment of the magnetic field gradients with water molecule movement, the signal will increase or decrease. To extract and analyze the information from WM tracts, three main steps should be performed: 1) acquisition of the images, 2) modelling of the data at the voxel level, and 3) creation of tracts which connect the information across voxels (tractography).

Figure 6. Water diffusion

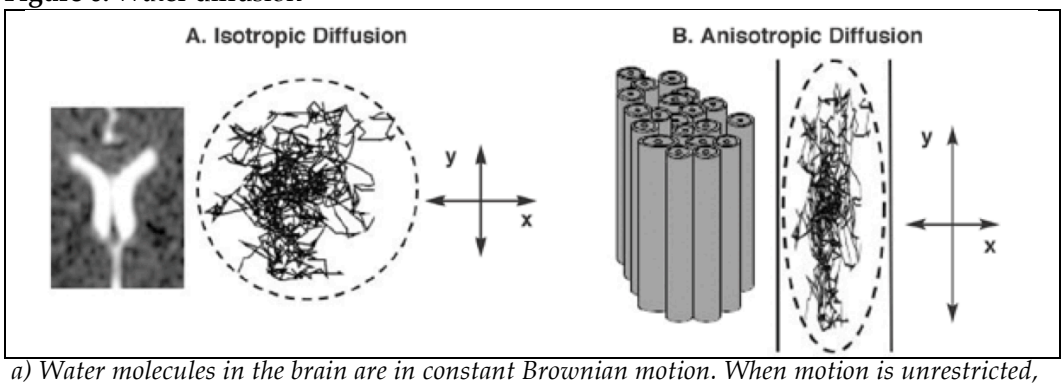

a) Water molecules in the brain are in constant Brownian motion. When motion is unrestricted, water molecules have no preferred direction of movement, and motion occurs equally and randomly in all directions (the diffusion is isotropic); B) in the presence of axons, the motion of water molecules will be restricted within the myelin sheath and will preferentially move along the longitudinal axis of the axon (water molecules will have a preferred movement along the y axis and the diffusion is anisotropic). The difference between the isotropic or anisotropic movement of water molecules is what is detected by diffusion-weighted imaging. Images from Rosenbloom et al., 2003.

1) Acquisition of the images: when designing an acquisition sequence, there are typically two main parameters to consider (although there are many more): the number of directions and the *b* value. The number of different alignments used to acquire these images is referred to as the number of directions. On the other hand, the *b* value comprises a set of physical constants and experimental parameters, such as the strength and duration of the magnetic field gradients. The same directions can be acquired using different *b* values. When an acquisition is made with only one *b*, it is called a single-shell acquisition; and when more than one *b* is acquired, it is called a multi-shell acquisition. For example, the Human Connectome Project uses 90 directions and 3 shells of *b* = 1000, 2000 & 3000. Nevertheless, the selection of parameters (the number of directions, *b* values, and the other factors not mentioned here) depends on the specific application. As is usually the case with MRI, a compromise solution must be found: more diffusion directions and higher *b* values yield better resolution. But, this comes at a cost. More directions implies a longer acquisition time, and increasing *b* values implies decreasing the signal-to-noise ratio (Wandell, 2016).

2) Modelling the data: there are many different ways to model data at the voxel level, and new models are being developed at a fast pace. Usually, for a single-shell acquisition with a small number of directions, the data is modeled using a diffusion tensor (usually abbreviated as DTI, for diffusion tensor imaging). A multi-shell acquisition combined with the acquisition of many directions (called high angular resolution diffusion imaging or HARDI), requires more complex models, such as the constrained spherical deconvolution (CSD) model (Jeurissen et al., 2014).

The mayor difference between the two is that the first model cannot model fiber crossings, as it will always give one (the predominant) direction (Tournier et al., 2011). In contrast, CSD models can report multiple fiber orientations. This difference is very relevant, given that around 90% of all the voxels in WM are estimated to include crossing fibers (Jeurissen et al., 2013).

3) Tractography: the third step consists of tractography algorithms, which combine the diffusion MRI voxel information to estimate the tracts. There are several options for performing tractography, and new improved algorithms are continuously being published. Classical tractography methods include local or global tractography and deterministic or probabilistic tractography. In local tractography, the algorithm starts from a seed and uses only this local information to decide on the next step (so in areas of high uncertainty the errors propagate upstream), while in global tractography the algorithm integrates information along the entire path. In local-deterministic tractography, the algorithm models the geometry of the diffusion data only, and there is only one possible direction at each step (Jackowski et al., 2004; Jones et al., 2002; Lazar et al., 2003; Melonakos et al., 2007; Mori and Barker, 1999; Pichon et al., 2005). In local-probabilistic tractography, model statistics for the diffusion data are also modeled, and many possible directions at each step are evaluated with different probabilities (Behrens et al., 2007; Friman et al., 2006; Jones and Pierpaoli, 2005; Lazar et al., 2005). In global methods, both deterministic and probabilistic methods can be applied, but the most important difference is that this approach makes use of previous knowledge. For example, if our participant is a healthy subject and we

want to find the optic radiation tract, we can use an atlas to tell the algorithm where to look (Yeatman et al., 2012b; Yendiki et al., 2011).

There is still a lot of work to do to improve DWI acquisition and analysis, and this is evinced by the continuous stream of new techniques and algorithms being developed to improve the technique, as well as by the publication of critical studies reporting results obtained using DWI analysis (Maier-Hein et al., 2016). There is no doubt that DWI is a very useful technique and that it will be more useful in the future, but care should be taken when analyzing, and most importantly, when interpreting the results (Wandell, 2016).

In any case, after performing the previous three steps, we obtain a model of our fiber tracts. From this point on, we can infer the underlying tissue in each voxel and calculate several indices, such as fractional anisotropy (FA), hindrance-modulated oriented anisotropy (HMOA) or apparent fiber density (AFD); these three measures provide information about WM tissue properties. FA is an index that provides a simple and robust indication to assess the degree of anisotropic diffusion occurring within a given tract. FA will be high in regions heavily organized in terms of orientation (e.g., corpus callosum), intermediate in regions with some degree of organization (e.g., WM regions that have no strong predominant axon fiber axis orientation), and low in tissues where the predominant cell shapes are not specifically oriented (e.g., grey matter). HMOA and AFD are relatively new and applied specifically to the more sophisticated CSD models (Dell'Acqua et al., 2013; Raffelt et al., 2012), and they are used as a compact measure of fiber density and connectivity along each tract

orientation. While HMOA/AFD are specific to the orientation of each tract, FA decreases where fibers cross due to local partial volume effects. Thus, although more accurate than FA, HMOA/AFD have not yet been as widely adopted as FA. To close on a technical note, it is important to remember that the diffusion field is in continuous evolution, that there are several (as in every other technique) known constraints (Jones et al., 2013), but that increasing efforts are being made to improve the information we can extract from DWI data, with tools such as SIFT/SIFT2 (Smith et al., 2015, 2013), LiFE (Pestilli et al., 2014) and Ensemble Tractography (Takemura et al., 2016).

Higher FA values have been associated with increased variations in axon count, density of axonal packing and myelination. Myelination occurs more actively during development but also in adulthood (Ishibashi et al., 2006), and leads to increases in the space occupied by axons in a given voxel and subsequent increases in FA (Stikov et al., 2011). These developmental effects of myelination and axon density on diffusion measurements have been confirmed in animal models and also in humans (Beaulieu et al., 2005; Pierpaoli et al., 2001).

Empirical evidence suggests that the development of cognitive abilities, such as reading is correlated with increases in FA values within tracts that connect relevant reading regions, such as the left arcuate fasciculus (Yeatman et al., 2012a). Thus, reading development is in part the result of microstructural changes in WM, as measured by FA, along tracts within the reading network (Wandell and Yeatman, 2013). Indeed, there is evidence showing that FA values in the left temporo-parietal lobe

correlate with reading performance in both poor and normal readers (Klingberg et al., 2000), which suggests that axons in this area are important for efficient structural connectivity between temporo-parietal and frontal regions. Studies such as this demonstrate how useful FA measures can be for investigating structural brain changes associated with specific cognitive functions. This explains why DWI has been gaining increased popularity among clinicians and researchers, providing a tool for studying WM architecture in living humans.

4.2.2 Cortical thickness

The human cerebral cortex constitutes a highly folded mantle of neurons, whose thickness varies on average between 1 and 4.5 mm depending on the region being examined (Fischl and Dale, 2000). The thickness of the cortex is of great interest and shows marked changes over development (Sowell et al., 2003). During infancy and early childhood there is an initial overproduction of neurons and synaptic connections followed by activity dependent fine-tuning which leads to synaptic pruning that continues well into adolescence (Shaw et al., 2006; Figure 7). Synaptic pruning refers to the fact that extra neurons and unused synaptic connections are eliminated to increase the efficiency of neuronal transmissions, leading to concomitant decreases in cortical thickness (Paolicelli et al., 2011; Tamnes et al., 2010). Therefore, across development grey matter loss occurs as part of the ultimate sculpting of the brain into the fully functioning adult nervous system and results in cortical thinning (Shaw et al., 2008; Sowell et al., 2003).

Figure 7. Rate of change in cortical thickness correlates with intelligence

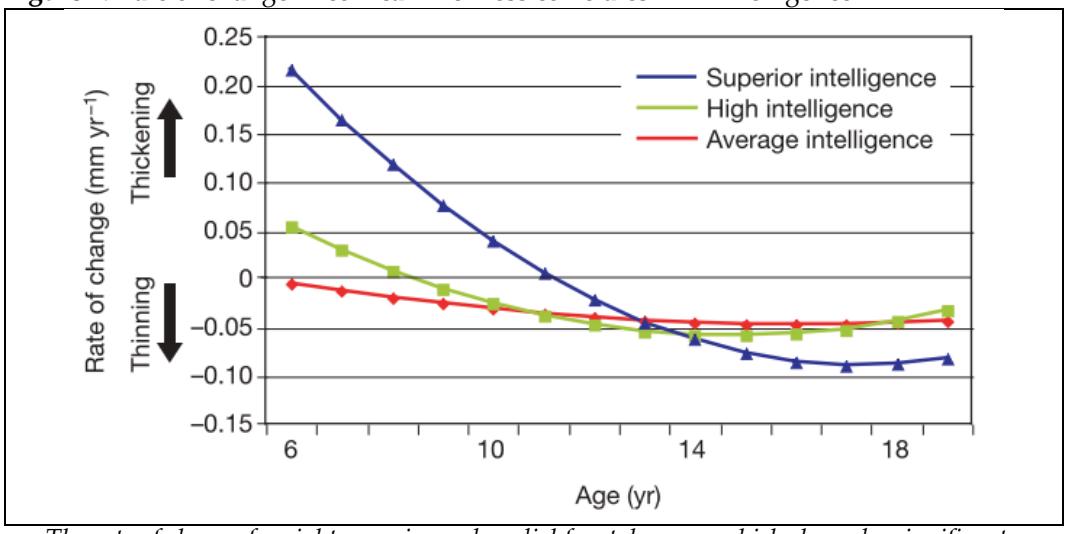

The rate of change for right superior and medial frontal gyrus, which showed a significant different developmental trajectory with age. Positive values indicate increasing cortical thickness. Negative values indicate cortical thinning. The point of intersection in the x-axis represents the age of maximum cortical thickness (5.6 years for average, 8.5 years for high, and 11.2 years for the superior intelligence group). Image from Shaw et al., 2006.

Empirical evidence has showed that vOT CT can be used to detect language lateralization, and that these CT values correlate with behavioral and fMRI data on a lexical decision task (Greve et al., 2013). In sum, CT can provide relevant information in relation to structural modulations in the form of neuronal loss and the reduced size of neural cell bodies, which in turn may be associated with the performance of cognitive abilities and relevant factors associated with language and reading.

There are several tools available to perform CT analysis, with Freesurfer (Fischl and Dale, 2000) being one of the most popular, because it is complete and reliable. In Freesurfer, the T1-weighted image is normalized and skull stripped before segmenting it into white and grey matter (see Figure 8). Once the boundary between white and grey matter has been delineated, a 2D mesh composed of small triangles is fitted and smoothed interpolating values across voxels, as the original tissue is continuous as well. If the smallest unit in a volumetric image is the voxel, the smallest

unit in the mesh is the 'vertex', which is precisely the vertex of each individual triangle of the mesh. For each vertex, different indices are calculated, such as CT, gyrification and cortical volume. Finally, the mesh is inflated until all the gray matter is covered, informed by the delimitations imposed by the pia mater. The CT at each vertex is the difference between the vertex at the pial surface and the corresponding vertex at the WM surface.

Figure 8. Freesurfer's cortical thickness pipeline

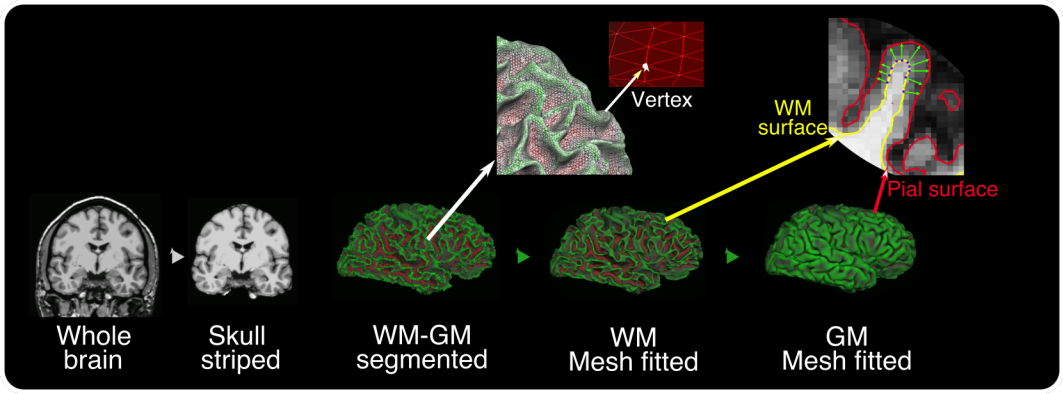

Freesurfer surface reconstruction pipeline. Skull stripped T1-weighted images have the WM and the grey matter boundary segmented, and afterwards a mesh is fitted to this boundary. The mesh is inflated until the boundary between the grey matter and the pial matter is found. The cortical thickness is the perpendicular distance between the WM and pial surfaces. Adapted from Freesurfer online course materials.

4.2.3 Quantitative MRI

MRI sequences are typically designed to reveal qualitative tissue contrast, but there are several scientific (and clinical) advantages in using quantitative MRI (qMRI) methods (Mezer et al., 2013; Tofts, 2003). Nowadays, the qualitative nature of the MRI measurements makes it difficult (or impossible, for example, when comparing different groups scanned in different locations) to compare data from different scanners. With qMRI the tissue properties are stable and comparable between scanners, similar to body temperature or blood pressure measurements.

Figure 9. Diffusion-weighted imaging and quantitative MRI

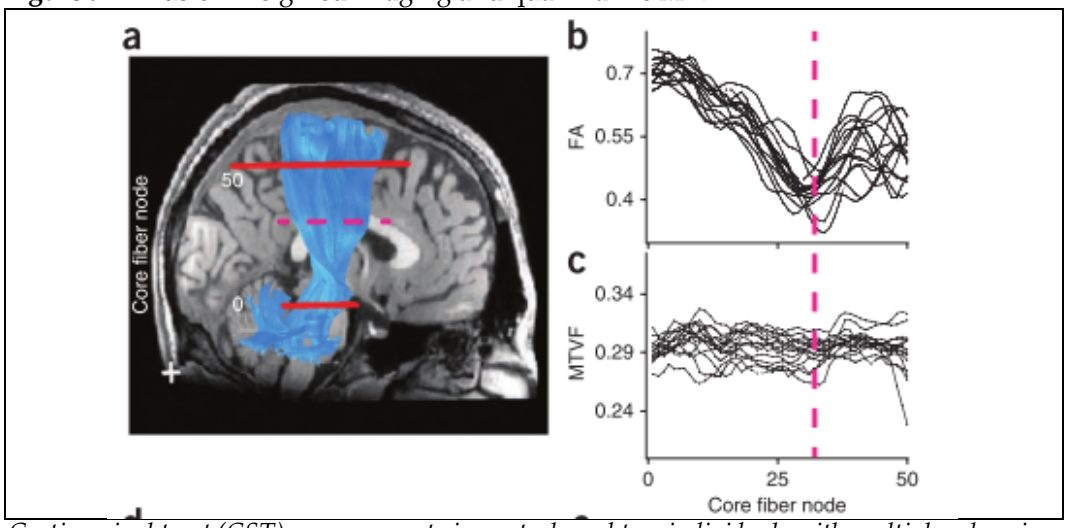

Corticospinal tract (CST) measurements in controls and two individuals with multiple sclerosis. a) The estimated right CST (blue) is overlaid on a sagittal T1-weighted image. The two solid red lines show axial planes that designate the measurement region; the centroid of the tract (core fiber) is calculated and sampled into 50 nodes. The CST intersection with the callosal fibers is designated by the dashed fuchsia line. b & c) The curves show FA and MTVF values measured at different nodes along the CST from different control subjects (N = 15). The FA value, but not the MTVF value, declines in the region where the CST intersects callosal fibers (dashed fuchsia line). Images from Mezer et al. (2013).

For example, CT is a qualitative measure: it is derived from a statistical analysis of uncalibrated MRI images that depend on multiple biological factors. By contrast, quantitative measurements can specify several biological tissue properties, such as T1, macromolecular tissue volume (MTV), magnetization transfer, or T2 (Mezer et al., 2013; Stikov et al., 2011; see Figure 9). For example, brain macromolecules (measured with MTV) are principally cell membranes and proteins, while in the case of WM, approximately 50% are myelin sheaths, so MTV can be used as a proxy for the myelination of fiber tracts.

Furthermore, the coupling of diffusion with qMRI methods can provide insights into macroscopic tissue organization. Additionally, there has been some success in measuring specific features of the WM axons, including axon diameter (Assaf and Pasternak, 2008; Barazany et al., 2009; De Santis et al., 2014; Huang et al., 2015) and the ratio of the myelin sheath thickness

to axon diameter (Purger et al., 2016; Rushton, 1951). These tissue properties change during development, in response to experience, and across the life span (Lebel et al., 2012, 2008; Mezer et al., 2013; Wandell and Yeatman, 2013; Yeatman et al., 2014a), and can be used to explain individual differences in development and behavior (Gomez et al., 2017).

The functional and structural MRI techniques described above have been used in the experiments described in this doctoral dissertation. One of the main objectives of the present work has been to integrate different types of neuroimaging indexes to better examine and understand the role of the vOT in reading. In the next section, I review research evidence on language and reading, integrating what is known about the involvement of vOT and the sub-component thought to be specifically responsive to words, the VWFA.

5 NEUROBIOLOGY OF READING

The present chapter is divided into four sections. First, I review the literature on the neurobiology of the vOT and VWFA. Second and third, I revise our understanding of the relation between the pPC and IFG with the vOT and reading, stressing the importance of functional and structural connectivity between these critical regions for reading. Finally, I review extant knowledge on the functional and structural interactions among these three areas of interest: vOT, pPC and IFG.

5.1 vOT and VWFA

Reading is an extraordinarily complex cognitive ability. The process starts in the eye, when the light-dark contrast defining the letters enters the retina and hits the ganglion cells. The only part of the eye with enough resolution to discern the details of a letter is the fovea. Consequently, we can only read short words or small parts of larger words at a glance and have to move the eyes rapidly (i.e., make saccades) from one segment of a word to the next. The saccades are controlled cortically by the frontal eye fields (FEF) and subcortically by the superior colliculus. Once the foveal images are converted to neuronal spikes in the ganglion cells, the information flows through the thalamic lateral geniculate nucleus (LGN) into the visual cortex region V1 (Clascá et al., 2016). The visual cortex is organized retinotopically, as concentric cortical circles in the occipital pole. V1, at the center, responds to very basic features, such as lines and their orientations. The complexity of visual representations increases as these circles expand: the dorsal pathway is assumed to encode the 'where' and the ventral pathway the 'what' (Goodale and Milner, 1992). Looking

at the anatomy, dorsal visual cortices reach the pPC, while ventral cortices reach the vOT (see Figure 10a). The vOT is divided into specialized high-level visual regions that respond selectively to specific image categories and are believed to play an essential role in object perception. In particular, the cortical region inside the vOT recruited for visual word recognition is referred to as the VWFA (Dehaene and Cohen, 2011; Kanwisher, 2010), but see (Price and Devlin, 2011; Vogel et al., 2012b).

Figure 10. The vOT as the gateway between reading and language

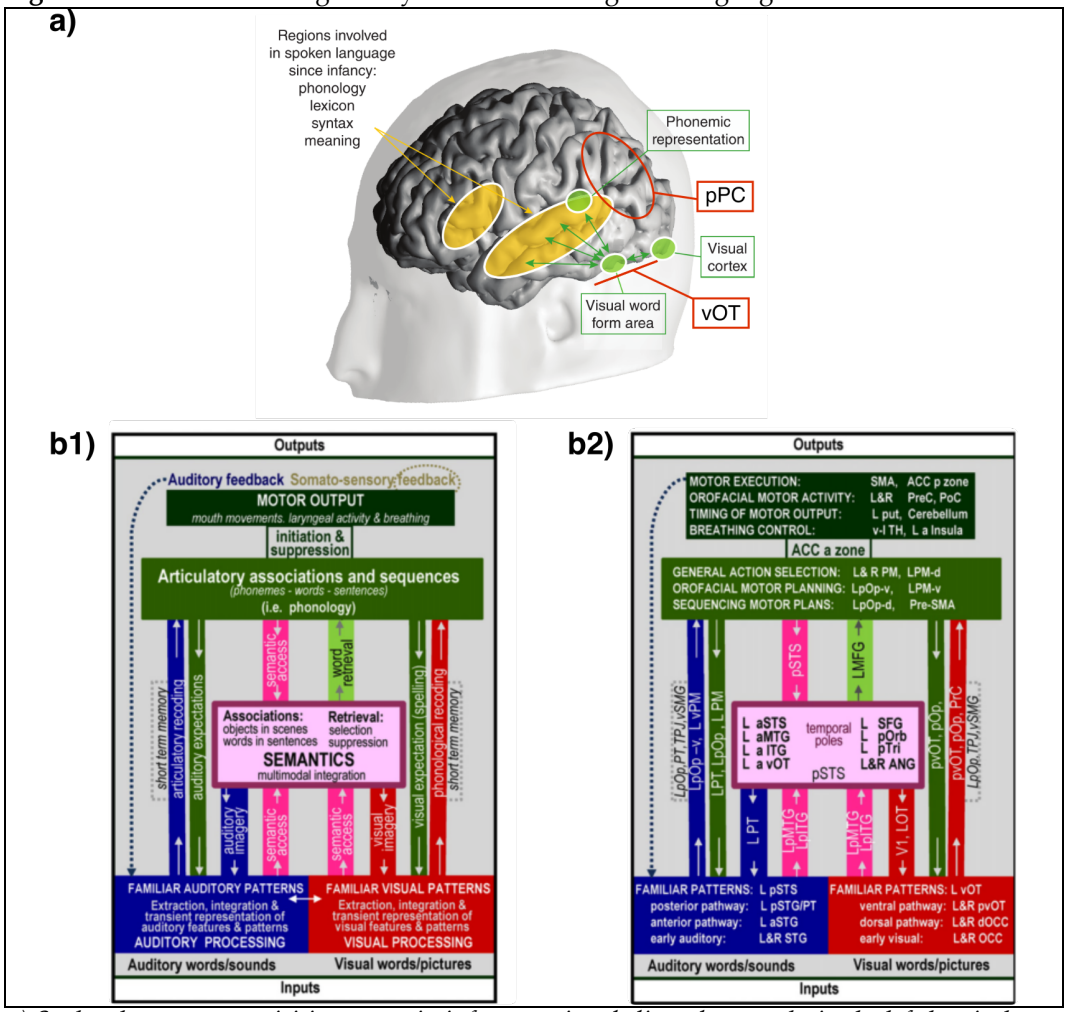

a) Spoken language acquisition starts in infancy, using dedicated networks in the left-hemisphere temporal and inferior frontal regions, and the acquisition of literacy consists in creating a new visual input pathway into this language network. Evidence suggests that the VWFA in the vOT is responsible for this gateway between systems. Images from Dehaene and Dehaene-Lambertz, 2016. b1) Functional and b2) anatomical models based on neuroimaging studies of language. See the role of the vOT as a gateway between vision and semantics. Images from Price, 2012,

If we hear or read a phrase in a known language, there will be some specific point in time when the individual words (*via* speech or print) are recognized and understood. In all language models (see Figure 10*b1/2* for an example), the semantic system that 'understands' the meaning is considered to be unique, and intrinsic to language. If, evolutionarily speaking, speech precedes reading by several thousand years, the neurobiology of reading must be an adaptation during learning that allows reading to be integrated into a speech system that is already in place (e.g., Rueckl et al., 2015). More specifically, contemporary models of reading (Jobard et al., 2003; Pugh et al., 2001) propose that the vOT, located in the ventral pathway, is the gateway from vision to language (although not exclusively, according to Richardson et al., 2011).

5.1.1 Principal theories

More than fifteen years ago Cohen, Dehaene and colleagues (Cohen et al., 2000, 2002) described how vOT regions participate in processing word forms. They proposed naming the word-responsive region within the vOT as the VWFA. While there is agreement that the VWFA is involved in the computations necessary for recognizing words, there is an ongoing theoretical debate between two prominent theories of word recognition: the local combination detector model (e.g., Dehaene et al., 2005; Dehaene and Cohen, 2011) and the interactive account (e.g., Price and Devlin, 2011, 2003). These theories critically differ on the question of whether word processing in the vOT is supported by rapid, automatic feedback from higher-order language areas.

The proponents of the local combination detector model (Dehaene and Cohen, 2011) argue that the visual stimulus feeds into the lexical level hierarchically, and that the orthographic representations feed into higher-level linguistic representations in a bottom-up manner. More specifically, the vOT would contain neurons sensitive to bigrams and the VWFA would process pre-lexical word abstractions. In contrast, the interactive account (Kronbichler et al., 2004; Price and Devlin, 2011) argues that there is a strong top-down influence from higher-level linguistic information on visual orthographic processing. One of the first studies refuting the pre-lexical hypothesis showed that VWFA activation is dependent on word frequency (Kronbichler et al., 2004), with more recent research reaching the same conclusion (Schuster et al., 2016; Yarkoni et al., 2008).

These studies, performed with fMRI, lacked sufficient temporal resolution to check whether different processes might occur in the same location but at different moments in time. A recent intracranial electrocorticography study, with very high temporal and spatial resolution (Hirshorn et al., 2016), supports both the pre-lexical and lexical theoretical accounts. Hirshorn et al.'s (2016) study showed that activity in the VWFA goes through multiple temporal stages of processing: early activity (from approximately 100-250ms after being presented with a word) is consistent with a pre-lexical representation of words, and later activity (from approximately 300-500ms) is consistent with a lexical representation.

In addition to the temporal differentiation, there is evidence for spatial differentiation as well. Price (2012) summarized: *"There is no doubt that an extensive region of the ventral occipitotemporal cortex is involved in skilled*

reading. Within this region, posterior areas are involved in visual feature extraction and more anterior areas are involved in lexico-semantic processing of the whole word. How the response properties in this system differ for written words and other stimuli is still a matter of debate" (p. 836). The need to assign different functionalities to different parts of the left vOT has also been highlighted by many other researchers (e.g., Cohen and Dehaene, 2004)

Another topic of discussion relates to the exclusivity of this region. Although there is agreement in regard to vOT involvement in different object recognition and categorization processes, some authors propose that there is an area with some form of neuronal 'recycling' and exclusivity for word recognition (Cohen and Dehaene, 2004). In contrast, others believe that there is no specialization for words and that the area is used for other high frequency types of visual stimuli as well (Devlin et al., 2006; Vogel et al., 2012b).

In sum, the debate can be summarized thus: is there an area in the vOT that deserves the name of visual word form area? If the answer is 'yes', that would mean that this area supports the representation of orthographic knowledge about graphemes, their combinatorial statistics, orthographic similarities between words, and word identity (Vinckier et al., 2007). If not, it would mean that this area has receptive properties tuned for general visual analysis, and that lexical knowledge emerges due to interactions with the spoken language network (Hirshorn et al., 2016; Price and Devlin, 2011).

5.1.2 Experimental designs used to examine the role of the vOT

A review of research that focuses on localizing VWFA using fMRI yields a surprising observation: different laboratories have used different functional contrasts, languages (transparent and opaque languages, including various writing systems, such as Japanese kanji) and different tasks to potentially identify, the same region dedicated to the visual recognition of words (the putative VWFA). The fMRI contrasts used can be as varied as words *versus* checkerboards (Bouhali et al., 2014; Cohen et al., 2002; Purcell et al., 2017), words *versus* consonant strings (Cohen et al., 2002; Devlin et al., 2006; Thesen et al., 2012), words *versus* false fonts (Olulade et al., 2015; Woodhead et al., 2011), words *versus* line drawings (Baker et al., 2007; Bruno et al., 2008), words *versus* phase-scrambled words (Ben-Shachar et al., 2011, 2007; Rauschecker et al., 2012; Wang et al., 2014; Yeatman et al., 2014b, 2013), words *versus* pseudowords (Boukrina et al., 2013; Graves et al., 2010; Kronbichler et al., 2004), or the most common contrast: words *versus* null/fixation (Cohen et al., 2008, 2000, Dehaene et al., 2010, 2002; Duncan et al., 2009; Glezer et al., 2016, 2015, 2009; Glezer and Riesenhuber, 2013; Longcamp et al., 2011; Twomey et al., 2011; Wang et al., 2014; Wright et al., 2008).

Furthermore, there is evidence of task effects in the activation of the vOT (Kay and Yeatman, 2017; Oliver et al., 2016; Vogel et al., 2012a), and again, across the literature we found many different tasks were used in the experimental designs for studies focused on the vOT. For example, some of the implemented tasks were visual lexical decision tasks (Boukrina et al., 2013; Cohen et al., 2000; Kronbichler et al., 2007; Twomey et al., 2011), phonological lexical decision tasks (Bruno et al., 2008; Kronbichler et al.,

2004; Schurz et al., 2010), n-back tasks (Baker et al., 2007; Dehaene et al., 2002; Duncan et al., 2009; James et al., 2005; Nestor et al., 2013; Wright et al., 2008), perceptual tasks (Ben-Shachar et al., 2011, 2007; Binder et al., 2006; Blackburne et al., 2014; Glezer et al., 2016, 2015, 2009; Glezer and Riesenhuber, 2013; Rauschecker et al., 2012; Vogel et al., 2012b; Yeatman et al., 2014b, 2013), reading aloud (Szwed et al., 2011), semantic judgments (Cohen et al., 2008; Glezer et al., 2009; Thesen et al., 2012; Wang et al., 2014; Wright et al., 2008), or no task at all or passive reading (Cohen et al., 2002; Longcamp et al., 2011; Mano et al., 2013; Woodhead et al., 2011). Some of the functional differences reported could also be due to the different rates of stimuli presentation, as different types of stimuli (such as words or false fonts) have different processing requirements (Vogel et al., 2012b). Interestingly, there is a pattern present in the literature where studies using low-level reading tasks (e.g., passive silent reading; Cohen et al., 2002; Dehaene et al., 2010; Pegado et al., 2011) align with the local combination detector model, supporting the prelexical computational role of the vOT. By contrast, studies using high-level reading tasks (e.g., lexical decision; Seghier and Price, 2013; Twomey et al., 2011; Woollams et al., 2011), favor an interactive account of the vOT.

Even using exactly the same localizer/contrast/task it is difficult to unequivocally identify the same functional area across subjects due to individual variability both in different activation patterns and different brain shapes (Glezer and Riesenhuber, 2013). It is not surprising, then, to find that in previous research different topographical positions for supposedly the same functional cortical area have been consistently reported.

Along this line, several authors have acknowledged the existence of a posterior-anterior distinction in VWFA function (Cohen and Dehaene, 2004; Vogel et al., 2012b; Xue and Poldrack, 2007). Depending on the anterior-posterior position specified, Xue and Poldrack (2007) review various models which suggest different functions: visuo-perceptual *versus* lexico-semantic (Simons et al., 2003), unimodal *versus* multimodal (Cohen et al., 2004), and specialization for local combination *versus* larger fragments of words (Cohen and Dehaene, 2004; Dehaene et al., 2005) . Based on those studies, coordinates have been proposed for a number of VWFA components distributed along the y-axis (Cohen and Dehaene, 2004; Vogel et al., 2012b): anterior VWFA (aVWFA; Talairach: –43, –48, –12; MNI152: –45, –51, –12), classical VWFA (cVWFA; Talairach: –43, –54, –12; MNI152: –45, –57, –12), and posterior VWFAs (pVWFA; Talairach: –43, –68, –12; MNI152: –45, –72, –10).

What seems to be clear is that various subregions of the VWFA are sensitive to different contrasts. If distinct areas show separate response profiles for different contrasts, one can assume that they are responsible for different computations in the visual word recognition process. For example, it has been proposed that one should use word *versus* object stimuli to detect the anterior VWFA (Price and Devlin, 2003); and words versus visually matched non-words (consonant strings, false fonts) to detect the middle and posterior VWFA, although mixed results have been reported using this strategy (Ben-Shachar et al., 2007; James et al., 2005; Xue et al., 2006). Although this selectivity is well known, in most experiments the VWFA is still treated as a single location within the vOT,

and the motivations for selecting one or another localizer are not usually specified.

Along these lines, discussions regarding the location of the VWFA have also been linked to one of the central theoretical discussions: whether or not the VWFA is strictly involved in visual word form processing. According to Büchel et al. (1998), words in non-visual modalities have yielded more anterior activations (average Talairach y = -43) than those typical of the VWFA (average Talairach y = -60). Furthermore, the anterior activations were sensitive to the semantic demands of the task, whereas the posterior activations were not modulated by reading demands even in the case of reading pseudo-words *versus* random letter strings. Thus, Cohen and Dehaene (2004) suggested that the VWFA must be differentiated from anterior vOT regions which are increasingly cross-modal and are more engaged in semantic processing.

It is worth noting that reviewing the experimental designs used in previous studies to examine the role of the vOT gets even more complicated. Most researchers tend to use independent localizers to identify the VWFA and then this region(s) are used to examine functional activation related to a specific task. Acknowledging this issue, several studies have centered on methods to improve the localization of the VWFA. For example, one study checked the consistency and variability of different functional localizers (Duncan et al., 2009), another study evaluated the individual variability of these functional localizers, arguing that a group analysis might exclude some effects (Glezer and Riesenhuber, 2013), and two methodological papers have proposed methods to define

language specific functional ROIs in individual space (Fedorenko et al., 2010; Julian et al., 2012).

In sum, it seems that the heterogeneity of methods previously employed is related to central theoretical discrepancies regarding the role of the vOT in visual word recognition. Further and more refined work is required to integrate all of these previous findings and theoretical proposals, and new studies are required to improve the spatial and temporal location of the putative VWFA(s).

5.2 Posterior parietal cortex (pPC)

Another important part of the reading system related to the vOT is located near the angular gyrus (AG) and the intraparietal sulcus (IPS) in the pPC. The AG is sometimes referred to as temporo-parieto-occipital cortex in the language and reading literature (Seghier, 2013), indicating its anatomical location at the junction of the occipital, temporal and parietal lobes (see Figure 11). It is probably not accidental then that the AG is considered an important intermodal interface (Binder et al., 2009), as confirmed by studies associating it with semantic processing, word reading and comprehension, number processing, the default mode network, memory retrieval, attention and spatial cognition, reasoning and social cognition (Seghier, 2013).

Figure 11. pPC

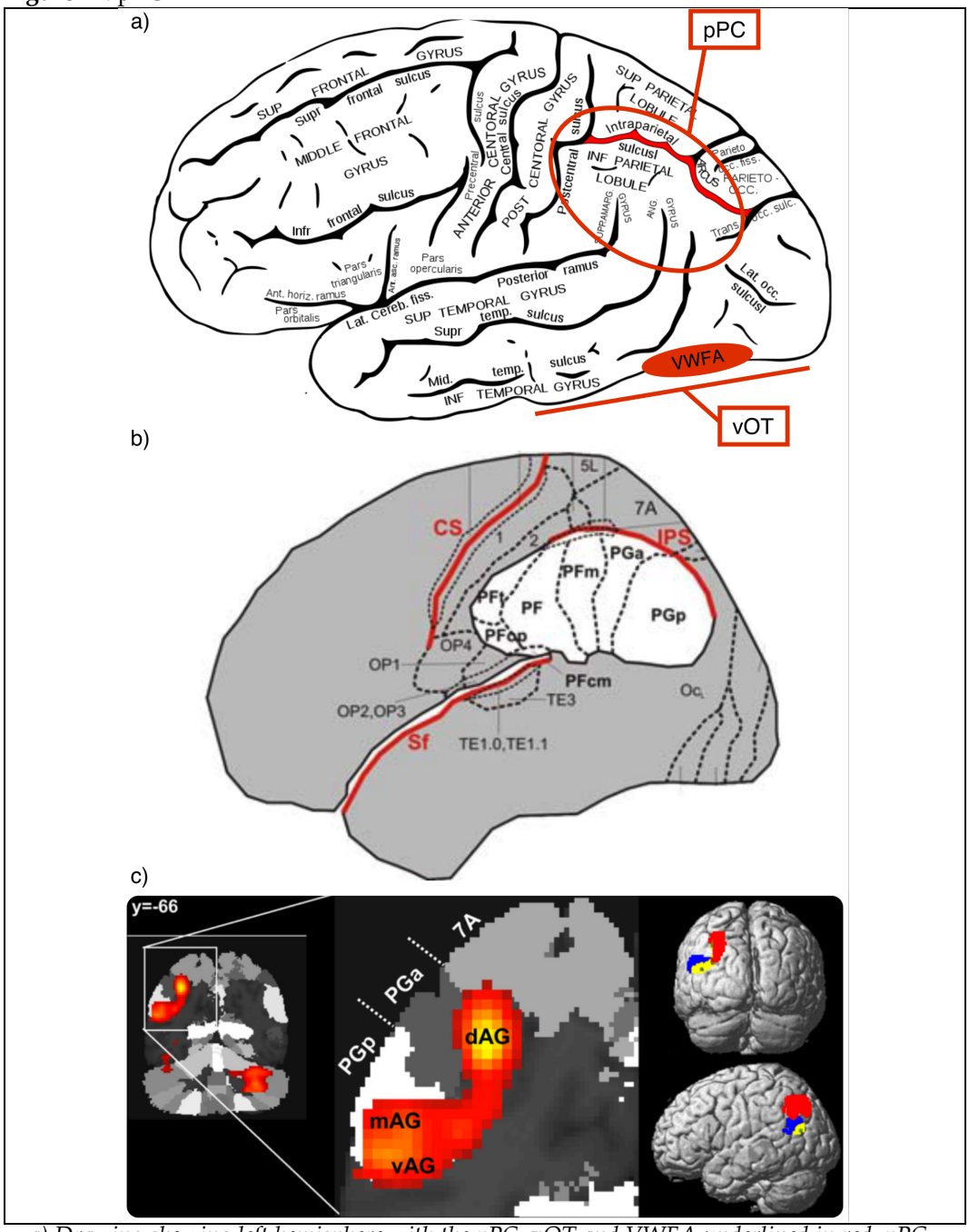

a) Drawing showing left hemisphere with the pPC, vOT and VWFA underlined in red. pPC includes the supramarginal gyrus, angular gyrus and the intraparietal sulcus. Image from Wikipedia. b) Schematic drawing of a lateral view of inferior parietal lobule areas as provided by the parcellation in Caspers et al. (2006). Notice the IPS in red. Image from Caspers et al., 2008. c) Subdivision of the AG in dorsal, medial and ventral regions with a fMRI experiment: the extent of the semantic activation in the left AG overlapped on the probabilistic cytoarchitechtonic rendering (coronal view at y=-66, with a zoom on the left AG). Image from Seghier et al., 2010

It is worth noting that the AG is not a single region with homogeneous anatomical and functional properties, and that there is large variability across studies in terms of the localization of activations in this region. This variability has been the origin of previous anatomical, connectivity, or

functional parcellation proposals focused on the AG. Anatomically, the rostral PGa and the caudal PGp (PG is one of the cytoarchitectonic parietal regions defined by von Economo and Koskinas, 1925) are the most consistent cytoarchitechtonic subdivisions of the AG, with high consistency across subjects (Caspers et al., 2013, 2008, 2006): results for both functional and structural connectivity studies similarly locate PGa and PGp subdivisions (Uddin et al., 2010). Functionally, these subdivisions are related to the type of task the AG is involved in. For example, using a written semantic decision task, Seghier et al.'s (2010) study showed a reliable intersection between the semantic network and the default network in the AG. They created 3 subdivisions: the first is located at the site of the overlap between the two networks, and involved in semantic associations regardless of the presence or absence of a stimulus; the second, dorsal to the overlap, is involved in searching for semantics in all visual stimuli; and the third, ventral to the overlap, is involved in the conceptual identification of visual inputs.

Specifically, the study of AG contributions to language has an extensive tradition, since it was first associated with word processing by Dejerine (1891) and also popularized by the language models of Geschwind (1970). According to Seghier (2013), *"what emerges from this large literature is that the AG engages in reading when semantic associations are made, an involvement that is particularly enhanced during sentence reading and more generally in comprehension of speech and written language"* (p. 49). Furthermore, semantic processing is the most consistent function attributed to the AG (Binder et al., 2009), and the AG has been shown to be part of a pathway that relies on phonology to decode visual word forms (Schlaggar and McCandliss,

2007). As part of the dorsal pathway, the AG typically shows stronger activation for reading pseudowords and low-frequency words compared to high frequency words (Borowsky and Besner, 2006; Mechelli et al., 2003; Tagamets et al., 2000), reflecting the demands on accessing phonology from sublexical orthographic codes (Carreiras et al., 2014; Price, 2012).

Finally, the AG is one of the major functional and structural hubs, linking different subsystems functionally (Tomasi and Volkow, 2011), and enervated by several main WM tracts, such as the superior longitudinal fasciculus, middle longitudinal fasciculus, inferior longitudinal fascicle, occipitofrontal fascicle, and inferior longitudinal fascicle (Seghier, 2013). Importantly, it was suggested that the AG can also be reached by the vOF (Yeatman et al., 2013).

Another interesting region in the pPC is the intraparietal sulcus (iPS), which delimits the angular and supramarginal gyrus medially (see Figure 11*a*-*b*). Topographically, the iPS has been organized into 6 different areas, denominated numerically from IPS0 to IPS5. The first one, IPS0, is contiguous ventrally to the visual cortex region V3a, and the rest are organized along the ventroposterior-dorsalanterior axis (Konen and Kastner, 2008; Wang et al., 2015). It has been shown that the iPS plays a key role in controlling spatial attention (Lauritzen et al., 2009; Saalmann et al., 2007), although Kay and Yeatman (2016) extended this hypothesis suggesting that the iPS is the region that induces task sensitivity in the VWFA as well (they claim that responses in the iPS predict the top-down enhancement of VWFA responses). In this vein, Vogel et al. (2012a) and

Zhou et al. (2016) showed that the VWFA is functionally connected to the iPS, and forms part of the dorsal attention network, suggesting that top-down effects from the IPS to the VWFA play an important role in text reading. Furthermore, regarding structural connectivity, the iPS is of interest because the dorsal endpoints of the vOF terminate in this region as well (Yeatman et al., 2014b). It seems that the vOF plays an important role in linking the ventral part of the vOT with the dorsal occipital cortex and pPC.

To conclude this section, it is worth mentioning that Pugh and colleagues (Pugh et al., 2001) introduced an interesting hypothesis concerning the relationship between the pPC and VWFA. They proposed that the apparent specialization of the VWFA arises because of a 'teaching signal' that is delivered from the pPC to vOT cortex. Studies comparing adult and children suggest that the size of the teaching signal varies with skill and experience (Church et al., 2011) and task demands (Kay and Yeatman, 2017). An alternative hypothesis is that the pPC supervises the vOT reading pathways in the event that word forms are degraded by being presented in unfamiliar orientations or spacing (Cohen et al., 2008; Dehaene et al., 2010), an hypothesis that was supported by transcranial magnetic stimulation showing that pPC stimulation increases sensitivity to signals initiated in the visual cortex (Silvanto et al., 2009).

5.3 IFG

According to the dual-stream hypothesis, the dorsal and ventral streams start in the visual cortex and join again in the IFG. Classically (Brodmann, 1909; Vogt, 1910), this region was divided into three different parts: two in

the anterior part at the ventral pathway named *pars orbitalis* and *pars triangularis*, and one in the posterior part at the dorsal pathway, named *pars opercularis*. These subdivisions were based on cellular and neuroanatomical studies. Brodmann proposed a categorization of IFG subregions based on cytoarchitechtonic differentiation. Vogt incorporated the distribution and amount of intracortical myelinated fibers, and other neuroanatomists have proposed similar parcellations of the IFG (see Amunts and Zilles, 2012 for a review and Figure 12*a* for Brodmann's proposal). Using modern techniques such as in vitro receptor autoradiography, more subdivisions have been proposed based on the regional distribution of transmitter receptors, since receptor distribution has proved to be a powerful indicator of functional diversity (Amunts et al., 2010; Figure 12*b*).

Figure 12. Classical and modern subdivisions of the IFG

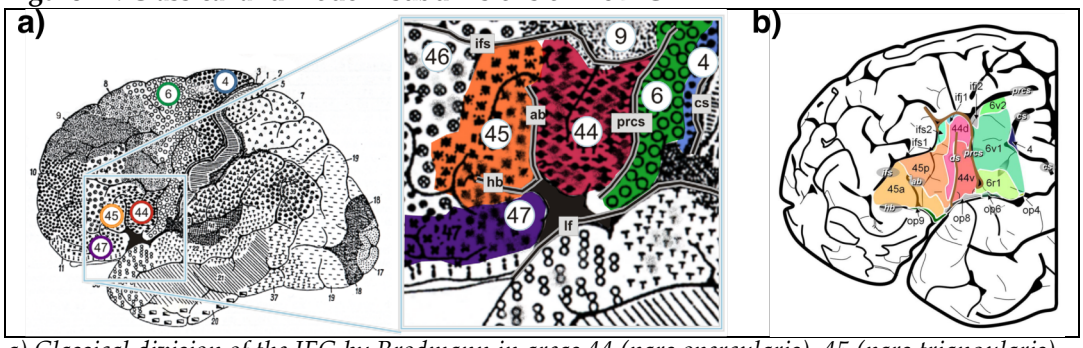

a) Classical division of the IFG by Brodmann in areas 44 (pars opercularis), 45 (pars triangularis), and 47 (pars orbitalis), and b) modern subdivisions based on the regional distribution of transmitter receptors. Images from Amunts et al., 2010

Neuroimaging studies on reading have also found a differential functional involvement of anterior and posterior IFG regions (Price, 2012; Uddén and Bahlmann, 2012), showing that the modulation of the ventral and dorsal pathways depends on the reading demands imposed by task and stimuli. Stronger posterior IFG engagement is typically found when stronger phonological demands are required by the task (Poldrack et al., 1999), and

stronger anterior IFG activation is typically found in studies using semantic reading tasks and when word retrieval during the reading task is semantically demanding, such as retrieving narratives (Badre and Wagner, 2002; Wagner et al., 2001). Furthermore, Vinckier et al.'s (2007) study found an activation gradient along the x-axis in the IFG, somehow analogous to the hierarchical coding of letter strings they found in the y-axis of the vOT.

Although reading starts in the visual cortex, there is evidence of early feedback from the IFG to the vOT during word recognition as well (Woodhead et al., 2014). The MEG literature on word processing shows evidence of a posterior to anterior timing, with occipital cortex activated first at 100-130ms, and (moving forward along the ventral stream) the vOT activated next at 150-170ms, and third sustained activity in the temporal and IFG cortex from around 200ms onwards (Cornelissen et al., 2009; Marinkovic et al., 2003; Pylkkänen and McElree, 2007; Tarkiainen et al., 1999; Vartiainen et al., 2009; Wheat et al., 2010). However, some studies have reported an early response in the IFG at approximately 130 ms as well, preceding activation in the vOT (Cornelissen et al., 2009; Pammer et al., 2004; Wheat et al., 2010). These reports are consistent with other findings regarding the top-down facilitation of visual recognition performed by the orbitofrontal/*pars orbitalis* cortex (Bar et al., 2006). In a dynamic causal modelling experiment with MEG, Woodhead et al. (2014) showed that the IFG modulates vOT in the early stages of word processing, and showed a preference for words over false fonts. Furthermore, in a fMRI experiment, Olulade et al. (2015) showed functional connectivity between the IFG and the anterior VWFA in the

vOT (see also Mechelli et al., 2005; Oliver et al., 2016). These results suggest that the phonological remapping required for articulation is subserved by the IFG and that it likely involves constant access to orthographic representations established in the vOT. In this vein, Mechelli et al.'s (2005) study subdivided the vOT into anterior, middle and posterior locations, and found, in a dynamic causal modelling experiment, that only the anterior *pars triangularis* and anterior vOT showed significant forward connections, providing additional evidence for functional connections between the IFG and vOT that are modulated based on location, task and stimulus type. The control group in a functional connectivity experiment with dyslexic children (van der Mark et al., 2011) showed the same effect, with a seed located in the VWFA (defined as MNI -42, -54, -17). Furthermore, structural connectivity between the vOT and the anterior brain regions (that might reach the IFG) through the inferior fronto-occipito fasciculus (iFOF) and inferior longitudinal fasciculus (iLF) has also been reported (Yeatman et al., 2013).

On the other hand, although the vOT, pPC and the IFG are the areas specifically related to the hypothesis of this thesis, it is also important to mention the posterior MTG/STG because of its role in language and its contribution to the dorsal reading network. The MTG is located in the temporal lobe between the superior temporal (above) and inferior temporal (below) sulci, going along the anterior to posterior axis laterally. As has happened with other cortical areas, the MTG has been associated with many different functions. Regarding language, it seems that it is the posterior MTG that is mostly involved in accessing semantics: the posterior MTG would be linked with the *pars opercularis* through the

posterior STG, as part of the dorsal pathway model of reading (Acheson and Hagoort, 2013; Friederici, 2012).

5.4 Connectivity and integration

The existence of two different routes in reading (a ventral lexico-semantic route and a dorsal route linking orthography and phonology) is supported by a large number of functional studies and metanalytic reviews (Jobard et al., 2003; Oliver et al., 2017; Richardson et al., 2011; Schurz et al., 2010). However, considering that brain structure supports function, understanding the structural organization is critical for the study of functional activation. Research evidence from studies using DWI have shown that structural connections between temporal and frontal regions are mediated by different ventral and dorsal fiber tracts, in line with the dual-stream hypothesis (Friederici, 2012; Saur et al., 2008). For instance, Saur et al.'s (2008) study showed that within the dorsal pathway, there was WM connectivity going from the temporal lobe to the premotor cortex and afterwards to the *pars opercularis* via the arcuate and superior longitudinal fascicle, supporting sensory-motor mapping of sound-to-articulation. Sound-to-meaning mapping, in contrast, appears to be supported by the extreme fiber capsule system (EFCS), connecting the temporal cortex with the *pars triangularis* and *orbitalis* along the ventral pathway. These structural findings suggest that the different types of decoding required during the reading process found in fMRI studies are also supported by DWI evidence.

Later studies have shown that the development of WM connectivity parallels reading acquisition in children, and is predictive of future

reading performance (Yeatman et al., 2013, 2012a). Furthermore, it has been shown that WM tract structure changes in adult illiterates once they learn to read for the first time (Thiebaut de Schotten et al., 2012), adding evidence to the importance of these tracts for language.

Additionally, regarding the starting point of the arcuate fasciculus in the vOT, there is an ongoing discussion in the literature about the VWFA and the posterior arcuate fasciculus. Some authors have reported that the VWFA is enervated by the arcuate fasciculus, or at least by the posterior part of it (Bouhali et al., 2014). Others, in contrast, have reported that they were not able to identify such a connection (Wandell et al., 2012). Lately there have been claims that a newly 'rediscovered' tract, the vOF, terminates in the VWFA (Weiner et al., 2016b; Yeatman et al., 2014b; see Figure 13) and connects it to the IPS in the pPC (Kay and Yeatman, 2017). In an interesting post-mortem single case study, Greenblatt (1973) reported that damage to a tract that corresponds to the modern definition of the vOF results in pure alexia, also called alexia without agraphia or word blindness. He suggested that damage affecting either the AG or the visual cortices, or the circuitry carrying signals between them (allegedly the vOF), may result in the letter-by-letter reading typically present in individuals with alexia.

Figure 13. WM tracts involved in reading

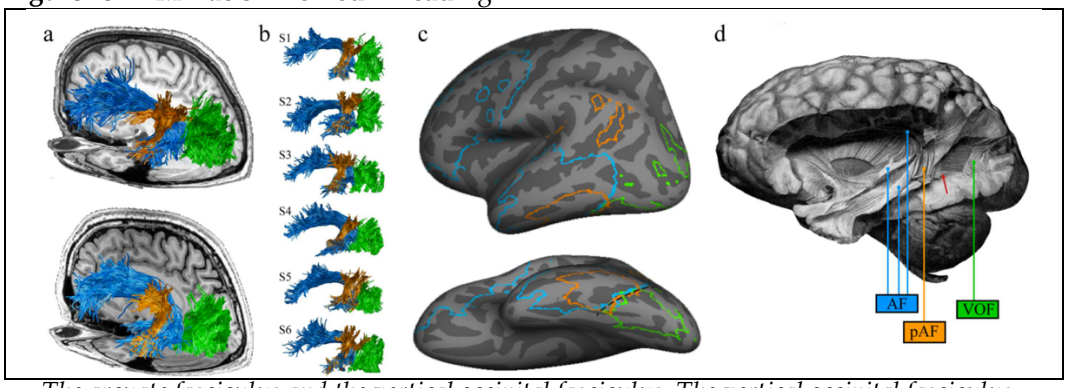

The arcuate fasciculus and the vertical occipital fasciculus. The vertical occipital fasciculus (VOF; green), the arcuate fasciculus (AF; blue) and the posterior segment of the arcuate fasciculus (pAF; orange) are shown in living and postmortem human brains. a) The VOF, AF, and pAF are shown for two representative subjects against the background of their T1-weighted anatomy. b) Renderings of the VOF, AF, and pAF for six additional subjects to illustrate variability. For some subjects, there is a clear separation between the pAF and VOF (S1 and S2), while for others, there is no sharp boundary between the VOF and the pAF (S4 and S5). c) Cortical endpoints for these three pathways were defined for 37 subjects. Cortical alignment was used to transform each individual's endpoint map to the FreeSurfer average template (www.freesurfer.net), and regions with consistent, intersubject overlap are shown for each pathway. Outlined cortical extents indicate locations in which the AF, pAF, or VOF terminated in more than 10 subjects. The black dashed line highlights the cortical location where the three pathways converge (posterior occipitotemporal sulcus extending into the lateral fusiform gyrus). Images from Weiner et al., 2016b.

The posterior portion of the arcuate fasciculus has terminations on the vOT surface that are slightly anterior to the vOF and that project to the supramarginal/angular gyri. Recent evidence (Yeatman et al., 2014b, 2013; own data) suggests that the supramarginal and angular gyri might be if not directly connected, a few centimeters anterior to the dorsal vOF projections (communication over this distance could be managed by the U-fiber system). Furthermore, it is known that the pPC is anatomically linked to the IFG (Kucyi et al., 2012).

The connectivity pattern of the vOT described in this section is in accordance with the connectivity bias hypothesis (Hannagan et al., 2015). This hypothesis proposes that the VWFA owes its properties to constraints arising from its connectivity with other brain areas. Bouhali et al. (2014) showed in a structural connectivity study with adults that the connectivity bias hypothesis was consistent: the VWFA preferentially

connected to the left-hemisphere lateral temporal and inferior frontal areas where language processing is often found. In a similar vein, Fan et al.'s (2014) study showed the existence of a differential connectivity gradient along the anterior-posterior axis of the vOT and, furthermore, they showed that this connectivity pattern could distinguish between typical and atypical readers, stressing the importance of these WM tracts for skilled reading. Nevertheless, brain connectivity effects found in readers could be the outcome of learning to read, instead of its precursor. To test the hypothesis that the VWFA owes its specialization to a pre-existing connectivity pattern, Saygin et al. (2016) measured brain connectivity in children before and after they learned to read. They showed that the connections that were already in place in pre-readers could be used to anticipate where the VWFA would appear once they learned to read.

As a side note, I would like to mention the increasing number of published neuroimaging studies in the visual word processing research arena. However, in order to further contribute to the field, it is important that future studies on this topic integrate indexes from multiple techniques. Along these lines, recent studies have combined MEG, CT and DWI (Kemmotsu et al., 2012), cytoarchitecture and qMRI data combined with behavioral and functional activations (Gomez et al., 2017; Weiner et al., 2016a), and studies including more sophisticated statistical techniques such as SEM linking CT, fMRI and behavioral data (Wendelken et al., 2011). The present doctoral dissertation employs functional and structural indexes combined with sophisticated statistical techniques to try to further elucidate the mechanism(s) that facilitate visual word recognition and

advance our knowledge of the interactions between structure and function underpinning reading behavior.

To conclude, I would like to highlight the importance of understanding visual word recognition using a multimodal and integrative approach that allows us to develop more refined and precise models of reading. If we are able to create models that link the neuroimaging results to individual behavior, it will be possible to create a baseline model and a database of typical reader behavior, characterized by a parameter range of functional and structural data. This would not only satisfy purely scientific interest by contributing to an old theoretical debate, but can crucially contribute to a better understanding of the overall brain function, and improve diagnosis and treatment for atypical readers.

6 HYPOTHESES

In this chapter, I introduce the main scientific questions that motivated this doctoral dissertation based on the previous literature review. The chapter is organized into three sections corresponding to the three main hypotheses. Each hypothesis is tested in an independent experiment, and therefore, the next three chapters correspond to the three specific (but related) experiments carried out to test our predictions.

The three hypotheses revolve around the idea of characterizing the vOT and associated regions in visual word recognition. Although it is clear that there is a word responsive region in the vOT (Baker et al., 2007; Price, 2012), many questions remain unanswered. Reading is such a complex process that it can be studied from many different perspectives. Even methodologically, there are a large number of decisions to make and the techniques used by cognitive neuroscientists are in constant evolution. This heterogeneity in terms of perspectives and methods sometimes makes it difficult to integrate results from earlier and more recent studies in order to resolve the mixed findings and inconsistencies in theoretical accounts concerning the involvement of the VWFA in reading i.e.: what specific role does it play? What are the temporal dynamics of its involvement? And, are there different VWFAs within the vOT that deal with the different subprocesses required in reading?

Other authors have expressed similar concerns: "*We conclude that the left occipitotemporal visual word-form area, far from being an homogeneous structure, presents a high degree of functional and spatial hierarchical organization which must result from a tuning process during reading*

acquisition" (Vinckier et al., 2007; p. 143). In line with this complexity, it is possible to find evidence in the literature supporting the claims and implications of either of the two main theoretical accounts: the local combination detector model (e.g., Dehaene et al., 2005; Dehaene and Cohen, 2011) and the interactive account (e.g., Price and Devlin, 2011, 2003).

The experiments reported in this dissertation use a multimodal MRI approach to address these questions. By integrating our findings with relevant information from previous studies and contributing to the development of a coherent theoretical view, I hope this work can serve as the initial scaffolding for more parsimonious models that describe the role of the vOT in reading. In these experiments we develop a series of behavioral, functional, and structural measurements of the cortical regions and connecting white-matter tracts involved in visual word recognition at the subject level.

6.1 Hypothesis 1: Is there more than one VWFA?

Previous evidence strongly supports the idea that visual word recognition involves a cascade of cognitive processes. The light-dark contrasts captured and converted to electrical spikes in the eye's ganglion cells go through the LGN to the visual cortices, and before the visual recognition process is completed, many different language-related cortical areas are involved including vOT, pPC and IFG. This means that various areas perform different sub-processes in interaction with each other, and that the same areas may perform different activities at different moments in time (Hirshorn et al., 2016).

6.1.1 Hypothesis 1.1: Do different functional contrasts localize different cortical areas (or VWFAs) within the vOT?

The literature suggests that the area known as the VWFA is not a fixed cortical region. Depending on the functional contrast used, different areas with different roles have been reported (see Figure 14*a*). Therefore, by carefully selecting the functional contrasts used in a given study, it should be possible to identify different cortical areas which, although all reported in the literature as the 'VWFA', in fact, perform different computational operations with respect to the visual word recognition process.

Beginning with the visual cortex and continuing along the vOT, we find various cortical areas that are sensitive to words (see top black line in Figure 14*b* showing the raw fMRI signal corresponding to real words). For the visual cortex and the first hierarchical steps within the vOT (i.e., more posterior regions), we can assume that similar cortical computations will be carried out whether we show words or pseudowords, since these have visually equivalent shapes (see the second dashed pink line in Figure 14*b)*. Further along the vOT (i.e., in more anterior regions), we expect some differentiation: although words and pseudowords include the same letter shapes and both are pronounceable, the former have meaning while the latter do not. Finally, if we use a highly perceptual stimulus such as a phase-scrambled word with no sharp edges as a contrast, we expect greater differentiation in the visual cortex (see the third dashed red line in Figure 14*b).* In sum, the contrast we obtain for each voxel along the posterior-anterior axis of the vOT (i.e., the arrows in Figure 14*b*) depends on the second term in the functional subtraction.

Figure 14. Hypothesis: influence of the functional contrasts in the VWFA localization

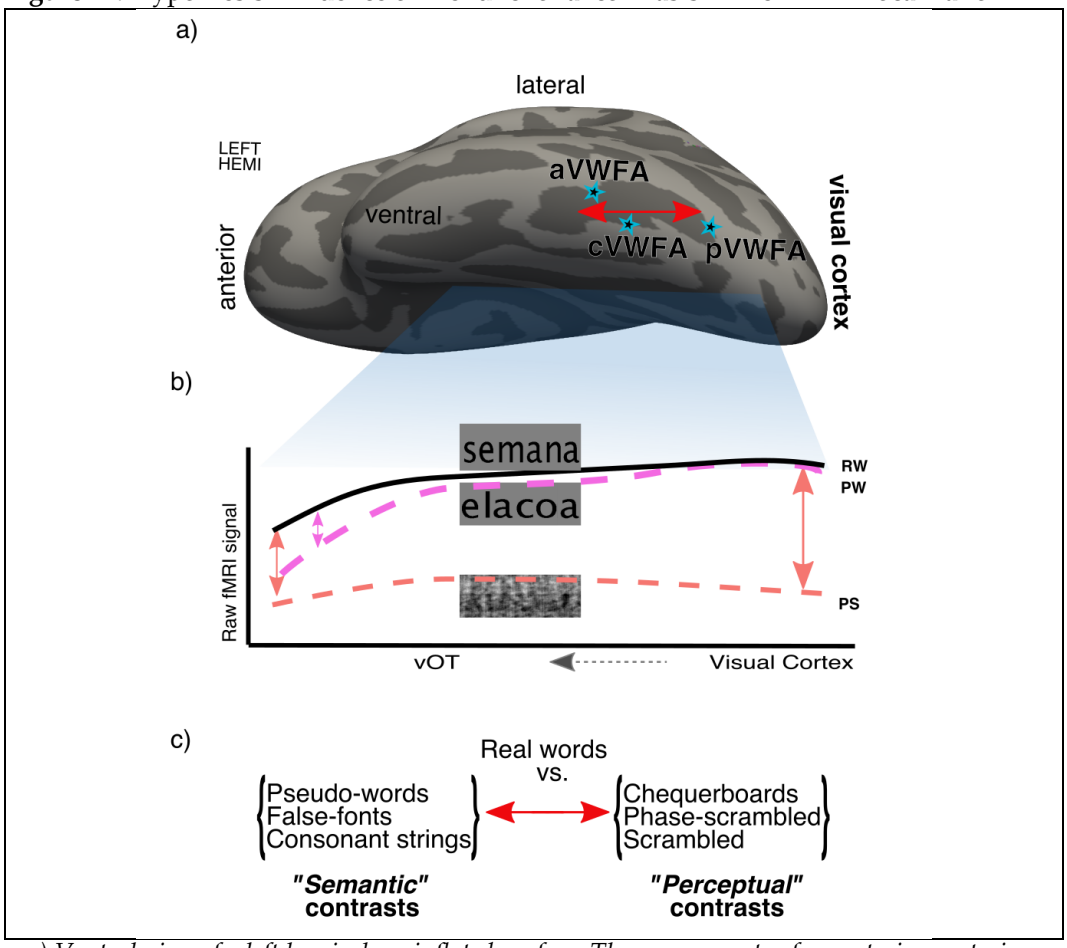

a) Ventral view of a left hemisphere inflated surface. There are reports of an anterior-posterior gradient along the vOT, and claims of differentiated anterior, classical and posterior VWFAs. b) Conceptual drawings of the raw fMRI signals for real words (RW), pseudowords (PW) and phase-scrambled words (PS). Depending on the characteristics of the contrast, and the task of the cortical area, we should be able to identify different cortical locations along the vOT. For example, as a word and a pseudoword are visually equivalent, we should not expect differences in the visual cortices. c) Definition of two types of contrasts, "semantic" contrasts and "perceptual" contrasts: the main component of what is left in the semantic contrasts would be lexico-semantic, the main component of what is left in the perceptual contrasts would be visual letter- and word-form information (on top of the rest of the lexico-semantic and other language information).

We hypothesize that contrasts using word-like stimuli such as pseudowords (PW), false fonts (FF) and consonant strings (CS) will group together and be localized in a different vOT cortical area relative to more visual stimuli such as phase-scrambled words (PS), scrambled words (SD) or chequerboards (CB). This is because subtractions using word-like stimuli remove contributions from the word and letter forms from the visual processing cortex (i.e., PW will remove everything except lexico-semantics, but CS and FF will remove the general letter- and word-form

information leaving the rest of the language information related to the word). We call the first group 'semantic' contrasts because (at least for the pseudo-words) this contrast shows what is left after all the visual, letter- and word-form, orthographical and phonological content has been subtracted from a real word. We call the second group 'perceptual' contrasts because they isolate the signal related to perceptual letter- and word-form information, in top of the rest of the language information present in the other contrasts as well. In short, all six contrasts carry semantic, orthographic and phonological information, but only the perceptual contrasts carry the perceptual letter- and word-form information, since in the semantic contrasts this signal have been removed. Consequently, in addition to the semantic/more anterior and perceptual/more posterior hypothesis, we expect the perceptual contrasts to be more robust and to have higher T values relative to the semantic contrasts.

In sum, out of all possible contrasts that can be computed from the stimuli, we will focus on the main contrasts previously used in the scientific literature. If we consider the real word versus fixation (**RWvsNull**) a special case, we hypothesize that as we have indicated, the selected contrasts will segregate into two groups: 1) *Semantic contrasts* with Real Words versus Pseudo Words (**RWvsPW**), Real Words versus Consonant Strings (**RWvsCS**), and Real Words versus False Fonts (**RWvsFF**), and 2) *Perceptual contrasts* comprising Real Words versus checkerboards (**RWvsCB**), Real Words versus Scrambled Words (**RWvsSD)**, and Real Words versus Phase-Scrambled Words (**RWvsPS**). Moreover, if this hypothesis is confirmed, we predict that the semantic

contrasts should be more anterior than the perceptual contrasts, i.e.: the raw signal related to semantic stimuli will be separable from the raw signal related to real words, and located more anteriorly in the vOT (see Figure 14*b*).

6.1.2 Hypothesis 1.2: Does the localization of the VWFA vary depending on the fMRI design used (block, event-related)?

It is a common practice in the literature to use independent localizers and, then use these localized cortical areas as ROIs in a given fMRI experimental design. Block designs are more commonly used to identify cortical ROIs using independent localizers due to their superior statistical power. Results from these block design localizers are then applied to either block or event-related functional tasks. However, block fMRI designs detect more sustained neuronal activity, and event-related fMRI designs detect more transient activity. Thus, in principle, the same functional contrasts might yield slightly different cortical areas depending on the nature of the fMRI design used to obtain the localizer. Here, using the same stimuli, presentation times and MRI sequences, we will examine whether or not the results obtained from block or event-related fMRI reading localizers differ.

6.1.3 Hypothesis 1.3: Is the functional localization of reading-related regions reliable across time?

Although inter- and intra-subject variability is expected and inherent to neuroimaging techniques, here we aimed to examine to what extent the functional localization of reading related-regions might vary across time when using the same functional localizer. If our first hypothesis is right,

perceptual contrasts will involve cortical regions closer to sensory visual areas and will discern less abstract qualities relative to semantic contrasts. So, we expect perceptual as opposed to semantic functional contrasts to have higher T values and to be more stable in a test-retest examination.

6.1.4 Hypothesis 1.4: Is the location of the different VWFAs associated with the location of the different WM fiber tracts connecting them?

If, as hypothesized, perceptual/semantic contrasts systematically detect differentiated functional areas along the y-axis of vOT, we expect that their pattern of structural connectivity will be different as well. According to the connectivity bias hypothesis (Hannagan et al., 2015), and recent findings with pre-readers (Saygin et al., 2016), the vOT reading regions are where they are because of their predisposition to connect to the rest of the language areas. Furthermore, previous evidence suggests that both the pAF and the vOF are necessary for word reading (Greenblatt, 1973), so I hypothesize that both tracts will be found in association with the different (perceptual and semantic) VWFAs.

This hypothesis is based on previous findings. On the one hand, some studies (especially from Brian Wandell's lab which tends to use the perceptual RWvsPS contrast to identify vOT regions) have defined a WM fiber tract, called the vOF, which innervates posterior vOT regions. On the other hand, based on an examination of findings from other labs, semantic contrasts use the pPC (angular gyrus) to test for word selectivity, and this suggests connectivity supported by a different fiber tract: the posterior arcuate fasciculus (pAF). In Figure 15*a1* we see a more anterior VWFA

(MNI Y = -50) innervated by the *'arcuate posterior segment'* or pAF. Figure 15*a2* shows results from a study that examined structural connectivity for a gradient of ROIs along the longitudinal axis in the vOT. ROI 5 corresponds to the classical VWFA at MNI Y = -58 and shows connectivity with the pPC. In contrast, the more posterior ROI 3 at MNI Y = -75 shows connectivity with the dorsal occipital area, near the iPS, which roughly corresponds to the vOF reported in Figure 15*b1-b2* (both images from studies by Wandell's lab).

Figure 15. Arcuate fasciculus and vertical occipital fasciculus

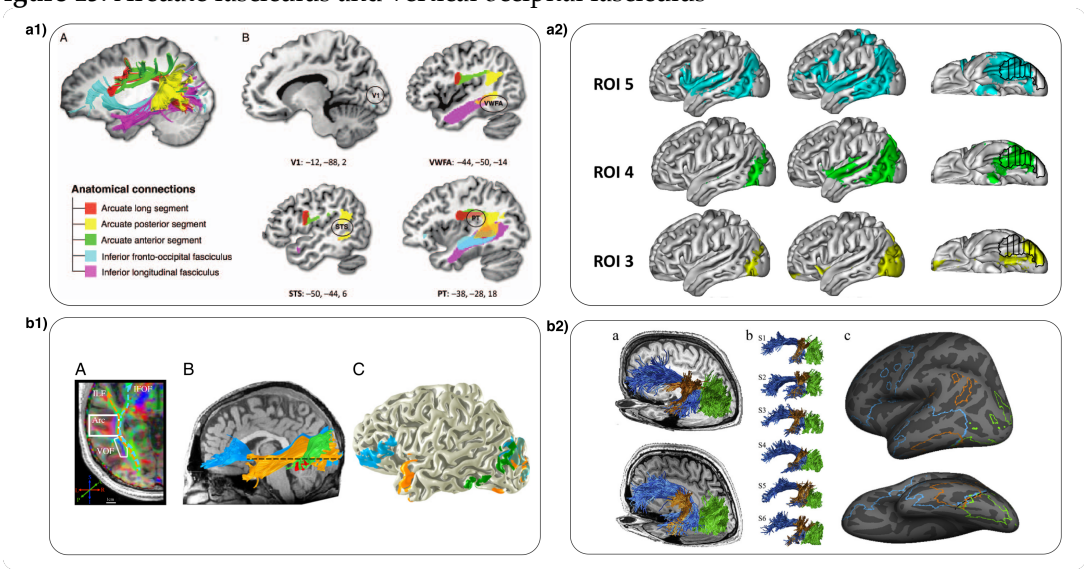

a) VWFA innervated by the posterior arcuate fasciculus: a1) In this case, the VWFA was calculated using letter strings (4 letter long low-case orthographically legal pseudowords) versus chequerboards, was more anterior (-44, -50, -14), and researchers claim the located VWFA region was connected to the posterior arcuate fasciculus. Image from Thiebaut de Schotten et al., 2012; a2) Structural connectivity showing that when seeding the classical VWFA (ROI 5) connectivity goes to the pPC, but when using more posterior ROIs (ROI 3) connectivity stays in the occipital lobe. Image from Bouhali et al., 2014. In contrast, b1) here researchers used the RWvsPS contrast to locate the VWFA, which usually results in a more posterior localization, with no connectivity to the pAF. Image from Yeatman et al., 2014. b2) Image from a recent paper providing a justification for separating the pAF(brown) from the vOF(green) tracts. Image from Weiner et al., 2016.

6.1.5 Hypothesis 1.5: Do separate VWFAs within the vOT make different contributions to reading behavior?

Extensive empirical evidence from studies using lexical decision tasks has shown that typical readers detect high-frequency words more quickly

than pseudowords, but more slowly than consonant strings. It is clear that although these stimuli are similar (letters), the detection of consonant strings is performed perceptually (it is impossible to read and phonetically pronounce them). In contrast, to detect a pseudoword, it is necessary to read the word and access the related phonology to discern whether or not it is a real word. When a high-frequency word is read, familiarity with such words means that both semantic and phonological systems are accessed. We predict that the functional activation of different cortical areas within the vOT, pPC and the IFG will predict individual reading behavior for words and non-words on a lexical decision task that was performed outside of the scanner.

6.2 Hypothesis 2: Does the functional segregation of the vOT extend through the reading network?

This hypothesis is a follow up from the previous set of predictions. According to the dual-stream hypothesis, after the involvement of the visual cortex the word recognition process follows the dorsal and ventral reading streams. If the abovementioned hypotheses for the vOT are correct (meaning that we can segregate the different VWFAs both functionally and structurally), we would expect these differences to be mirrored in other critical regions of the language network that are structurally connected to the vOT, such as the pPC and IFG.

6.2.1 Hypothesis 2.1: Does the pPC segregate semantic and perceptual contrasts?

Another important part of the reading system is located near the AG and iPS in the pPC. Previous empirical evidence suggests that the (anterior)

VWFA and the AG are innervated by the pAF. Meanwhile, the (posterior) VWFA connects to the iPS via the vOF. This suggests that if there are differential activations in the vOT as a function of the semantic versus perceptual nature of the functional contrasts, we should expect that this difference will be also be found in the pPC, and that these differences will possibly be modulated by the various WM fiber tracts innervating pPC regions.

6.2.2 Hypothesis 2.2: Is the pPC associated with reading behavior?

If the previous hypotheses are confirmed, we will find two separate areas located in the pPC: the iPS, related to perceptual contrasts and connected to the vOT via the vOF; and, the AG, related to semantic contrasts and connected to the vOT via the pAF. Here, we will examine if functional activation in these pPC regions predicts reading behavior, based on the hypothesis that the semantic contrasts will predict in the AG while the perceptual contrasts will do so in the iPS.

6.2.3 Hypothesis 2.3: Does the IFG dissociate between semantic and perceptual contrasts?

As reviewed in the previous chapter, there is extensive evidence showing the involvement of the IFG in reading. Specifically, there are reports of gradients analogous to the y–axis in the vOT (Olulade et al., 2015; Vinckier et al., 2007), and reports showing that the anterior part of the IFG is more involved in semantic processing, while the posterior part is more involved in phonological processing. Functional connectivity studies have also shown different patterns of connectivity between anterior and posterior vOT with IFG (Mechelli et al., 2005). Therefore, we expect to

observe differences in the IFG, with the semantic contrasts showing functional activation located anteriorly to the functional activation observed for perceptual contrasts.

6.2.4 Hypothesis 2.4: Is the IFG associated with reading behavior?

If the previous hypotheses are confirmed, semantic vs. perceptual contrasts will enable us to distinguish two separate functional areas in the IFG , one more anterior and one more posterior. As for vOT and pPC, we will examine if functional activation in these areas predicts reading behavior.

6.3 Hypothesis 3: Integration

If the first hypothesis was devoted entirely to the vOT and the second to establishing parallelisms between the vOT and the pPC and IFG, this third hypothesis relates to integration between these three core regions in the reading network.

6.3.1 Hypothesis 3.1: What is the structural connectivity pattern of the three regions? Can we locate vOF and pAF using our functional contrasts?

In Hypothesis 1.4 we expected that the different VWFAs would be associated with the vOF and pAF WM tracts. Here, we extend this hypothesis in two ways by positing that: 1) the rest of the regions functionally identified in the language areas should be structurally connected as well, and we should be able to find these WM tracts systematically, and 2) the new vOF and pAF WM tracts found using

functional ROIs should coincide with the structurally determined vOF and pAF WM tracts identified in Experiment 1.

6.3.2 Hypothesis 3.2: Is functional activation in the main reading regions associated? Does the structure contribute to this association?

We hypothesize that functional activation in the main reading regions in vOT, pPC and IFG will be strongly correlated, and that the WM properties of the tracts connecting these regions can boost this correlation.

6.3.3 Hypothesis 3.3: Does functional activation in various reading regions differently contribute to predicting reading behavior? Does the structure also contribute?

Previously, we hypothesized that functional activation in the core reading regions would predict reading behavior. Here, we intend to integrate these findings and examine if the combined functional activation in these three regions can further explain reading behavior variance. Further, we seek to examine if adding WM microstructure indexes from the tracts connecting cortical regions in the regression model will further increase the percentage of reading behavior variance that can be explained relative to that already explained by functional activation in the three main regions. In this regard, we hypothesize that the inclusion of functional and structural indexes related to the main reading regions will make a meaningful contribution to explaining overall reading behavior, and that the variance explained by these models will be numerically higher for functional indexes based on perceptual contrasts relative to those based on semantic contrasts.

In the following three empirical chapters, we present the three main studies designed to test all of these hypotheses, describing the methods, results and providing specific discussions for the main results found in each experiment. Later, in the general discussion, we will relate the main findings from all of these studies to these three groups of hypotheses.

7 Experiment 1: Multimodal localization of the VWFA(s)

In order to study the variability of VWFA localizations in vOT and their relation to regional WM structure, we conducted an MRI experiment using functional and diffusion-weighted imaging. Our objectives were to investigate: 1) the effect of selecting different contrasts to identify the VWFA; 2) the influence of using two different fMRI designs (i.e., block, event-related); 3) the reliability of the effects across time (test-retest); 4) the relation between the functional and structural results; and, 5) the capacity of the different functional contrasts to predict individual reading behavior.

7.1 Methods

7.1.1 Participants

MRI and behavioral data from 100 sessions were collected at the BCBL's Miramon facilities. Data from 3 sessions were excluded from further analysis due to incidental findings or technical problems with data acquisition. The 97 valid sessions were performed by a total of 66 different participants, of which 31 underwent a second identical session separated by 7-10 days. Therefore, this data was divided into two experiments: the Main experiment and the Test-Retest experiment. For the Main experiment, first day acquisition sessions from the 66 unique participants were used. For the Test-Retest experiment, only those 31 participants that had participated in two acquisition sessions (first and second day) were selected.

All participants were right-handed healthy young adults (age 24.15 ± 3.70 years; 40 females; see Figure 16), with no history of psychiatric, neurological, attention or learning disorders, with normal or corrected-to-normal vision. All of them gave written informed consent in compliance with the ethical regulations established by the BCBL Ethics Committee and the guidelines of the Helsinki Declaration. Furthermore, all the participants were screened to check for outliers in intelligence (using the Kaufman Brief Intelligence Test, second edition; KBIT-2; Kaufman and Kaufman, 1993) and an objective measure of vocabulary which is an adaptation of the Boston Naming Test (Kaplan et al., 1983) that controls for cognates in Spanish, Basque and English. All participants were highly proficient in Spanish.

Figure 16. Age distribution of participants

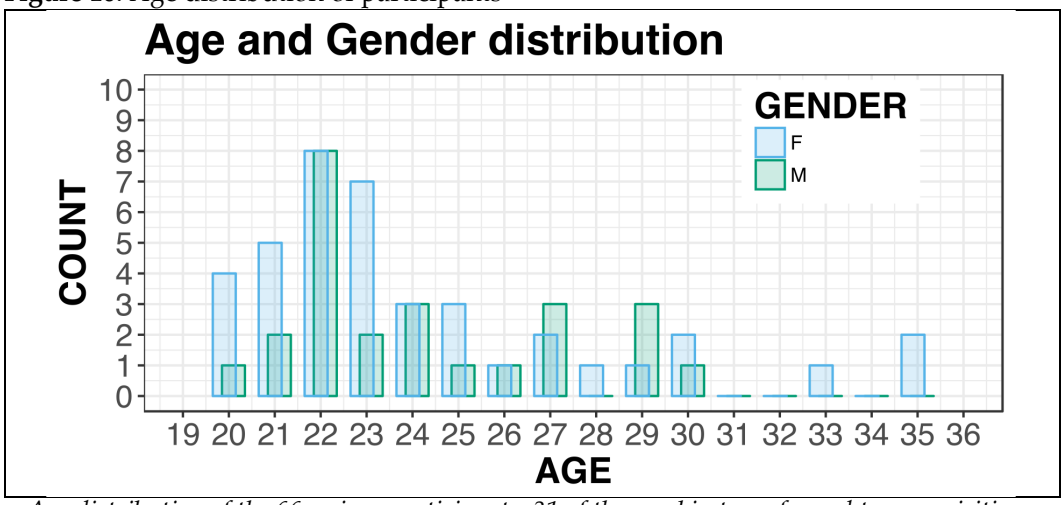

Age distribution of the 66 unique participants. 31 of these subjects performed two acquisition sessions.

7.1.2 Materials and procedures

In all acquisition sessions, two functional localizers where acquired using two different fMRI designs: block and event-related. For both functional localizers the stimuli and the task were the same. The stimuli were organized into eight experimental conditions and one task condition and

were presented in black at the center of the screen against a grey background (RGB = 128, 128, 128; see Figure 17, *i* to *viii*). The task condition (see Figure 17, *t1*) used stimuli from the 8 main conditions. As soon as a black rectangle appeared framing the stimulus participants were instructed to press a button. Two full sets of stimuli were designed, with a total of 80 stimuli per condition per set. These sets were counterbalanced across subjects. Next, we describe the materials used in each of the 8 main experimental conditions:

i. Real Word, High Frequency (RWH): 4-to-6 letter-length Spanish words selected from the EsPal database (Duchon et al., 2013) with frequencies ranging from 50 to 500. Since most of the participants were Spanish-Basque bilinguals, words were checked for cross-language cognates in Basque using the E-Hitz database (Perea et al., 2006). We also used an algorithm for the stochastic optimization of stimuli (SOS; Armstrong et al., 2012) to create two definitive counterbalanced sets of 80-word lists, equating them in terms of frequency, number of letters, bigram frequency, concreteness and number of neighbors.

ii. Real Word, Low Frequency (RWL): the same procedure described for RWH was followed for RWL, with the exception that RWL frequencies were within the .5 and 5 interval. Henceforth, we refer to the combined set of RWH and RWL as Real Words (RW).

iii. Pseudowords (PW): generated using the Wuggy tool (Keuleers and Brysbaert, 2010) on a pool of words comprising 50% randomly selected from RWH and 50% randomly selected from RWL.

iv. Consonant strings (CS): generated by substituting all vowels in the PW with random consonants to equate their length to the other stimuli.

v. Phase scrambled words (PS): generated by shifting the word image in the frequency domain, using the tools provided by the Stanford Vistasoft package (https://github.com/vistalab/vistasoft/wiki) on a pool of words comprising 50% randomly selected from RWH and 50% randomly selected from RWL.

vi. Scrambled words (SD): designed by creating 10 x 10 pixel tiles and mixing them randomly, using words from a pool comprising 50% randomly selected from RWH and 50% randomly selected from RWL.

vii. Checkerboards (CB): consisting of 15 pixel size black and white squares, with a length equated to the length of RW.

viii. False fonts (FF): Georgian was used as the letter system of choice to produce FF, with a letter-by-letter translation. FF were generated using words from a pool comprising 50% randomly selected from RWH and 50% randomly selected from RWL .

Figure 17. Examples of stimuli for the conditions used in the functional localizers

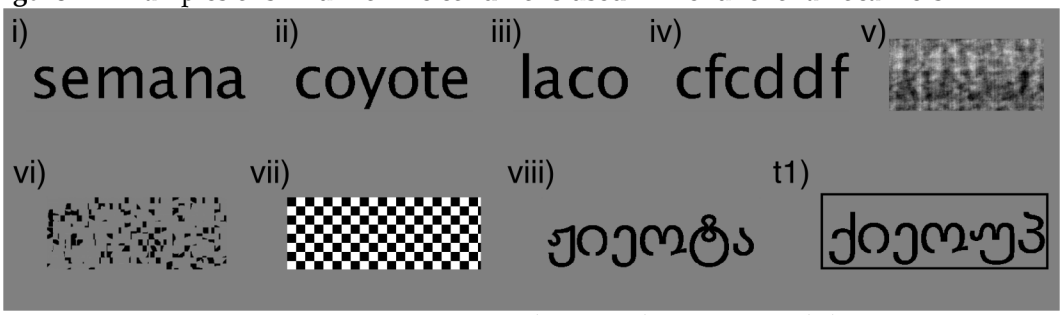

Examples of stimuli for the 8 experimental conditions and the task included in the functional localizers. i) High frequency words (RWH), ii) Low frequency words (RWL), iii) Pseudowords (PW), iv) Consonant strings (CS), v) Phase scrambled words (PS), vi) Scrambled words (SD), vii) Checkerboards (CB), viii) False fonts (FF), t1) Example of task stimuli.

The event-related fMRI design consisted of one functional run. Four consecutive stimuli of the same condition were presented every 2.4 s (the study repetition time, TR), with each item being presented for 400 ms, followed by a 200 ms blank space. Aside from the counterbalancing for the two sets of stimuli (one set used in the localizer inside the scanner, the other set used in the lexical decision task with real words, pseudowords and consonant strings that participants performed outside of the scanner), the order of presentation for the conditions was pseudo-randomized in 9 different orderings based on an algorithm designed to maximize the efficiency of the recovery of the blood oxygen level-dependent (BOLD) response for each condition (Optseq II; Dale, 1999) and to generate inter-trial intervals of variable duration to build an appropriate baseline or null events for the fMRI design (Optseq II; Dale, 1999). Thus, there were a total of 18 different counterbalances (2 sets of materials X 9 orderings) that were randomly assigned to each participant. The Test-Retest group was presented with the same counterbalanced sets and ordering in sessions I and II.

The block fMRI localizer used the same stimuli in two separate functional runs. Each run consisted of 2 activation blocks per condition and fixation

blocks of the same length that were interleaved with activation blocks. Activation blocks lasted 12 s and included 20 stimuli of the same condition each presented for 400 ms and followed by a 200 ms blank space. Thus, four stimuli of the same condition were presented every 2.4 s (study TR), so in total there were the same number of stimuli per condition presented in the block and event-related fMRI localizers. At the end of some blocks (randomized), one or two additional images were added for the task condition (see Figure 17*t1*).

In both block and event-related functional designs, the task consisted in a perceptual task where participants were asked to press a button when a rectangle appeared around a regular stimulus (see Figure 17). These task stimuli were modeled separately in the block and event-related general linear models (GLM), and were not taken into consideration in subsequent analyses. Furthermore, the MRI acquisition sessions were divided into 3 sections (i.e., A, B, C), separated by resting breaks. The order of sections A-B-C was randomized across subjects to control for potential habituation and fatigue effects. For the Test-Retest group, acquisition sessions were separated by 7-10 days to both minimize structural changes and avoid habituation.

Outside the scanner, the following tests were administered to participants: an intelligence test (K-BIT2; Kaufman and Kaufman, 1993), a vocabulary measure which is an adaptation of the Boston Naming Test (Kaplan et al., 1983), and a lexical decision task. The lexical decision task was intended to obtain a behavioral measure of participants' abilities to discern between real words, pseudowords and consonant strings. The stimuli used for the

lexical decision task was the set of stimuli that was not used for the fMRI localizer, and included 120 words, 120 pseudowords and 60 consonant strings.

7.1.3 MRI acquisition

The participants were scanned in a 3T Siemens TRIO whole-body MRI scanner (Siemens Medical Solutions, Erlangen, Germany), using a 32-channel head coil. Headphones (MR Confon) were used to dampen background scanner noise and to enable communication with experimenters while in the scanner. Participants viewed stimuli back-projected onto a screen by a mirror mounted on the head coil. To limit head movement, the area between participants' heads and the coil was padded with foam and participants were asked to remain as still as possible. For the functional tasks, participants were provided with a response pad. For both the block and event-related fMRI designs, images were acquired using the same gradient-echo echo-planar pulse sequence with the following acquisition parameters: TR = 2400 ms, time echo (TE) = 24 ms, 47 contiguous 2.5 mm isotropic axial slices, 10% inter-slice gap, flip angle (FA) = 90º, field of view (FoV) = 200 mm. Prior to each scan, four volumes were discarded to allow for T1-Equilibration effects. For the event-related design, the order of the study conditions and the inter-trial intervals of variable duration corresponding to the MR frames that served as baseline or null events (i.e., a fixation cross presented in the center of the screen, 30% of the total collected functional volumes) were determined with an algorithm designed to maximize the efficiency of the recovery of the BOLD response (Optseq II; Dale, 1999).

Structural T1-weighted images were acquired with a multi-echo (ME) MPRAGE sequence with TE-s = 1.64, 3.5, 5.36, 7.22 ms, TR = 2530 ms, FA = 7º, FoV = 256 mm, 176 slices and voxel size = 1 mm3 (isotropic). Additionally, a T2-weighted image was acquired with TE-s = 425 ms, TR = 3200 ms, FoV= 256 mm, 176 slices and voxel size = 1 mm3 (isotropic).

Diffusion weighted images (DWI) were acquired in 3 different sequences: two with one phase encoding directions (A >> P) and one with 6 *b0*-s using the opposite phase encoding direction (P >> A) to compensate for spatial distortions. These files had a *b* of 1000 s/mm^2 and 35 directions one, and a *b* of 2500 s/mm^2 and 65 directions the other one (both had 5 intercalated *b0*-s). All three files were acquired using the following parameters: TR = 6766 ms, TE = 110 ms, FA = 90º, isotropic 1.8mm voxel size, 78 slices with 0% gap, and were acquired with a multiband acceleration factor of 2.

7.1.4 MRI Data Processing and Analysis

The MRI data processing pipeline includes three main steps with components based on the nature of the data and the tools used to analyze them: 1) T1-weighted image reconstruction, 2) fMRI data analysis, and 3) DWI data analysis.

First, using Vistasoft and a custom Matlab script, all T1-weighted images were aligned along the ac-pc line and the midsagittal plane. These aligned T1s were used for the Freesurfer (Fischl, 2004) pipeline along with the participants' corresponding T2-weighted images, which further helps to inform the skull stripping process. The Freesurfer pipeline performs the

volumetric grey- and white-matter segmentations, providing several automated cortical parcellations that can be used in subsequent analyses and, additionally, converts the grey matter into a 2D mesh that can be used to display, visualize and analyze information. For both volumetric and surface images, Freesurfer also provides an averaged brain in MNI305 space that can be used to compare and visualize individual subject information.

For fMRI analysis we used standard SPM8 preprocessing routines. First, slice timing was performed on every functional image. Then, realignment for motion correction and 4mm smoothing and volume repair using ArtRepair5 (Mazaika et al., 2009) was applied to the images. In the last stage of preprocessing, all the functional images were co-registered to the ac-pc aligned anatomical T1-weighted image, and resliced from the original 2.5mm isotropic voxels to the 1mm isotropic voxels in anatomical space. Thus, all functional images were in the same space as the individual anatomical images so that the ROIs from Freesurfer could be used without further modifications. Note that the images were not normalized to the standard MNI152 template.

Statistical analyses were performed on individual subject space using the GLM. fMRI time series data were modeled as a series of impulses convolved with a canonical hemodynamic response function (HRF). The motion parameters for translation (i.e., x, y, and z) and rotation (i.e., yaw, pitch, and roll) were included as covariates of non-interest in the GLM. For the event-related fMRI design, each trial was modeled as an event, time-locked to the onset of the presentation of each character string. For

the block fMRI design, each block was modeled as an epoch of 12 seconds, time-locked to the beginning of the presentation of the first stimuli within each block. The resulting functions were used as covariates in a GLM, along with a basic set of cosine functions that high-pass filtered the data, and a covariate for session effects. The least-squares parameter estimates of the height of the best-fitting canonical HRF for each study condition were used in pairwise contrasts. For both block and event-related fMRI designs, the functional volumes associated with the task conditions were modelled separately and were not taken into consideration in subsequent analyses.

The resulting individual T-stat map images (one per subject, contrast and fMRI experimental design) were translated to the individual cortical surface using Freesurfer's mri_vol2surf function, and then, using mri_surf2surf, all images were translated to the fsaverage space for inter-subject comparison. Using a custom Matlab script, all global maximas (GMax) were obtained per subject, contrast and design, and the data were converted to MNI152 coordinates by multiplying with an affine transformation matrix for further analysis and comparison with the literature. Finally, we thresholded the T values to capture GMax $\geq$ 1.65, which corresponds to a $p \leq 0.05$.

Finally, for DWI analysis, subject motion was initially corrected by co-registering each volume to the average of the non-diffusion weighted *b0* images (and gradient directions were adjusted to account for this co-registration). Using FSL's topup, the susceptibility induced off-resonance field was estimated, and eddy currents were corrected using FSL's eddy

tool (Smith et al., 2004). The $b = 1000$ and $b = 2500$ measurements were used to estimate fiber orientation distribution functions for each voxel using mrtrix3's multi-tissue constrained spherical deconvolution (CSD; lmax = 4; Jeurissen et al., 2014), and Freesurfer was used to inform the algorithm on the different types of tissues. Fiber tracts were estimated using probabilistic tractography (with 500,000 fibers) using the iFOD2 algorithm (Tournier et al., 2010). For each subject, the vertical occipital fasciculus (vOF) and posterior arcuate fasciculus (pAF) were identified using tools from the AFQ analysis pipeline (Yeatman et al., 2014b, 2012b). Using Vistasoft, Freesurfer's mri_vol2surf and custom scripts, the end-points of these tracts in the cortex were identified, and separated into two different groups: vOF and pAF endings in vOT and elsewhere outside of vOT, to create the vOT_vOF and vOT_pAF ROIs. For the vol2surf transformation, the voxels were matched with the surface 1 mm below the cortical surface. DWI data is not reliable for grey matter, so it is usually advisable to do the matching in white matter, right below the areas of interest. Nevertheless, tract information is usually stronger in the sulci and is typically lost in the gyri. We see this as a limitation of the technique, not a characteristic of the brain.

7.1.5 ROI definition

From Freesurfer's automated aparc parcellation we extracted one extensive cortical area of interest to be used as a mask in subsequent fMRI analyses. This cortical area covered the entire ventro-occipito-temporal (vOT) region, and was constructed by including fusiform, inferior temporal and lateral occipital regions from the aparc parcellation. As the response to words in the primary visual cortex was not part of this study,

regions V1 and V2 were excluded from this mask. Values on the y-axis ≤ -30 in the MNI152 space were also excluded from this mask (see Figure 18*a-b*).

To further characterize the functional activations and structural differences in our main vOT cortical area of interest, we also created 2 different sets of ROIs named *litVWFA* and *aa-ca-cp-pp* within the vOT (see Figure 18*c* and definitions below). As the name suggests, the *litVWFA* set comprises 3 ROIs based on previously published coordinates in the literature (Cohen and Dehaene, 2004; Vogel et al., 2012b), called the anterior, classical and posterior VWFAs (*aVWFA, cVWFA, pVWFA*). The coordinates for the center-points of these areas were: *aVWFA* (Talairach: –43, –48, –12; MNI152: –45, –51, –12), *cVWFA* (Talairach: –43, –54, –12; MNI152: –45, –57, –12), and *pVWFA* (Talairach: –43, –68, –12; MNI152: –45, –72, –10). These ROIs were created to serve as a reference for our own results and to perform statistical analyses.

Nevertheless, as there is an overlap between the *aVWFA* and *cVWFA* and, the described ROIs left some empty spaces, we created the *aa-ca-cp-pp* set of ROIs as well (see Figure 18*c*). This allowed us to systematically cover the *litVWFA* ROIs and most importantly, the whole lateral occipito-temporal sulcus along the anterior-posterior gradient avoiding any overlaps and leaving no empty spaces. The sub-ROIs were created manually and called anterior-anterior (*aa*), central-anterior (*ca*), central-posterior (*cp*) and posterior-posterior (*pp*), hence the set of the 4 ROIs was abbreviated to *aa-ca-cp-pp*.

Figure 18. vOT cortical area of interest and two sets of ROIs.

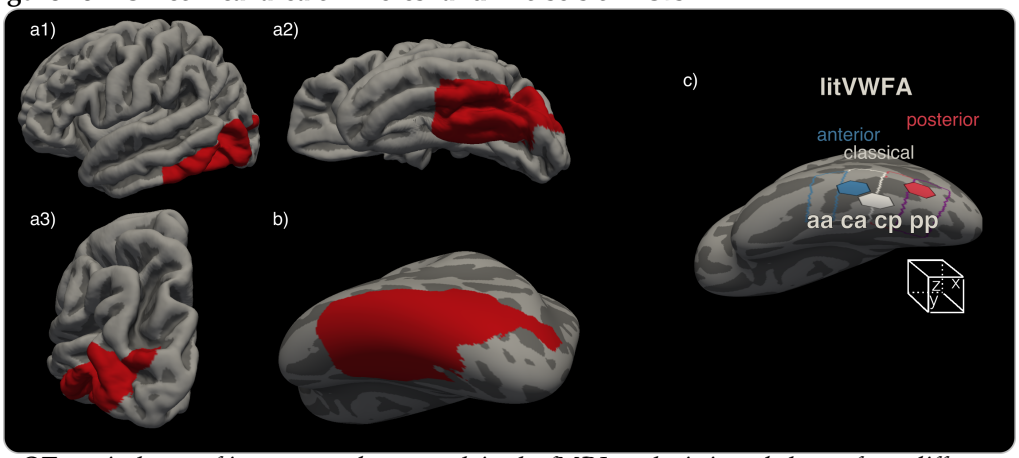

vOT cortical area of interest used as a mask in the fMRI analysis in red shown from different orientations and on folded and inflated surfaces. In a) we see the left hemisphere pial surface in the typical a1) sagittal (lateral), a2) axial (ventral), and a3) coronal (posterior) positions. b) shows vOT on an inflated Freesurfer fsaverage brain; dark areas indicate sulci and light areas indicate gyri. Note: this is in fsaverage space, so the cortical area of interest will be different for each individual. c) Exploratory ROIs in the vOT cortical area of interest: the litVWFA set of 3 ROIs and the aa-ca-cp-pp set of 4 ROIs. As the name suggests, litVWFA comprises 3 ROIs described previously in the literature, named anterior VWFA (aVWFA), classical VWFA (cVWFA), and posterior VWFA (pVWFA). The other four ROIs in aa-ca-cp-pp were manually designed to cover the litVWFA ROIs and the lateral occipito-temporal sulcus without overlaps or empty spaces between them. They were organized along an anterior-posterior gradient, and were named anterior-anterior (aa), central-anterior (ca), central-posterior (cp) and posterior-posterior (pp), hence the name aa-ca-cp-pp.

To create the *litVWFA* set of ROIs, we converted the three MNI152 coordinates reported in the literature to the MNI305 space, selected the nearest surface vertex corresponding to the coordinate, and created one vertex 2D surface label. Then, using Freesurfer's mris_label_calc tool, each label was dilated 8 times. The dilation factor was randomly chosen, yielding an approximate area (different for every subject) of 1.8 cm^2 (equivalent to a 1.3 cm side square).

The objective of the *litVWFA* and *aa-ca-cp-pp* ROIs was to characterize the functional activations and to relate them to existing literature. Furthermore, this study had the objective of relating functional activations to the endpoints of two tracts of interest: vOF and pAF. In order to do this, we created two additional ROIs per subject, corresponding to the endpoints of these tracts in the vOT: vOT_vOF and vOT_pAF. Both ROIs

were translated to fsaverage surface space using Freesurfer's mri_surf2surf. Although at the individual subject level the vOT tract endings were separated along an anterior-posterior axis, we wanted to create a probabilistic map and check for a 'probabilistic intersection' that could be used to study the hypothesized functional gradient. For this purpose, once in common space, the intersection between vOT_vOF and vOT_pAF was calculated as including those vertexes where at least 20% of the subjects had both tracts. The percentage of subjects was averaged at each vertex, for example: if 100% of subjects had both tracts at a vertex, this vertex was considered to be part of the intersection with 100% probability; if at another vertex 20% of the subjects had one of the tracts, and 80% the other tract, this vertex was marked as 50%; if in another vertex 15% of subjects had one of the tracts while 100% of the subjects had the other tract, the vertex was not considered to be part of the intersection.

7.1.6 Data Analysis

Within each fMRI design (i.e. block, event-related), and for every contrast and subject, the T value of the GMax inside the vOT cortical area and inside the abovementioned ROIs was located (with MNI X, Y, Z coordinates) and saved for analysis.

All analyses focused on the main contrasts previously used in the scientific literature. First, we analyzed the most extensively used contrast, real word versus fixation (**RWvsNull**), on its own. To statistically check the word selectivity gradient along the Y-axis, we performed a 4 (ROI) repeated-measures analysis of variance (ANOVA) to compare the T values inside each ROI as described in the methods section. Block and

event-related designs were conducted individually, as we were not interested in studying the effects of the fMRI design in this experiment (stronger activation for a block design was expected).

Second, we examined the following six contrasts found in the literature: 1) Real Words versus checkerboards (**RWvsCB**), 2) Real Words versus Scrambled Words (**RWvsSD)**, 3) Real Words versus Phase-Scrambled Words (**RWvsPS**), 4) Real Words versus Pseudo Words (**RWvsPW**), 5) Real Words versus Consonant Strings (**RWvsCS**), and 6) Real Words versus False Fonts (**RWvsFF**). First, we conducted a repeated-measures ANOVA using the GMax Y value for each contrast as the dependent variable in order to test the hypothesis of an anterior/posterior gradient related to the semantic/perceptual nature of the contrasts. Then, we repeated the same analyses for the X and Z axes to explore if there was an analogous functional gradient along these axes. To further examine to what extent the activations for the contrasts of interest organized as semantic or perceptual, we performed a hierarchical cluster analysis, as implemented by R's hclust (Murtagh, 1985), including each contrast's GMax T (mean and standard deviation) values.

Third, we checked for the test-retest reliability of our fMRI results. For this purpose, we selected the acquisition sessions of the 31 subjects assigned to the Test-Retest experiment. These subjects had repeated the experiment after 7-10 days. For this experiment, all the previously mentioned analyses were also conducted including an additional factor, Test-Retest: day1, day2.

Fourth, to examine the correspondence between the vOF and pAF tract endings in the vOT and the functional coordinates reported in the literature, we ran 2 chi-square tests, one per tract (vOF, pAF). To this end, we created a dichotomous variable per tract and ROI (*aVWFA*, *pVWFA*). For each subject, we indicated if the tract ending in question fell inside the ROI or not (at least one vertex). We did not consider *cVWFA* due to the fact that very few subjects showed any correspondence between the *cVWFA* and the ending of either the vOT or pAF tracts.

Fifth, we studied the relation of the vOF and pAF tracts to the functional activations of our contrasts of interest (RWvsPW/CS/FF/CB/SD/PS). We superimposed the mean of the contrast and cluster GMaxs on top of the vOF and pAF tract terminations to visually inspect their associations. Then, we statistically tested the hypothesis that the location of the semantic contrasts is related to vOT_pAF and the perceptual contrast to the vOT_vOF. For the semantic contrasts, we expected the average T for vOT_pAF ROI to be higher than that for the vOT_vOF ROI. The opposite was predicted for the perceptual contrast. To this end, we performed 12 different t-tests, one per Design and Contrast. The T values were thresholded to be higher than zero before averaging.

Finally, to examine if functional activations within the vOT for the various contrasts of interest predicted individual reading ability, we conducted linear regression analyses at each vertex. The reading ability scores were obtained from the lexical decision task that participants had performed outside the scanner. The complete analysis procedure consisted of the following steps: 1) obtain the reaction times for the selected stimuli in the

lexical decision task: consonant strings (CS), pseudowords (PW), and real words (RW). For this analysis, we removed the reaction time measurements corresponding to incorrect trials, and all values below 200ms and above 2 standard deviations from the mean. To obtain a single value per subject and stimuli, we averaged the values. 2) The functional activation maps were smoothed in the cortex using a Gaussian filter with a full width at half maximum (FWHM) of 5 mm. 3) We performed 18 different linear regressions at each vertex inside the vOT cortical area of interest: the functional activation T values (RWvsPS/CB/SD/PW/CS/FF) were used as independent variables and the behavioral data (CS, PW, and RW reaction times) as dependent variables. 4) Statistical cluster-wise corrections for multiple comparisons were carried out using FreeSurfer tools based on non-parametric Monte Carlo testing. We used an initial cluster-forming vertex-wise threshold of $p < 0.05$, and only those clusters with a corrected value of $p < 0.05$ were considered statistically significant.

7.2 Results

First, we characterized the GMaxs per design, contrast and subject in the vOT cortical area of interest, as well as in the different y-axis ROIs selected based on previous literature. Second, based on the data obtained from these contrasts, we examined if the functional activations derived from these contrasts tended to group together. Third, we checked for the reliability of these results using data from the Test-Retest experiment. Fourth, we characterized two tracts of interest for the vOT, the vOF and pAF, and investigated how these tracts were related to the contrast activations in the functional localizers. Finally, we examined if the

functional activation data in the vOT predicted individual reading behavior.

7.2.1 fMRI characterization of the vOT

7.2.1.1 RWvsNull

According to the literature, the most extensively used contrast to localize the VWFA is RWvsNull, masked either with 1) another contrast or 2) an ROI (usually a sphere) around the Talairach or MNI coordinates reported in previous studies that had focused on the VWFA (Glezer and Riesenhuber, 2013; Vogel et al., 2012b). To evaluate the adequacy of using the RWvsNull contrast to locate the VWFA, we analyzed the activation produced by this contrast in the vOT. To this end, we computed the across-subject average T value at each vertex. *Figure 19a-b* shows these averaged T values, accompanied by histograms representing these T values along the X-, Y-, and Z-axes (Figure 19*c*). On the Y-axis, we observed a gradual increase in the T values from Y = -35 to Y=-102.

To further examine this gradient statistically, we conducted two repeated measures ANOVAS. The first ANOVA included the *aa-ca-cp-pp* ROI as the independent measure (*aa, ca, cp, pp*; see Figure 18) and the T value of the GMax as the dependent measure. The second ANOVA included the *litVWFA* ROI (*aVWFA, cVWFA, pVWFA*; see Figure 18) ANOVA and the T value of the GMax as the dependent measure. Both ANOVAs revealed a main effect of anterior-posterior vOT ROI divisions, ($F(2,96) \geq 49.92$, $ps < .001$). Post-hoc analysis revealed that this effect was driven by systematically stronger T-values in all the posterior regions (for example: *cVWFA* higher than *aVWFA,* and *pVWFA* higher than both *aVWFA* and

cVWFA; all individual t-tests with *p*s < .01). This effect was confirmed in both block and event-related fMRI designs, although as expected the block design values were systematically higher than the event-related ones (see Figure 19*d*).

Figure 19. Average T values in the vOT for the RWvsNull contrast (block design)

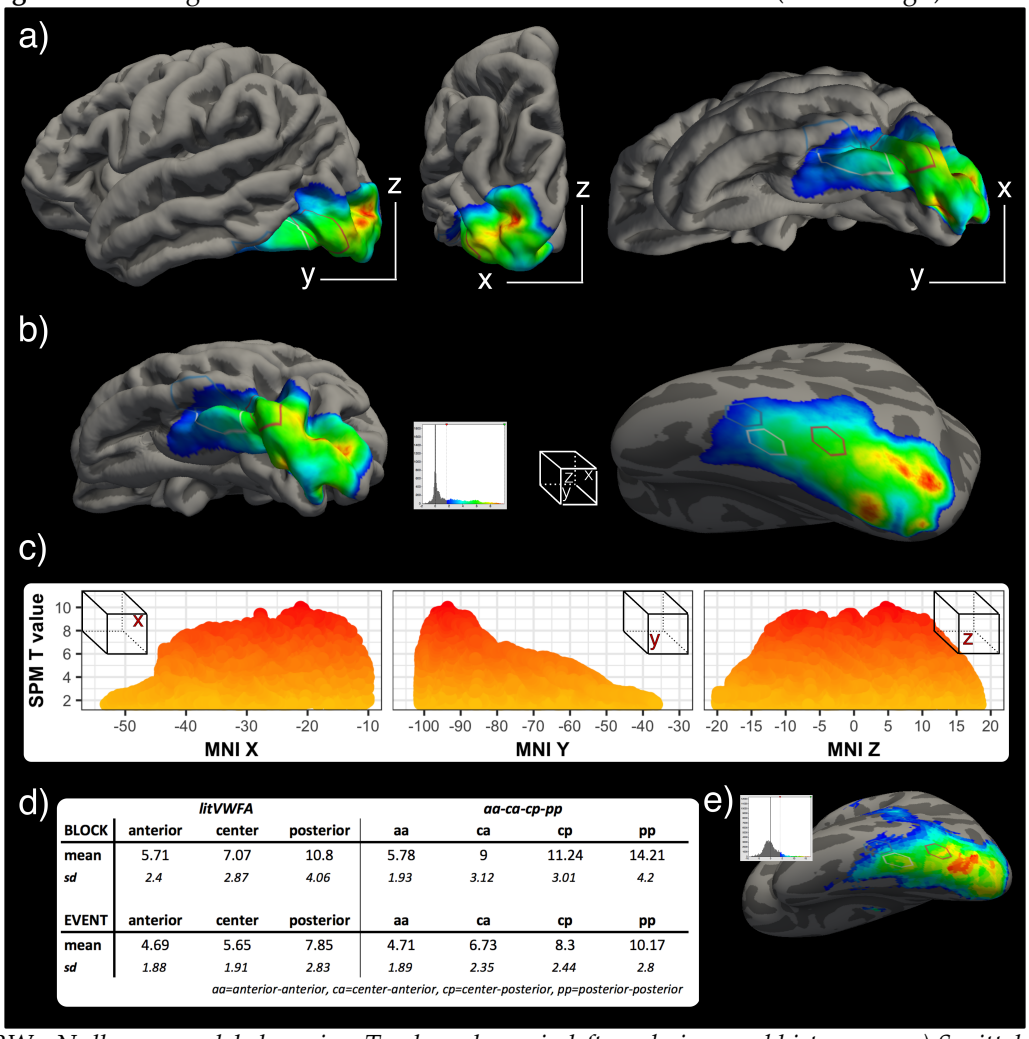

	litVWFA			aa-ca-cp-pp			
BLOCK	anterior	center	posterior	aa	ca	cp	pp
mean	5.71	7.07	10.8	5.78	9	11.24	14.21
sd	*2.4*	*2.87*	*4.06*	*1.93*	*3.12*	*3.01*	*4.2*
EVENT	anterior	center	posterior	aa	ca	cp	pp
mean	4.69	5.65	7.85	4.71	6.73	8.3	10.17
sd	*1.88*	*1.91*	*2.83*	*1.89*	*2.35*	*2.44*	*2.8*

aa=anterior-anterior, ca=center-anterior, cp=center-posterior, pp=posterior-posterior

RWvsNull average global maxima T values shown in left renderings and histograms. a) Sagittal, coronal and axial pial surface in fsaverage space; b) pial and inflated surfaces oriented identically allowing for visualization of the average global maxima T-value overlay; c) average GMax T values along each independent X, Y and Z coordinate; d) the table shows the mean and standard deviation (sd) T values inside the litVWFA and aa-ca-cp--pp ROIs; and, e) whole-brain analysis for the RWvsNull contrast using a q < 0.01 voxel-wise FDR corrected threshold.

Importantly, the smallest averaged GMax T value in this analysis was 4.69 (see Figure 19*d*). This T-value corresponded to a *p*-value ≤ 0.000001 uncorrected, which is above the typical thresholds used in previous fMRI

studies. In fact, a review of the previous published studies over the last 15 years using RWvsNull as a contrast for localizing the VWFA revealed that the most restrictive voxel-wise corrected threshold applied in these studies was $q < 0.01$ FDR corrected (Nestor et al., 2013). Additionally, we performed a whole-brain group analysis for the RWvsNull contrast using the same $q < 0.01$ voxel-wise FDR-corrected threshold. This analysis similarly yielded activated voxels along the entire vOT for both the block and event-related fMRI designs (see Figure 19*e*). This result suggests that the statistical thresholds used in previous fMRI studies for the contrast RWvsNull might have resulted in activation across the entire vOT, as well and, thus, the use of a second masking contrast (e.g., RWvsCB) or a sphere ROI around the classical VWFA coordinates (e.g., *anterior-classical-posterior VWFA*) might have been the *de facto* determining factor for localizing the word selective areas in vOT.

7.2.1.2 Analysis of other relevant functional contrasts

To examine the hypothesis that the selection of the contrast has an impact on the localization of VWFA, we analyzed the GMax of the RWvsCB/SD/PS/PW/CS/FF contrasts in the vOT (for both block and event-related designs). We analyzed 4 different measures: the T value itself, and the X, Y, Z GMax location coordinates. All the 12 average X, Y, Z coordinate contrasts (6 contrasts, for both block and event-related designs) lay along the lateral occipito-temporal sulcus (see Figure 20*a*).

For both block and event-related designs, as expected, the averages of the perceptual (RWvsCB/SD/PS) contrasts were organized within the posterior part of the lateral occipito-temporal sulcus, coinciding roughly

with the *pVWFA*. In contrast, the averages of the semantic (RWvsPW/CS/FF) contrasts were organized within the anterior part of the sulcus, in the vicinity of the *aVWFA* and *cVWFA*. The enlarged image in Figure 20*a* shows the lateral occipito-temporal sulcus, with a blue dashed line separating the two hypothesized groups.

Figure 20*b* shows the same average contrasts plotted in X, Y, Z format: in *b*1) the mean MNI X (medial to lateral) and mean MNI Y (anterior to posterior) positions of the averages of the contrasts, and in *b*2) the mean MNI Z (ventral to dorsal) and mean MNI Y positions. The size of the dark center of every contrast is scaled to the mean T value of each contrast. The size of the outer colored external circle is scaled to the standard deviations of the X-Y and Z-Y coordinates. This serves as an indicator of the spatial variability of the contrast: a bigger outer circle means that the GMaxs were more spread out. The color is assigned depending on the originally assigned group (perceptual or semantic). Additionally, the coordinates of the 3 literature VWFA ROIs (*aVWFA*, *cVWFA* and *pVWFA*) are marked with a grey dark cross for reference.

Figure 20. Perceptual and semantic contrast's average locations in vOT

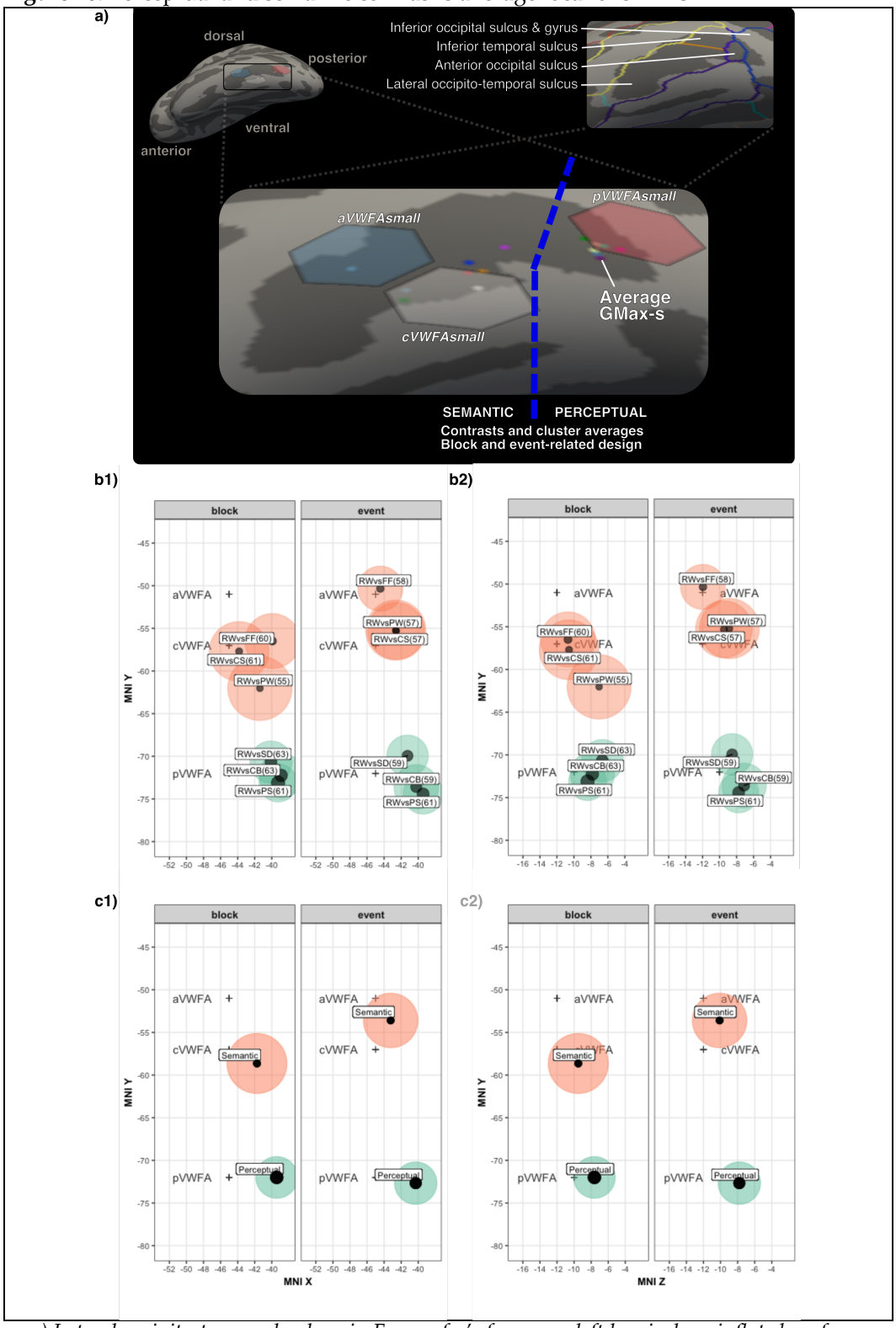

a) Lateral occipito-temporal sulcus in Freesurfer's fsaverage left hemisphere inflated surface showing the block and event-related average GMax for the semantic (RWvsCS-PW-FF) and perceptual (RWvsPS-CB-SD) contrasts. Notice the litVWFA set of ROIs drawn in for reference and comparison with results from literature. b) Same information plotted in X,Y (b1) and Z,Y (b2). The size of the inner black circle indicated the average T value, and the size of the outer circle is scaled to the standard deviation of the coordinate positions (bigger circle indicates a larger data spread). The color of the outer circle indicates if the contrast is semantic (green) or perceptual (red). c) Analogous plots, but with clustered averaged values. In all plots the litVWFA coordinates have been included as small dark gray crosses for reference.

To statistically test the anterior-posterior segregation of contrasts, we performed a series of ANOVAs. First, we performed three separate 2 (Design: block, event-related) X 6 (Contrast: RWvsPS/CB/SD/PW/CS/FF) repeated-measure ANOVAs, one per MNI coordinate (i.e., X, Y and Z) as dependent measures.

The ANOVA for the Y coordinate revealed the main effect of Contrast ($F(6,292) = 32.47$, $p < 0.0001$, $R^2_{Adj} = 0.68$). Post-hoc analysis showed systematic one-to-one statistically significant differences for contrasts belonging to the perceptual group versus contrasts belonging to the semantic group (all ps < 0.001): all semantic contrasts were more anterior to the perceptual contrasts. No differences emerged for contrasts within the same perceptual or semantic group (all *p*s ≥ 0.15).

Additionally, with the objective of statistically exploring the medial-lateral and dorsal-ventral segregations of contrasts, we tested the X and Z axes. The analysis for the X coordinate showed that the main effect of Design and Contrast ($F(11,494) = 4.71$, $p < 0.0001$, $R^2_{Adj} = 0.19$), was subsumed by a statistically significant Design X Contrast interaction ($p = 0.02$). Post-hoc analyses revealed that this interaction was due to the significant difference between block and event-related designs for the RWvsFF contrast. The rest of the contrasts did not show differences as a function of Design, p ≥ 0.84.

The analysis for the Z coordinate only revealed a main effect of Contrast ($F(6,292) = 4.71$, $p = 0.004$, $R^2_{Adj} = 0.60$). In this case, post-hoc analysis showed that this main effect emerged because the RWvsFF contrast was

statistically different (ps $\leq$ 0.04) from the RWvsCB/PS/SD perceptual contrasts and from the RWvsPW (p = 0.04) semantic contrast.

Additionally, we performed a hierarchical cluster analysis on the averaged GMax T values. For both block and event-related fMRI designs, the clustering algorithm grouped semantic contrasts together, on the one hand, and perceptual contrasts together, on the other. These results confirm the original allocation of the different contrasts to either the perceptual or semantic groups, for both block and event-related fMRI designs. As a summary, we plot the grouped contrasts in Figure 20c (which is analogous to Figure 20b, but shows the averages for the grouped perceptual and semantic contrasts).

Table 2. Means and standard deviations of T values per contrast and fMRI design

	BLOCK		***EVENT***	
PERCEPTUAL	**mean**	***sd***	**mean**	***sd***
Cluster	5.40	*1.60*	4.70	*1.60*
RWvsCB	5.35	*1.60*	4.53	1.72
RWvsPS	5.79	*1.74*	5.09	1.61
RWvsSD	5.07	*1.40*	4.52	1.39
SEMANTIC	**mean**	***sd***	**mean**	***sd***
Cluster	2.90	*0.80*	2.90	*0.70*
RWvsCS	2.83	*0.76*	2.77	*0.73*
RWvsFF	3.29	*0.93*	3.09	*0.74*
RWvsPW	2.66	*0.61*	2.70	*0.61*

In sum, our results revealed a y-axis segregation of functional reading contrasts based on their semantic *versus* perceptual nature. We showed consistently that contrasts of a semantic nature produce activations that are more anterior and lateralized along the lateral occipito-temporal sulcus relative to activations for perceptual contrasts. All contrast

averages lie approximately in the center of the sulcus, except the contrast RWvsFF.

7.2.1.3 Reliability over time: the test-retest effect

To check for the robustness of the previous functional results across time, we conducted a test-retest analysis. To this end, we repeated the main analyses previously performed, adding the factor Test-Retest (day1, day2), with the 31 subjects included in the Test-Retest experiment.

RWvsNull

To check whether or not the anterior-posterior gradient found in the Main Experiment was reproduced in the Test-Retest experiment, we conducted two analogous mixed-model ANOVAs. The first was a 4 (ROI: *aa*, *ca*, *cp*, *pp*) X 2 (Test-Retest: day1, day2) ANOVA, and the second a 3 (ROI: aVWFA, cVWFA, pVWFA) X 2 (Test-Retest: day1, day2) ANOVA. In both cases, the T value of the GMax was the dependent variable. There was no interaction and no Test-Retest main effect in these ANOVAs ($ps \geq 0.14$). Most importantly, the main effect of an anterior-posterior gradient was replicated. Please refer to Table 3, which is analogous to the table in Figure 19*d*.

Table 3. Average T values for the Test-Retest analysis.

	litVWFA						*aa-ca-cp-pp*							
BLOCK	**anterior**		**classical**		**posterior**		**aa**		**ca**		**cp**		**pp**	
Test-Retest	Day 1	Day 2	Day 1	Day 2	Day 1	Day 2	Day 1	Day 2	Day 1	Day 2	Day 1	Day 2	Day 1	Day 2
mean	5.24	5.49	6.74	7.00	10.65	9.52	5.99	5.67	9.27	8.46	11.38	10.80	14.35	14.10
sd	*2.49*	*2.45*	*2.69*	*3.03*	*3.89*	*3.43*	*2.22*	*2.43*	*3.22*	*2.93*	*3.76*	*3.13*	*3.93*	*4.16*
EVENT	**anterior**		**classical**		**posterior**		**aa**		**ca**		**cp**		**pp**	
Test-Retest	Day 1	Day 2	Day 1	Day 2	Day 1	Day 2	Day 1	Day 2	Day 1	Day 2	Day 1	Day 2	Day 1	Day 2
mean	4.29	3.14	5.64	4.34	7.48	5.82	4.63	3.82	6.94	5.96	8.24	7.06	10.14	9.43
sd	*1.88*	*1.07*	*2.08*	*2.42*	*3.18*	*2.03*	*2.29*	*1.61*	*3.07*	*2.24*	*3.04*	*2.55*	*3.42*	*2.83*

aa=anterior-anterior, ca=center-anterior, cp=center-posterior, pp=posterior-posterior

The results are divided into the two ROI sets: litVWFA and aa-cc-cp-pp, corresponding to the ROIs defined in Figure 18*c. The individual ROIs are organized from anterior to posterior within each set. Each mean and standard deviation is presented twice, corresponding to day 1 or day 2. As expected, block design values are systematically higher than event-related values, and values corresponding to more posterior ROIs areas are higher than those for more anterior areas.*

Perceptual and semantic contrasts

We tested if the localization of the different regions along the vOT, using the semantic RWvsPW/CS/FF and perceptual RWvsCB/PS/SD contrasts was reliable across time. In these analyses, we only used the Y-axis coordinate of the individual GMax values and the T values as dependent measures. First, we performed a 2 (Design: block, event-related), X 2 (Contrast: RWvsPW/CS/FF/CB/PS/SD) X 2 (Test-Retest: day1, day2) repeated measures ANOVAs, using the Y coordinate of the individual GMax values as the dependent variable. There was no Test-Retest main effect or interaction ($p \geq 0.81$). As in the Main experiment, there was only a Contrast main effect ($F(7,279.9) = 19.64$, $p < 0.0001$, $R^2_{Adj} = 0.58$). Post-hoc analysis reproduced the same systematic one-to-one statistically significant differences for contrasts belonging to the perceptual group versus contrasts belonging to the semantic group (all ps < 0.003): all semantic contrasts were more anterior to perceptual contrasts. As expected, no differences emerged between contrasts within the same perceptual or semantic group (all ps ≥ 0.22). Furthermore, the clustering analysis using the T values as the dependent measure grouped the

contrasts as expected, putting RWvsPS/CB/SD in the perceptual and RWvsPW/CS/FF in the semantic groups, respectively.

In sum, our results confirm that the Y-axis functional segregation observed in the vOT is a robust and reproducible phenomenon across time (i.e., 7-10 days). Next, we proceed to relate this functional segregation to the two WM tracts of interest: the pAF and vOF.

7.2.2 DWI characterization of the vOT

In the previous section, results consistently confirmed a functional segregation of semantic and perceptual contrasts along the Y-axis of vOT, and demonstrated that semantic contrasts were related to the regions *aVWFA*/*cVWFA* delineated by previous studies, while perceptual contrasts were associated with the *pVWFA* region delineated in previous studies. To test the hypothesis of a topographical relation between this functional segregation and the pAF and vOF WM tracts, we conducted two analyses. The first was intended to relate the WM tract cortical endings with the literature coordinates (i.e., *litVWFA*): *aVWFA* coincides with a high-density area in pAF, and *pVWFA* is located in the vicinity of the ventral high-density area of vOF (see Figure 21). In the second analysis we related these tracts to our own functional findings.

To understand the relation between the VWFAs reported in the literature and the cortical regions innervated by the vOF and pAF WM tracts, per tract, we created a dichotomous variable indicating if the subject had the tract (at least one vertex) inside the ROI (*aVWFA*, *pVWFA*) or not. We did not consider *cVWFA* due to the fact that very few subjects had either WM

tract ending in this region. We ran a chi-square test for each tract (Figure 21*a*), and the results showed that there was a clear relation between the most anterior and posterior VWFAs reported in the literature and the cortical endings of the pAF and vOF tracts, respectively ($\chi^2(2, N = 66) \geq 36.75$, $ps < 0.001$).

Figure 21. vOF and pAF tract cortical endings in the vOT coincide with litVWFAs

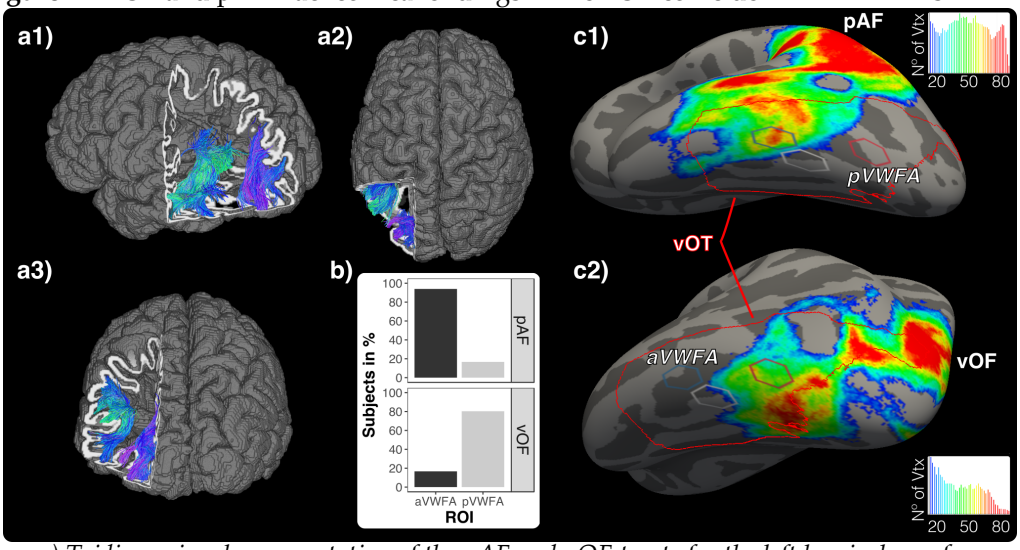

a) Tridimensional representation of the pAF and vOF tracts for the left hemisphere of a representative subject, in typical a1) sagittal (medial), a2) axial (dorsal), and a3) coronal (posterior) views. b) Barplot showing the number of subjects with at least one tract vertex inside the aVWFA or pVWFA, for both the pAF and vOF. c) Average inflated surface rendering with overlaid probability maps (thresholded at 20%) of the c1) pAF and c2) vOF tract cortical endings in the vOT cortex (vOT cortical area of interest is outlined in red). The red color in the probabilistic map indicates a high percentage of subjects with the tract on that vertex, green indicates medium and blue low. Note the outlines of the litVWFAs superposed: aVWFA coincides with the pAF, pVWFA with vOF while cVWFA coincides with neither. The histograms indicate the percentage of subjects on the x-axis, and the number of vertex (count) on the y-axis.

Next, to examine the hypothesized relationship between the functional segregation of semantic and perceptual contrasts along the Y-axis of the vOT and the pAF and vOF WM tracts innervating the vOT, we superimposed the contrasts on the vOF and pARC WM tract cortical endings (we maintained the litVWFA ROIs for reference; see Figure 22*a*). The center image in Figure 22*a* shows the relation between contrasts and WM tracts: perceptual contrasts lie posterior to the intersection between the pAF and vOF; semantic contrasts, although more sparse, roughly lie

anterior to this intersection. The intersection was calculated as the vertex where both tracts were present for at least 20% of the subjects. For further comparisons see Figure 22*b-c*, which, analogous to Figure 20*b-c*, shows the contrast and cluster information separately for the X-Y and Z-Y axes. The only difference in this case, is that a projection of the pAF and vOF WM tracts has been drawn in. At every point the tract present in the greater percentage of subjects was selected. All the semantic contrasts roughly lie in the pAF tract and *aVWFA*, while perceptual contrasts lie in the vOF tract and *pVWFA*.

Figure 22. Relationship between fMRI designs, type of contrasts and tracts in vOT

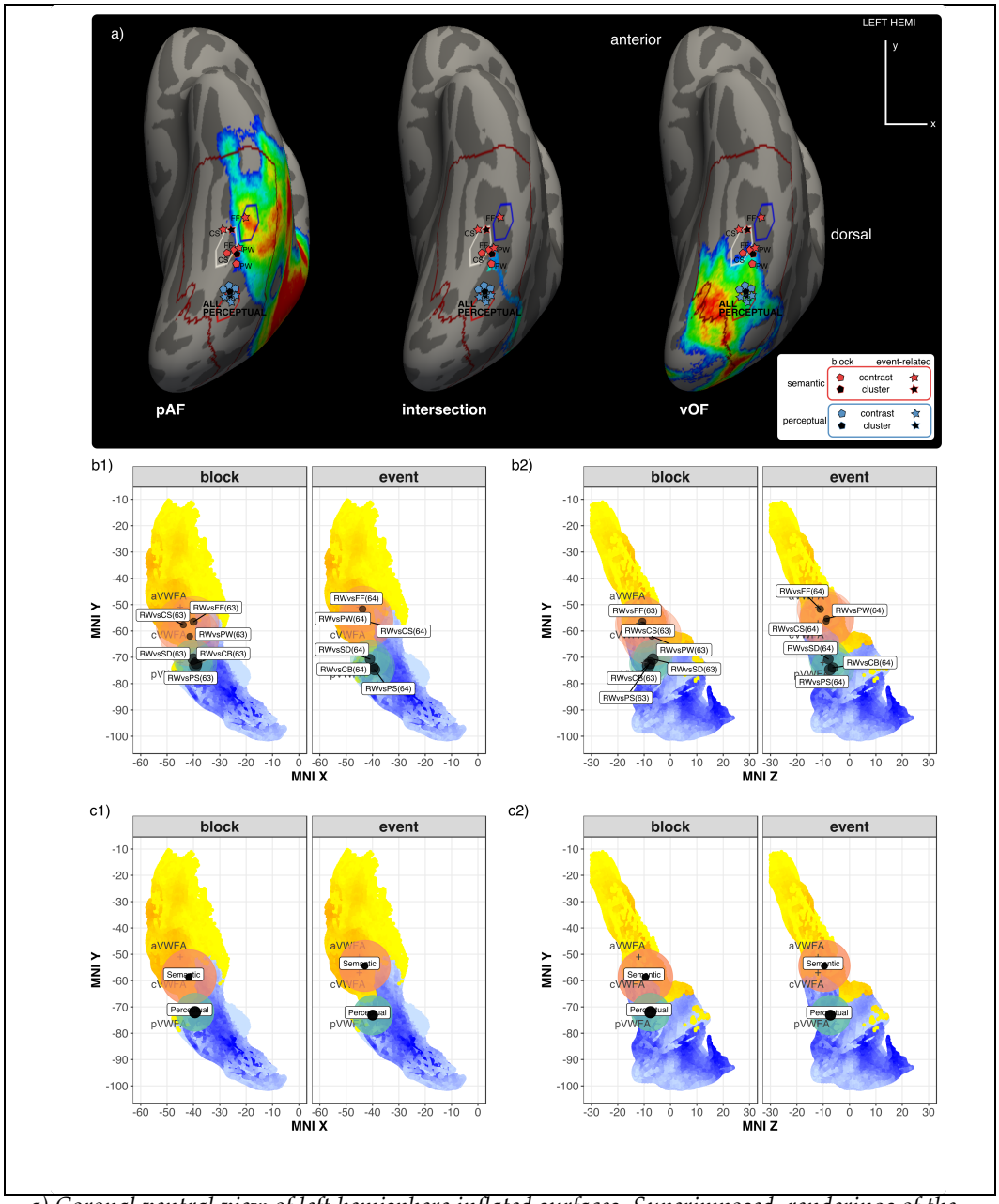

a) Coronal ventral view of left hemisphere inflated surfaces. Superimposed, renderings of the pAF and vOF cortical endings, along with their intersection. On top of the tracts, the averaged functional coordinates have been plotted. See the legend for a guide to understanding the location of every Design/Contrast average. The semantic and perceptual contrasts are roughly separated by the intersection of the two tracts. The litVWFA set of ROIs was drawn as well for reference and comparison with results from the literature. b) Same information plotted in X,Y (b1) and Z,Y (b2). The size of the inner black circle indicates the average T value, and the size of the outer circle is scaled to the standard deviation of the coordinate positions (bigger circle indicates larger data spread). The color of the outer circle indicates if the contrast is semantic (green) or perceptual (red). c) Analogous plots, but with clustered averaged values. In all plots, the litVWFA coordinates have been included as small crosses for reference.

To statistically check the relationship between the tracts and our previous functional segregation of semantic and perceptual contrasts results, we performed 12 different one-sided t-tests, one per fMRI design and

contrast. We compared the average vertex-wise T values of the contrasts inside the ROIs as defined by the cortical endings of the WM tracts. For example, our hypothesis was that the perceptual RWvsPS functional contrast would have higher vertex-wise average T values in the vOF ROI than in the pAF ROI. In contrast, we expected that the semantic RWvsPW average T value in the vOF ROI would be lower than that for the pAF ROI. All the resulting t-tests were significant (ps ≤ 0.05), except for the block design RWvsCS and RWvsPW contrasts (ps ≤ 0.1). These results confirmed our hypothesis of a relation between the WM tracts and the observed functional segregation.

In sum, these results showed an association between the functional location of the semantic contrasts and the pAF WM tract, and between the functional location of the perceptual contrasts and the vOF WM tract; as well as an overlap with the *a-c-p-VWFA* regions previously reported in the literature.

7.2.3 Prediction of behavioral results

Next, we tested the hypothesis that individual reading abilities, measured by a lexical decision task, can be predicted by functional activations in the vOT. To this end, only for the block design, we performed separated vertex-wise linear regression analyses restricted to the vOT using the T values for the 3 perceptual and 3 semantic contrasts as independent variables and individual average reaction times (RTs) to RW, PW and CS as dependent variables. This analysis yielded a total of 18 vertex-wise regressions. Results revealed a systematic predictive capacity for all the perceptual contrasts (i.e., RWvsPS/CB/SD) in vOT clusters for RW, PW

and CS (see Figure 23). The cortical area corresponding to the most posterior part of the lateral occipito-temporal sulcus systematically showed a significant association with reading behavior, precisely where the average GMax values of the perceptual contrasts were located (see 7.2.1.2.- Analysis of other relevant functional contrasts). On the other hand, semantic contrasts did not consistently predict reading behavior.

Figure 23. Functional activation in vOT cortical areas predicting reading behavior

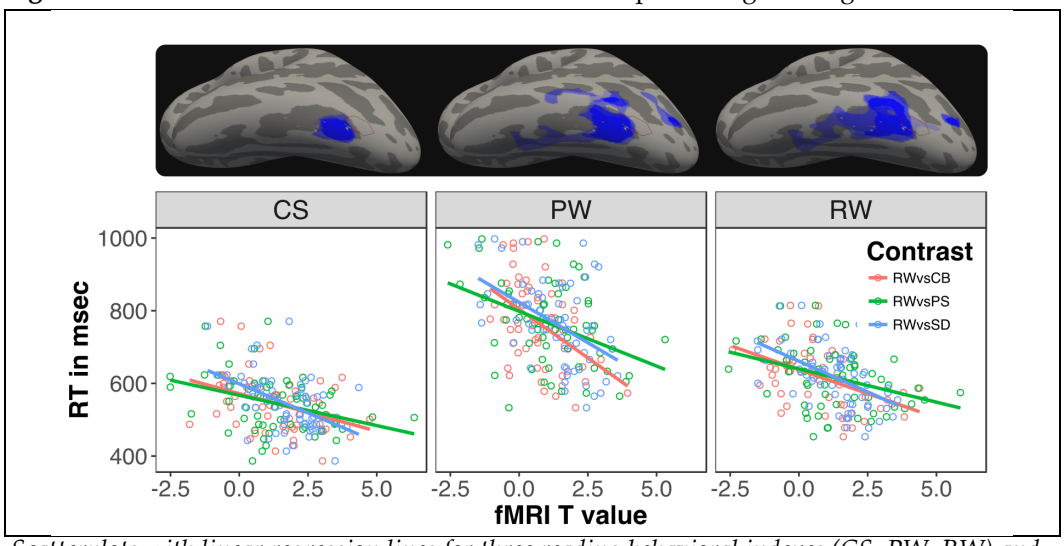

Scatterplots with linear regression lines for three reading behavioral indexes (CS, PW, RW) and the three perceptual contrasts (RWvsCB/PS/SD). The horizontal axis shows the T value of the most significant vertex (which is different in each of the 9 cases, but always in the posterior part of the lateral occipito-temporal sulcus). The vertical axis shows the average reaction time in milliseconds for the reading behavior measures. In the top row we rendered the clusters where the prediction was significant, with clusters being vertex-wise (p = 0.05) and cluster-wise (p = 0.05) corrected. In each rendering the significant clusters from the three main contrasts were superposed with some degree of transparency so the overlapping areas could be better appreciated. Furthermore, for reference, the layout of the pVWFA from the literature and the average GMax values were rendered: the overlapped predictive clusters and the GMax of the perceptual clusters coincide in the posterior part of the lateral occipito-temporal sulcus.

7.3 Discussion

The present experiment aimed to both functionally and structurally characterize the visual word responsive areas within vOT cortex. To this end, we ran two experiments: the Main experiment with 66 healthy young adults that performed reading-related tasks inside and outside of the scanner, and the Test-Retest experiment that consisted of a subset of 31

subjects who participated in the Main experiment and then in the Retest part of the study after 7-10 days.

Most voxels in the vOT are highly responsive to words

First, we focused on the most widely used contrasts to identify the VWFA: RWvsNull. Our findings showed a strong gradient along the y-axis, with higher-to-lower T values along posterior-to-anterior vOT. Moreover, our results across both block and event-related fMRI designs revealed that the statistical thresholds used in previous fMRI studies for the contrast RWvsNull can yield activations along the entire extent of vOT and, thus, the use of a second masking contrast (e.g., RWvsSD/CB) or classical VWFA coordinates (Cohen and Dehaene, 2004), to further constrain the results obtained from the functional RWvsNull contrast, might have been the determining factor in locating VWFAs. In this case, the located 'VWFA' may, in fact, have instead corresponded topographically to the area identified by the secondary masking contrast/coordinate criterion.

In other words, this result implies that when the VWFA is localized using the RWvsNull functional contrast in combination with a 1) mask created from another contrast or 2) within an ROI (sphere, for example) created around a published coordinate, the RWvsNull contrast does not add information to either 1) or 2). The information in 1) and 2) alone is what determines the purported location of the VWFA, since the functional RWvsNull contrast itself will be highly significant across the entire vOT.

The "semantic" and "perceptual" VWFAs

Our main results confirmed our hypothesis: the perceptual (RWvsCB/PS/SD) and semantic functional contrasts (RWvsPW/CS/FF) identified different cortical regions within the vOT. All perceptual functional contrasts yielded activations that lay close together, with minimal spatial variability, in the posterior part of the lateral occipitotemporal sulcus. Conversely, for the semantic functional contrasts, the spatial variability was broader, occupying a larger part of the mid-section of the lateral occipitotemporal sulcus.

As previously indicated, the perceptual and semantic functional contrasts subtract different information from RWs. On the one hand, in the case of the three perceptual contrasts, purely visual information in terms of light-dark contrasts is removed from RWs. Subtracting a CB of the same size as the RW constitutes a more raw subtraction than using word scrambling (phase or pixel). However, in all these three cases (CB, PS, SD) what is left from the subtraction is theoretically the same: whole words with intact orthography, phonology and lexico-semantics. On the other hand, among the three semantic contrasts, different aspects of the word remain after subtracting PWs/CSs/FFs from RWs. Semantics should be present after all three subtractions, as only RWs carry meaning. But when we read pseudowords we still have to access phonology and even orthography, which is not the case for CS or FF. Nevertheless, we should expect differences between RWvsCS and RWvsFF as well. Although our FF has all the characteristics of a real script, our subjects were not as familiar with this script as they were with the script used for CS. This difference is such

that in some studies, the contrast between CS and FF has been used to detect the 'letter-form' area (Thesen et al., 2012).

As important as the finding that perceptual and semantic contrasts cluster within vOT, were the localizations of these clusters. As hypothesized, the perceptual functional contrasts localized a region within the vOT systematically posterior to the region localized by semantic contrasts. To examine if this effect was clearly established in results reported in the previous empirical research on vOT, we did an extensive literature review of 105 papers. There were some consistent examples suggesting an anterior-posterior gradient in the same direction as that found for our data (Brem et al., 2010; Stigliani et al., 2015; Vinckier et al., 2007; Weiner et al., 2016a; Xue and Poldrack, 2007). An example related to our semantic contrasts is the above-cited study from Thesen et al. (2012). In this study, the VWFA was explicitly localized using first the RWvsCS functional contrast at the individual-subject level, and then a group average was computed. Importantly, Thesen et al. obtained similar localizations to those reported here. Examples related to our perceptual contrasts, include two studies using RWvsPS (Ben-Shachar et al., 2011, 2007) which reported more posterior regions than the typical MNI Y-axis values = -65. However, there are counter examples to these studies. For example, studies by Cohen et al. (2002) and Rauschecker et al. (2012), using the RWvsCB and RWvsPS contrasts, report MNI coordinates in line with the classical VWFA which are not as posterior as our results suggest.

Nevertheless, in our experiment we explicitly tested the main functional contrast previously used in this area of research across two different fMRI

designs and, regardless of the exact MNI coordinate obtained, our results are unequivocal with regard to the fact that the positions of the cortical areas identified by semantic and perceptual functional contrasts are inherently different. Therefore, we can safely assume that these distinct regions within the vOT perform different computations in the completion of a visual word recognition task. With this in mind, and for the sake of brevity, from now on we refer to the cortical regions identified by the semantic and perceptual functional contrasts as semantic VWFA (semVWFA) and perceptual VWFA (perVWFA), respectively.

Based on these results confirming that vOT computes information hierarchically in a posterior-to-anterior direction, the relatively anterior location of semVWFA relative to perVWFA becomes especially relevant in regard to the roles played by these VWFAs. We suggest that for perVWFA the word is a purely visual object. In contrast, semVWFA constitutes the initial region within the vOT stream that deals with the word as a language unit. This idea aligns well with other results from studies examining the fusiform face area (FFA). In parallel with our VWFA results, some previous work has reported a mid-fusiform FFA and a posterior fusiform FFA (Grill-Spector et al., 2004; Weiner et al., 2016a; Weiner and Grill-Spector, 2012). Some studies (Stigliani et al., 2015; Weiner et al., 2016a) have actually reported a mid-occipito-temporal sulcus character-sensitive area and a posterior-occipito-temporal sulcus character-sensitive area. These regions coincide respectively with the semVWFA and perVWFA observed in our results. Interestingly, these studies find the posterior VWFA in both hemispheres, but only find the mid VWFA in the left hemisphere, effectively suggesting that the

perVWFA is more related to visual processing while the semVWFA is more related to computations carried out by the more extensive language network.

We will elaborate further on this idea below when we examine the structural connectivity patterns of the semVWFA and perVWFA. Nevertheless, before discussing the structural connectivity results, it is important to comment on the reliability and reproducibility of the functional results obtained here in terms of the localization of the perVWFA and semVWFA, as a function of two different fMRI designs (block, event-related) and a test-retest examination of the reliability of these results.

Block and event-related fMRI designs identify similar VWFAs

As expected, our results confirmed that the perceptual contrasts showed higher T values and less variability, relative to the semantic functional contrasts. This result was predicted on the basis that the RW and semantic raw signals are more similar than the RW and perceptual signals. Also as expected, we found that the block fMRI design provided higher T values and less variability than the event-related fMRI design.

It has been reported that while fMRI event-related designs capture transient cortical activity, fMRI block designs capture sustained activation (Brockway, 2000; Buckner et al., 1996; D'Esposito et al., 1999; Dale and Buckner, 1997; Friston et al., 1999; Rombouts et al., 1997; Schacter et al., 1997). Although in Figure 20*b* we observed that overall the functional activation averages obtained from the semantic contrast in the event-

related fMRI design were more anterior than the ones obtained from the block fMRI design, our results did not show statistically significant main effects or interactions for the factor fMRI Design. There may, in fact, be some consistent differences for these designs (as the same pattern of results can be observed in the test-retest data), and it was simply a lack of power /or the inherent variability of the data which led to the non-significant differences we found for these two different types of fMRI design. In any case, the results confirm the systematicity of the identification and segregation of perVWFA and semVWFA.

Researchers interested in the sustained versus transient effects of fMRI designs who may want to further evaluate these differences could use different variations. For example, we used the same stimuli in both designs: in the fMRI block design we used 2 functional runs with (as per the name) blocks of the same stimuli one after the other and with long rest periods, while in the fMRI event-related design we used randomized stimulus order, short rest periods and one functional run. In both cases, we presented the stimuli for 400ms with a blank period of 200ms, and used the same fMRI sequence with 2.4sec TRs. Variations such as modifying the duration of the presentation of the stimuli or using faster multiband data acquisitions might be useful in terms of further examining potential differences between these types of fMRI designs.

However, the null effect found here in terms of the type of fMRI design is important, because it confirms the segregation of perVWFA and semVWFA within the vOT across designs. This is in line with several previous studies (e.g., Glezer et al., 2016, 2015), that used a block design

for their independent localizers (with more statistical power) and an event-related design for their main experimental design. Nevertheless, as stated above, we did this in a fairly controlled manner. If a combination of both designs is to be used for the independent localizer and actual fMRI experimental task, it is advisable to first check if within the scope of the study there may be some impact related to the sustained vs. transient nature of block vs. event-related localizers.

Reliability over time of the localization of the VWFAs

We tested the robustness of our functional results in a Test-Retest experiment with 31 subjects and successfully replicated the perVWFA and semVWFA segregation for both the block and event-related fMRI designs. We performed our test with healthy young adults and a 7-10 day delay; within this brief time interval we would not expect any improvements in reading abilities or structural changes. Nevertheless, considering individual subject variability, this is a remarkable and relevant result.

Future studies may want to further examine the effects of using longer temporal intervals in regard to test-retest reliability for the localization of the VWFAs reported here. Moreover, being further trained in reading or having a period of extensive exposure to reading may be conditions of special relevance in terms of examining changes in the location of these VWFAs in comparison with a control reading group. Finally, to examine the location of these VWFAs in low and high skill readers at different temporal intervals could not only inform us regarding any differences in the location of VWFA for such groups, but also help determine if either

group is more or less likely to show differences in dedicated vOT regions involved in performing perceptual and semantic operations over time.

In any case, the relative location of the contrasts is far more important than the exact location of the average contrast (i.e., semantic functional contrasts were consistently located in the anterior vOT relative to perceptual ones). And, as we will see below, the semantic contrasts were related to the cortical endings of the pAF WM tract and the perceptual contrasts were associated with the cortical endings of the vOF WM tract, which has importance consequences for the localization of these different VWFAs and their interactions with other brain regions.

Overlap of the functional and structural perVWFA and semVWFA topography

Our results are aligned with the connectivity bias hypothesis (Dehaene and Dehaene-Lambertz, 2016; Hannagan et al., 2015; Saygin et al., 2016) and confirmed our hypothesis that perceptual functional contrasts would be more related to vOT_vOF tract endings, while semantic contrasts would be more related to the vOT_pAF cortical endings. Interestingly, we were also able to link the VWFA coordinates reported in the literature (aVWFA, cVWFA and pVWFA) to the tract cortical endings: the vOT_vOF cortical endings were related to the pVWFA, and the vOT_pAF cortical endings to the aVWFA. The cVWFA was located in the middle of these two tract endings. We think that the coordinates reported in cVWFA might relate to the averaged results obtained in meta-analytic studies which comprise various kinds of contrasts and tasks and, therefore, might be expected to produce results centered in this middle region.

Our results also confirmed that some discrepancies regarding the connectivity of the VWFA could be explained by the initial choice of functional contrasts. Studies highlighting the role of the pAF as the main WM fiber tract linking the VWFA to other regions (Bouhali et al., 2014; Thiebaut de Schotten et al., 2012) reported a more anterior VWFA than studies supporting an additional role for the vOF WM fiber tract in this regard (Weiner et al., 2016b; Yeatman et al., 2014b, 2013). Our results linked the anterior VWFA to the semVWFA and the more posterior VWFA to the perVWFA, supporting the previously expressed idea that for the perVWFA a word is mostly a visual object while the semVWFA is the first region to deal with the word as a language unit.

In this chapter, we mainly examined the cortical endings of the vOF and pAF tracts and their overlap with perVWFA and semVWFA. In the next empirical chapter we further extend the work reported in the present experiment, examining other brain regions outside vOT that these WM tracts connect to which form part of the core reading network. The perVWFA connects to the iPS, which is part of the pPC and occipital cortex, whereas the semVWFA connects to a region in the pPC centered on the AG. According to Weiner et al. (2016; p. 2): *"For example, in terms of function, the vOF connects dorsal and ventral visual regions and is believed to carry signals that are important for a variety of perceptual functions (Takemura et al., 2015; Yeatman et al., 2014), while the pAF is intermingled with the arcuate and principally terminates in cortical regions that are important for language (Catani et al., 2005; Catani & Thiebaut de Schotten, 2008)"*. Along these lines, as we discuss in the next chapters, in our DWI analysis we observed that

the pAF continues to the IFG through the anterior arcuate fasciculus (aAF).

Therefore, the next chapter will be entirely dedicated to studying the relationship between the vOT and the areas connected via the vOF (iPS), pAF (AG), and aAF (IFG).

Reading behavior is associated with functional activation in the vOT

Finally, we examined if functional activation within the vOT predicted individual differences in reading behavior. Reading behavior was operationalized as reaction times in a lexical decision task that participants performed outside the scanner. Interestingly, our results showed that only the perceptual contrasts consistently predicted word and pseudoword reading in a patch of cortex in the posterior lateral occipitotemporal sulcus that coincides with the perVWFA. The semantic contrasts did not yield such consistent and systematic results: some contrasts were associated only with some of the lexical decision measurements (with different locations found depending on the behavioral measure), and other contrasts did not show any association at all with reading performance in the lexical decision task (e.g., RWvsPW).

This result is in line with some of the points already discussed above. We think that the consistent prediction of reaction times, regardless of the type of strings presented in the lexical decision task (RWs/PWs/CSs), for all the perceptual contrasts (RWvsPS/CB/SD) might be due to the fact that all visual word processing goes through the same visual feature extraction location in the posterior lateral occipitotemporal sulcus.

Furthermore, as can be seen in Figure 23, the reaction times from the lexical decision task for CS was the reading behavior most strongly localized in the perVWFA. CS detection is fast and it may rely only on visual characteristics, without reading per se being required or even possible. Therefore, at this point, it would reasonable to assume that the perVWFA is not exclusive for words and is involved in 'modality agnostic' visual feature extraction.

Conclusion

Our functional and structural results suggest that there is a computational continuum dedicated to visual word processing in the vOT. A combination of functional contrasts of different types (semantic and perceptual) with the pAF and vOF cortical endings was able to consistently localize two segregated VWFAs involved in visual word recognition in the lateral occipitotemporal sulcus. Temporally, we interpret this as demonstrating that the first processing stage is in the posterior lateral occipitotemporal sulcus, innervated by the vOF, and is responsible for visual feature extraction. A more anterior and centrally located part of the same lateral occipitotemporal sulcus, innervated by the pAF, is the next processing stage and constitutes the first interface with the language network.

In the next empirical chapter we will investigate the interactions of the regions identified within the vOT with other cortical areas (pPC and IFG) that are structurally connected with the vOT via the vOF and pAF WM tracts. This will allow us to further examine if the results observed in this first experiment extend to other language areas.

8 EXPERIMENT 2: pPC and IFG

In the previous experiment, we provided evidence suggesting a functional segregation in the vOT based on the perceptual versus semantic characteristics of functional contrasts, and further demonstrated that this segregation it also related to the two WM fiber tracts innervating the vOT. The vOT seems to be the first processing stage right after vision, so that the visually accessed words reach the language system through an interactive computational process. The literature suggests that two of the main brain regions involved in this integrative process are the pPC (AG and IPS) and the IFG. In this experiment we seek to test if the pPC and the IFG, both connected to the vOT by the WM tracts identified in Experiment 1, contribute to the functional segregation observed in the vOT.

8.1 Methods

MRI and behavioral data from the unique 66 participants in the Main Experiment were used for this study. Please refer to Experiment 1 for full details regarding Participants, Materials and Procedures, MRI acquisition and MRI Data Processing. The ROI definition and Data Analysis, although similar in nature, are specific to this experiment.

8.1.1 ROI definition

Analogous to the procedure used in Experiment 1 to define the vOT, we defined the pPC and IFG cortical areas using masks which restricted subsequent fMRI analyses. For the pPC, using Freesurfer's automated grey matter parcellations, we extracted and added together the left supramarginal, inferior parietal, superior parietal cortices and occipital

superior/transversal sulcus. We extended the pPC by including the superior parietal and the occipital superior/transversal sulcus with the objective of covering the IPS in its entirety, as we wanted to include the occipito-parietal cortical endings of the vOF (see Figure 24*a1-a4* and Figure 24*b2*). For the IFG, we added together the Freesufer parcellations for the left *pars orbitalis*, *pars triangularis* and *pars orbitalis* (see Figure 24*c1* and *c2*).

Figure 24. Cortical areas of interest in the pPC and the IFG and tract ROIs in pPC

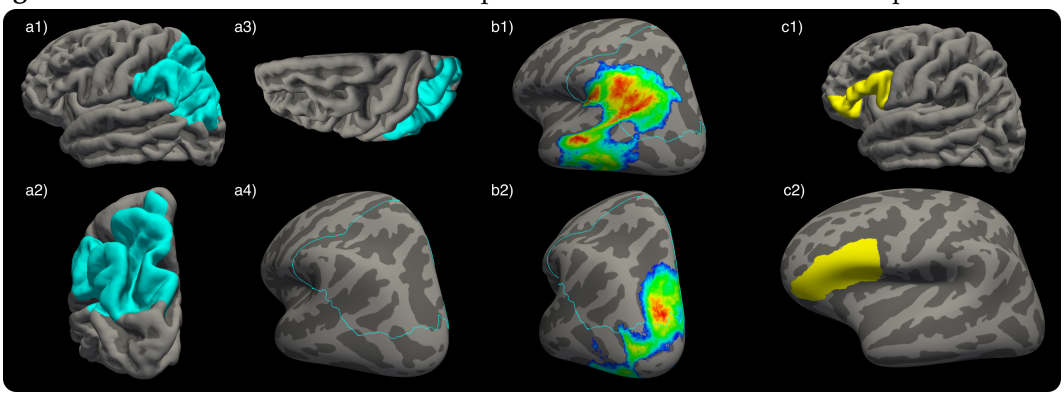

pPC (blue) and IFG (yellow) cortical areas of interest used as a mask in the fMRI analysis from different orientations and displayed on various surfaces. a) left hemisphere pial surface in the typical a1) sagittal (lateral), a2) axial (dorsal), and a3) coronal (posterior) positions. a4) shows the pPC on the inflated Freesurfer fsaverage brain, where the dark areas indicate sulci and the light areas indicate gyri. b1) shows the outline of the pPC cortical area of interest and the probabilistic map of the pAF tract cortical endings (minimum values in blue correspond to 35% of the subjects and maximum values in red to 92.5% of the subjects). b2) shows the outline of the pPC cortical area of interest and the probabilistic map of the vOF tract cortical endings (minimum values in blue correspond to 35% of the subjects and maximum values in red to 90.0% of the subjects). c1) shows the IFG in a sagittal rendering of the pial surface, and c2) shows the same but on an inflated surface. Note: this is in fsaverage space, the cortical area of interest will be different for each individual.

Two additional masks were created as a function of the cortical endings of the pAF and vOF WM tracts of interest: the pPC_pAF (see Figure 24*b1)* and pPC_vOF (see Figure 24*b2)* ROIs. These ROIs were created by masking the cortical tract endings with the pPC cortical area of interest for each WM tract. The renderings of the probabilistic maps of both tracts are displayed in Figure 24*b* for reference, but these ROIs were calculated and used at the individual level.

8.1.2 Data Analysis

We performed two separate fMRI analyses, inside the pPC and IFG masks. We used the same contrasts as in the previous experiment: RWvsPW/CS/FF/PS/CB/SD (for both block and event-related designs). Per fMRI design, contrast and subject, the T value of the GMax inside the above-described masks was located (with MNI X, Y, Z coordinates) and saved for analysis.

Afterwards, we conducted repeated-measures ANOVAs for each contrasts' GMax X, Y, and Z values to explore if there was a location gradient related to the semantic/perceptual characteristics of the contrasts of interest in the pPC and in the IFG. Additionally, to further examine to what extent the contrasts might reveal functional activation for semantic or perceptual contrast in different locations, we performed a hierarchical cluster analysis, as implemented by R's hclust (Murtagh, 1985), including each contrast's GMax T (mean and standard deviation) values, for both the pPC and the IFG.

The selected pPC cortical mask was quite large, and we were more interested in the AG and iPS. As our hypothesis stated that semantic contrasts would connect through the pAF to the AG while perceptual contrasts would connect to the iPS *via* the vOF, we also repeated the above-mentioned analysis within the ROIs defined by the pPC_pAF (Figure 24*b1*) and the pPC_vOF (Figure 24*b2*) tract cortical endings, separately. The per-subject GMax T, X, Y, Z values were obtained within each ROI. Additionally, a repeated-measures ANOVA was performed to compare the T values between the two ROIs.

To examine the relation between individual reading abilities (measured by the lexical decision task that participants performed outside the scanner) and functional activations, separate linear regression analyses were conducted at every vertex within the pPC and IFG. For the functional contrasts, we selected RWvsPW to represent the semantic contrasts and RWvsCB to represent the perceptual contrasts. For the lexical decision scores we used the average reaction time for RW and PW. Thus, in total we conducted four linear regression analyses in pPC and four in IFG: RWvsPW and RWvsCB predicting RW reaction times and RWvsPW and RWvsCB predicting PW reaction times.

8.2 Results

As indicated, first we characterized the global maximas (GMax) per design, contrast and subject for the pPC and IFG cortical areas of interest to examine potential functional dissociations related to the characteristics of the functional contrasts (i.e., perceptual, semantic). For this initial analysis, we conducted repeated-measures ANOVAs and a hierarchical cluster analysis. Second, for the pPC, we examined whether or not there was any association between the T values for the different contrast activations along the X-, Y-, and Z-axes, separately for the pPC_vOF and pPC_pAF ROIs. Finally, we examined if the functional activation in the pPC and IFG was predicted by the lexical decision behavioral data, as was done previously in Experiment 1 for the vOT.

8.2.1 pPC

8.2.1.1 fMRI characterization

To examine the hypothesis that the different contrasts yielded different cortical segregations within the pPC, first we analyzed the GMax T values for the RWvsCB/SD/PS/PW/CS/FF contrasts in the pPC and in the ROIs defined by the pPC_vOF and pPC_pAF (for both block and event-related designs).

When considering the whole fMRI pPC mask, semantic contrasts for both block and event-related designs showed an anterior versus posterior organization around the AG: RWvsPW was the most posterior one, RWvsCS was intermediate, and RWvsFF was the most anterior one. Perceptual contrasts were not systematically organized (see Figure 25*a*).

When the search for GMax was restricted to the pPC_pAF, the results were similar: in this case, all perceptual contrasts across both event-related and block fMRI designs were grouped in the same location around the AG, with the semantic RWvsPW contrast being localized in the same place but slightly dorsally, and RWvsCS/FF anterior to the RWvsPW maxima (see Figure 25*b*).

Finally, the averages for GMax in pPC_vOF showed a similar pattern: all contrasts were located around the intraparietal sulcus (iPS), and almost in the superior occipital sulcus for both fMRI designs. The RWvsCS contrast for both the event-related and the block fMRI designs was the only GMax that segregated, being located on the side of the iPS. The RWvsPW

contrasts for both fMRI designs, although part of the same semantic group, were located in the most ventral areas (see Figure 25*c*).

Figure 25. Average locations for perceptual and semantic contrasts in pPC

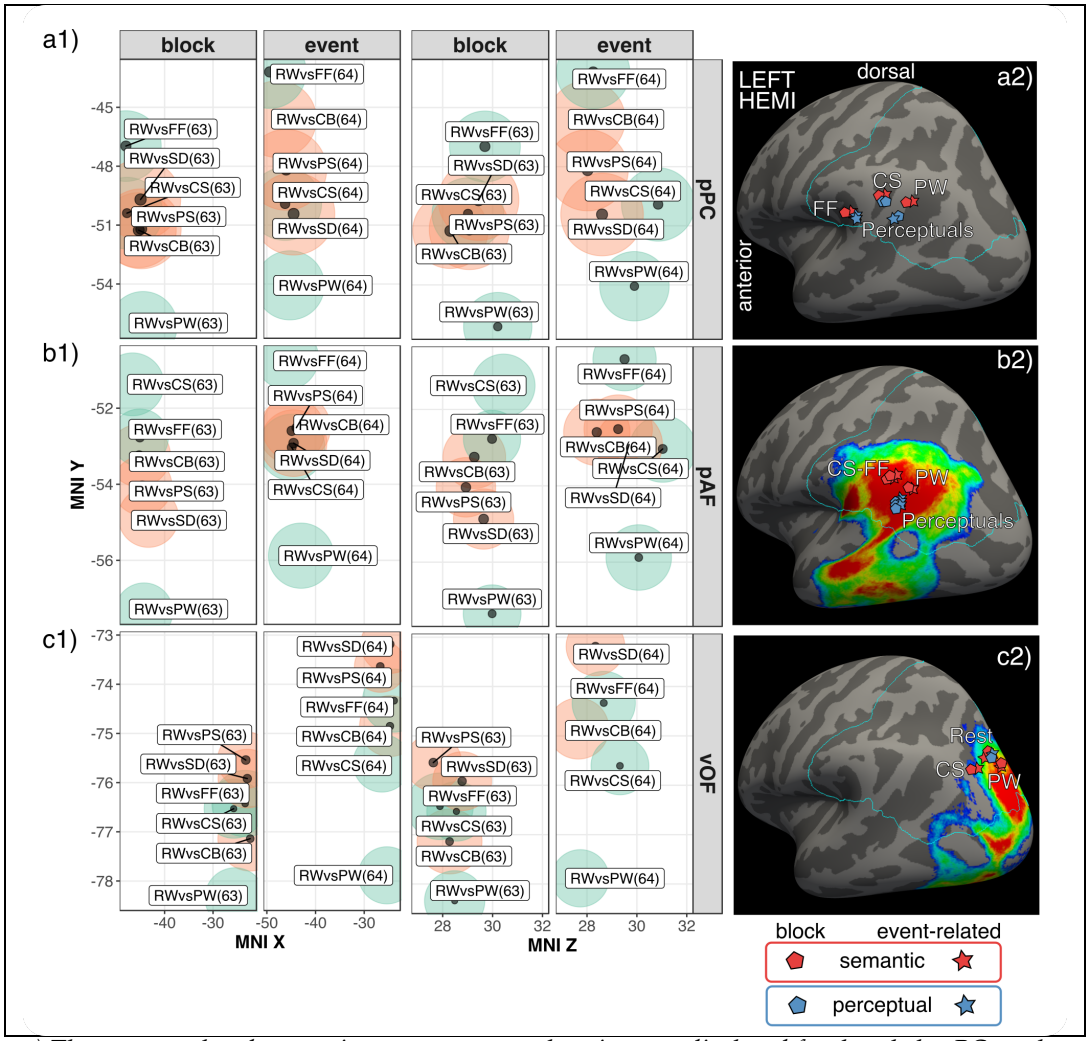

a) The perceptual and semantic contrast average locations are displayed for the whole pPC mask, and within the b) pPC_pAF, and c) pPC_vOF cortical ending ROIs. The same information is shown in a1-b1-c1) MNI X,Y and Z,Y plots and in a2-b2-c2) surface renderings. In the MNI X,Y,Z plots: the size of the inner black circle indicates the average T value, and the size of the outer circle is scaled to the standard deviation of the coordinate positions (bigger circle indicates more spread data). The color of the outer circle indicates if the contrast is semantic (green) or perceptual (red). In the surface renderings, all the 12 different contrasts have been located. Perceptual contrasts grouped together for pAF and vOF, but not for pPC. Semantic contrasts grouped together in block-event-related pairs, but the three contrasts did not group together in any ROI.

Furthermore, with the objective of statistically testing these differences, we performed a series of ANOVAs. First, we performed, per ROI (pPC, pPC_pAF, pPC_vOF) three separate 2 (Design: block, event) X 6 (Contrast: RWvsPS/CB/SD/PW/CS/FF) repeated-measure ANOVAs, one per MNI

coordinate (i.e., X, Y and Z) as dependent measures. We describe the results for these analyses below, organizing the results in different subsections as a function of the ROI used.

Analysis for the whole pPC mask

The ANOVA for the X and Y coordinates revealed a main effect of Contrast ($F(6,277.1) \geq 3.64$, $p < 0.001$, $R^2_{Adj} \geq 0.47$). Post-hoc analysis showed that on the X-axis this effect was driven by a statistically significant difference in the location of the RWvsFF contrast relative to the RWvsPW/SD contrast ($p \leq 0.05$). On the Y-axis this effect was driven only by RWvsPW, which was significantly more posterior than all the other contrasts ($p \leq 0.05$, although marginally for RWvsCS/SD). The ANOVA for the Z coordinate did not reveal any statistically significant effect.

For the T value (see Table 4), we performed both a clustering analysis and an ANOVA. The clustering analysis separated RWvsPW/CS into one group and the other four contrasts into another group. Similarly, the ANOVA showed that the main effect of Contrast was significant ($F(6,296.4) \geq 18.53$, $p < 0.0001$, $R^2_{Adj} \geq 0.76$), driven by statistically significant higher values for RWvsPS/SD/CB/FF than for RWvsPW/CS ($p \leq 0.001$). It is worth mentioning that RWvsCS was higher than RWvsPW, although this difference was only marginally significant ($p = 0.08$).

Analysis in the pPC_pAF ROI

The results of the analyses for the pPC_pAF ROI further qualify the results described for the analyses of the main pPC ROI. The ANOVA for

the Y-axis showed a main effect of Contrast (F(6,283.1) = 2.61, $p < 0.02$, $R^2_{Adj} = 0.41$). This main effect was due to the more posterior position for the RWvsPW contrast relative to the RWvsCS/FF contrast across both fMRI designs ($p \leq 0.02$). No significant effects emerged for the ANOVAs conducted for the X- and Z-axes. The ANOVA for the T value also showed a main effect of Contrast (F(6,287) ≥ 8.52, $p < 0.0001$, $R^2_{Adj} = 0.71$), driven by significantly lower values for the RWvsPW/CS contrasts relative to all other contrasts ($p \leq 0.02$).

Analysis in the pPC_vOF ROI

The X,Y,Z ANOVAS revealed no location main effects, all coordinate averages were centered in the iPS region. Nevertheless, all the interest lies in the T value. The ANOVA for the T value showed a main effect of Contrast (F(6,244.1) = 10.77, $p < 0.0001$, $R^2_{Adj} = 0.57$). This main effect was due to significantly higher values for all perceptual RWvsCB/PS/SD compared to semantic RWvsCS/PW/FF values ($p \leq 0.01$). The only non-significant differences were for RWvsCB and RWvsFF ($p = 0.3$). These results are analogous to what we saw in the vOT.

Differences in T between pPC_pAF and pPC_vOF

To examine if there were consistent differences in T values obtained in the pPC_vOF versus the pPC_pAF ROIs (see Table 4), we performed a repeated-measures ANOVA including ROI (pPC_pAF, pPC_vOF) as an additional factor along with the existing Contrast (RWvsPS/CB/SD/PW/FF/CS) and Design (block, event-related) factors. This ANOVA analysis (F(7,288.7) = 15.33, $p < 0.0001$, $R^2_{Adj} = 0.65$) revealed

a main effect for ROI, with the pPC_pAF ROI showing higher T values than the pPC_vOF ROI ($p < 0.001$) and a main effect for Contrast. This main effect was due to significantly higher values for all perceptual RWvsCB/PS/SD than for semantic RWvsCS/PW/FF values ($p \leq 0.03$). The only contrast that behaved differently from contrast conducted for the vOT was RWvsFF: there were non-significant differences for RWvsCB/PS and RWvsFF ($p \geq 0.2$), but significant differences for RWvsFF and RWvsFF ($p < 0.001$). No main effects or interactions involving the Design factor were statistically significant in this analysis ($p = 0.66$).

8.2.1.2 Prediction of behavioral results

Next, we examined if functional activation within the main pPC ROI could predict individual word and pseudoword reading abilities, as measured by the lexical decision task that participants had performed outside the scanner. To this end, only for the fMRI block design, we performed separated vertex-wise linear regression analyses restricted to the whole pPC mask using the T value of one perceptual (PWvsCB) and one semantic contrast (RWvsPW) as the independent variables, and the individual average reaction times (RTs) to RW and PW as the dependent values (these combinations yield a total of 4 vertex-wise regressions). The cluster-wise corrected results revealed a systematic predictive capacity for both the PWvsCB and the RWvsPW contrasts for pseudoword and word reading (see Figure 26).

Figure 26. Functional activation in pPC cortical areas predicting reading behavior

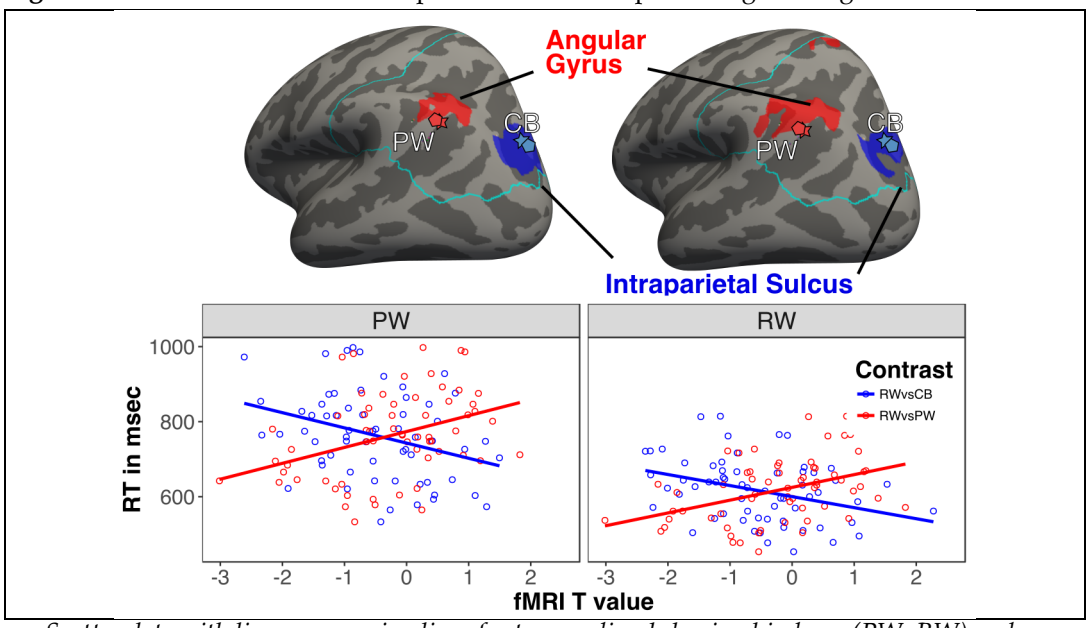

Scatterplots with linear regression lines for two reading behavioral indexes (PW, RW) and a perceptual (RWvsCB) and a semantic (RWvsPW) contrast. The horizontal axis shows the T value of the most significant vertex of the cluster (which is different in each of the 4 cases). The vertical axis shows the average reaction time in milliseconds for the reading behavior measures. In the top row we rendered the clusters where the prediction was significant, vertex-wise (p = 0.05) and cluster-wise (p = 0.05) corrected. In each rendering we composed the two most significant clusters predicting PW or RW RTs. Furthermore, for reference, the average GMax values were rendered as well. For the perceptual contrast, the average GMax location lies in the predictive clusters. For the semantic contrast, the average GMax location lies a few millimeters ventrally to the semantic clusters.

Consistent with our hypothesis, RWvsPW predicted activation in the AG for pseudoword and word reading and RWvsCB predicted activation in the iPS also for pseudoword and word reading. The direction of the correlation for RWvsPW in the angular gyrus with PW and RW RTs was positive, while for RWvsCB in the iPS with PW and RW RTs the correlation was negative.

Table 4. Means and standard deviations (sd) of T values per contrast and design

	pPC				*pPC_pAF*				*pPC_vOF*				*IFG*			
PERCEPTUAL	**mean**	***sd***	**mean**	***sd***	**mean**	***sd***	**mean**	***sd***	**mean**	***sd***	**mean**	***sd***	**mean**	***sd***	**mean**	***sd***
RWvsCB	3.74	*0.95*	3.58	*1.14*	3.30	*0.93*	3.32	*1.09*	2.82	*1.03*	2.86	*0.75*	3.58	*1.16*	3.51	*1.04*
RWvsPS	3.72	*1.21*	3.56	*1.18*	3.37	*1.02*	3.06	*1.07*	3.19	*0.98*	2.82	*0.92*	3.64	*1.13*	3.35	*0.97*
RWvsSD	3.80	*1.08*	3.65	*1.12*	3.34	*1.09*	3.28	*1.11*	3.12	*1.02*	2.83	*0.80*	3.72	*1.06*	3.53	*1.19*
SEMANTIC	**mean**	***sd***	**mean**	***sd***	**mean**	***sd***	**mean**	***sd***	**mean**	***sd***	**mean**	***sd***	**mean**	***sd***	**mean**	***sd***
RWvsCS	3.04	*0.77*	3.14	*0.83*	2.92	*0.81*	3.10	*0.92*	2.54	*0.57*	2.48	*0.80*	3.14	*0.92*	3.11	*0.82*
RWvsFF	3.52	*1.01*	3.42	*1.08*	3.13	*0.99*	3.04	*0.99*	2.66	*0.83*	2.68	*0.68*	3.49	*1.13*	3.46	*1.04*
RWvsPW	2.81	*0.66*	2.70	*0.65*	2.72	*0.67*	2.52	*0.61*	2.35	*0.63*	2.32	*0.43*	2.24	*0.76*	2.49	*0.61*
	BLOCK		***EVENT***		***BLOCK***		***EVENT***		***BLOCK***		***EVENT***		***BLOCK***		***EVENT***	

8.2.2 IFG

8.2.2.1 fMRI characterization

To examine the hypothesis that the different contrasts yielded different cortical segregations within the IFG, first we analyzed the GMax T values of the RWvsCB/SD/PS/PW/CS/FF contrasts for both block and event-related designs. As can be observed in Figure 27, all contrasts group together, except RWvsPW, which consistently across both block and event-related designs lies anteriorly to the rest of the contrasts.

Figure 27. Perceptual and semantic contrast's average locations in IFG

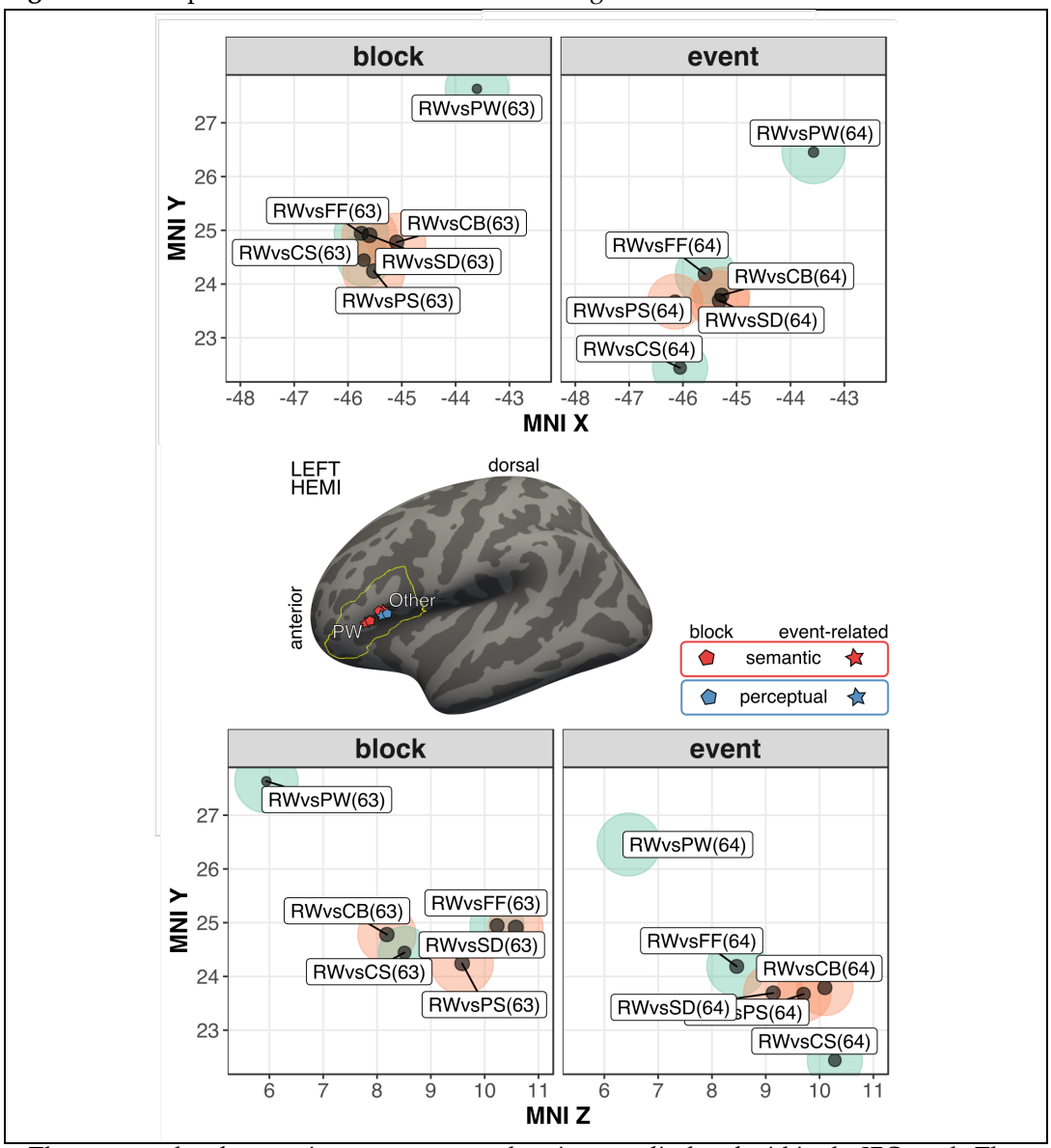

The perceptual and semantic contrast average locations are displayed within the IFG mask. The same information is shown in MNI X,Y and Z,Y plots and on surface renderings. In the MNI X,Y,Z plots: the size of the inner black circle indicates the average T value, and the size of the outer circle is scaled to the standard deviation of the coordinate position (bigger circle indicates greater data spread). The color of the outer circle indicates if the contrast is semantic (green) or perceptual (red). In the surface renderings, all the 12 different contrasts have been located. RWvsPW (for block and event-related) activation lies more anteriorly than the activation for the rest of the functional contrasts.

The ANOVA for the X-axis revealed a main effect of Contrast ($F(6,298.7) = 3.12$, $p < 0.005$, $R^2_{Adj} \geq 0.49$). Post-hoc analysis showed that this main effect was due to RWvsFF being more medial than the rest of the contrasts ($p \leq 0.03$), except RWvsCB ($p = 0.12$). The ANOVA for the Y-axis revealed a main effect of Contrast ($F(6,298.45) = 2.21$, $p < 0.04$, $R^2_{Adj} \geq 0.32$), which was

driven by a significant difference between RWvsPW and RWvsCS (p = 0.03). The analysis for the Z-axis revealed no statistically significant effects (p = 0.1). For the T value, the clustering analysis separated the T value of the RWvsPW contrast into one group and the remaining five contrasts into another group (see Table 4). The ANOVA for the T value revealed a main effect of Contrast (F(6,298.8) = 33.70, $p < 0.0001$, $R^2_{Adj} \geq 0.64$). Post-hoc analysis showed that this main effect was due to the fact that the RWvsPW contrast was smaller than the remaining contrasts ($p \leq 0.001$) and that RWvsCS, although bigger than RWvsPW, was smaller than the remaining contrasts ($p \leq 0.01$).

8.2.2.2 Prediction of behavioral results

Finally, we examined if functional activation within the IFG predicted individual word and pseudoword reading abilities, measured as reaction times in a lexical decision task outside the scanner. To this end, and only for the fMRI block design, we performed separate vertex-wise linear regression analyses restricted to the IFG mask. As in the pPC, we used the T value of one perceptual (RWvsCB) and one semantic contrast (RWvsPW) as independent variables, and the individual average reaction times (RTs) for RW and PW as the dependent variables (these combinations yielded a total of 4 vertex-wise regressions). The cluster-wise corrected results revealed a systematic predictive capacity for both the RWvsCB and the RWvsPW contrasts for pseudoword and word reading (see Figure 28).

Figure 28. Functional activation in IFG cortical areas predicting reading behavior

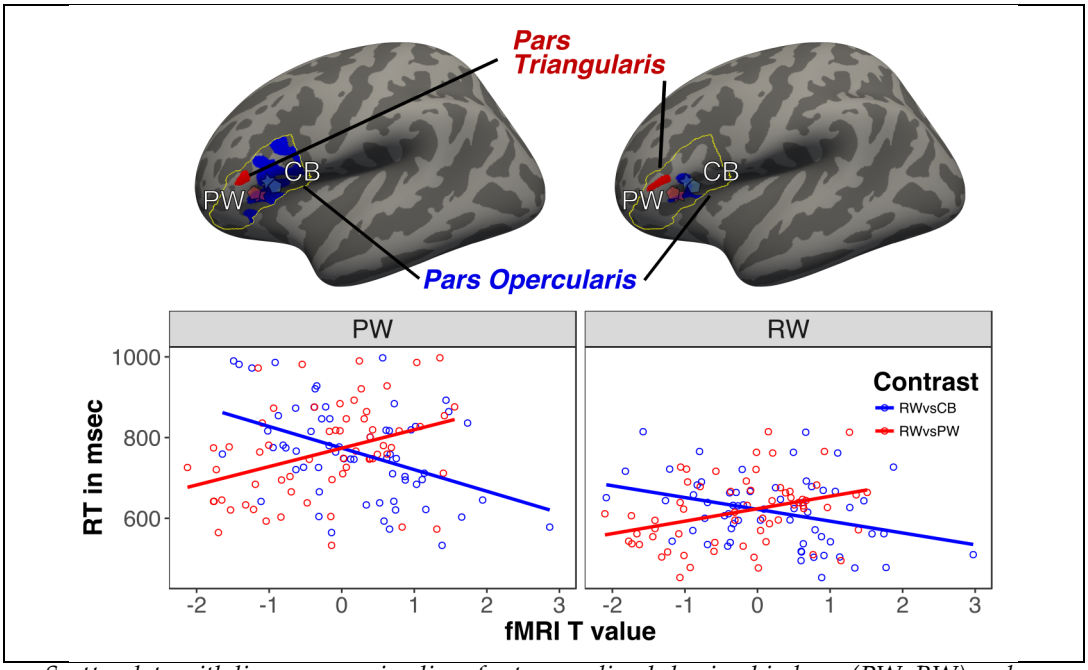

Scatterplots with linear regression lines for two reading behavioral indexes (PW, RW) and a perceptual (RWvsCB) and semantic contrast (RWvsPW). The horizontal axis shows the T value of the most significant vertex of the cluster (which is different in each of the 4 cases). The vertical axis shows the average RT in milliseconds for the reading behavior indexes. In the top row we rendered the clusters where the prediction was significant, vertex-wise ($p = 0.05$) and cluster-wise ($p = 0.05$) corrected. In each rendering we composed the two most significant clusters predicting PW or RW RTs. Furthermore, for reference, the average GMax values were rendered as well. For the perceptual contrast, the average GMax T location lay within the predictive clusters. For the semantic contrast, the average GMax T location lay a few millimeters ventrally to the semantic clusters.

These results are strikingly similar to the ones obtained for the pPC. In both cases RWvsPW positively predicted reading behavior, and RWvsCB negatively predicted reading behavior. Also, in both cases the average GMax locations coincided for RWvsCB, but lay a few millimeters more ventrally in the case of RWvsPW.

8.3 Discussion

This chapter was focused on examining potential parallelism between the vOT and the pPC and IFG related language areas. Unlike the findings observed for vOT in the previous chapter, the pPC and IFG results did not show such a clear segregation between perceptual and semantic functional contrasts. However, we found other subtle and relevant

differences that can shed further light on the computations carried out by the pPC and IFG along the visual word recognition process.

pPC: false fonts as a perceptual contrast

First, we analyzed the average locations in the X-, Y-, Z- axes and GMax T values for the whole pPC, pPC_vOF and pPC_pAF ROIs. The first remarkable finding was that the location averages for the whole pPC ROI were similar to those found for the much smaller pPC_pAF ROI. Logically, this was explained by the fact that most of the GMax T values for the big pPC ROI laid inside the smaller ROI defined by the pPC_pAF tract cortical endings. Also, these GMax T values were more organized in the pPC_pAF ROI, possibly due to lower variability for the data in this smaller ROI.

The second main finding was that in all three ROIs (i.e., whole pPC, pPC_vOF and pPC_pAF), the locations aligned well with the maximum probability areas of the cortical tract endings. In spite of this finding, we did not find any other strong spatial segregation such as that found for the vOT. The only systematic difference between the functional contrasts in this regard was found for the RWvsPW in the AG, which was located more posteriorly than the other semantic contrasts (e.g., RWvsCS/FF). In contrast, the average GMax T values offered more interesting results. In the iPS (demarcated by the pPC_vOF cortical endings in this case), the results mimic what we found in the vOT: all perceptual contrasts showed higher T values than semantic contrasts, with the exception of the RWvsFF and RWvsCB contrasts, which showed no differences. In the AG (demarcated by the pPC_pAF cortical endings in this case), we observed a

shift in how the RWvsFF related to the rest of the contrasts. Here the RWvsFF functional contrast behaved like the other perceptual contrasts, showing higher T values than the remaining semantic contrasts (i.e., RWvsPW and RWvsCS). Furthermore, it is worth mentioning that RWvsCS had marginally higher values than RWvsPW, as well.

It is not surprising that the perceptual contrasts showed higher T values than the semantic ones. If we remove only the visual perceptual information from the word signal, the semantics, phonology and orthography remain intact. Nevertheless, we think that the change (between vOT and pPC) shown for the RWvsFF contrast (and the tendency demonstrated for the RWvsCS contrast) tell an interesting story. As explained in the *Methods* section above, we built our FF based on a real script (i.e., Georgian). The vOT could not discern between the RWvsCS and the RWvsFF contrasts, and both were localized at the semVWFA instead of the perVWFA. The interesting element is that once they reached the "higher" computation areas (i.e., pPC), FFs did not seem to be treated like characters anymore. In the iPS, directly connected to the perVWFA, this effect was hardly discernible. But in the AG, the RWvsFF contrast was treated like a perceptual contrast. Thus, whereas vOT appeared to treat FFs as strange characters, the AG seemed to treat them as small drawings that control only for the dark/light features as the scrambled words do.

It is worth exploring this idea in futures studies. In most of the previous studies, FFs have not generally been based on real scripts (Brem et al., 2010), but on little drawings or random shapes created artificially in the lab to mimic a real script. In such cases, functional responses to FFs might

not reflect the statistical regularities found in a real script (Changizi et al., 2006; Changizi and Shimojo, 2005). An experiment comparing different types of FFs would help to elucidate this possibility, and help us further understand at which moment the pPC ceases to treat FFs as character strings and begins to treat them as drawings that function like perceptual stimuli.

The third and last relevant finding from the examination of the pPC was related to the fact that the most extreme perceptual and semantic functional contrasts predicted reading behavior. We selected RWvsCB as the 'most perceptual' contrast, as CBs are the selected stimuli that have the least close relationship to word stimuli. We selected RWvsPW as the most semantic contrast, because PW are the only stimuli that only leave the semantics out of a RW. There are two aspects to highlight in the reading behavior prediction findings: 1) Although we selected the whole pPC mask, the perceptual contrast predicted behavior in the iPS, and the semantic contrast predicted behavior in the AG; 2) The RWvsCB cortical activation cluster that predicted behavior coincided with the perceptual contrast average GMax T location, whereas the RWvsPW cortical activation cluster was a little bit more ventral than the semantic average GMax T location. We think that this is a remarkable finding that is consistent with our results for the perVWFA and semVWFA, and most importantly, it is in line with findings from previous studies. Using RWvsPS as contrasts, Ben-Shachar et al.'s (2011, 2007) studies have already shown iPS activations, while Kay and Yeatman (2017) have also demonstrated functional connectivity and task effects between the iPS and the VWFA. Meanwhile, AG has been extensively associated with

semantics in previous research (Binder and Desai, 2011; Seghier et al., 2010).

IFG: anterior IFG areas responded more semantically

Results in the IFG cortical area pointed in the same direction as the vOT results, with semantic processing associated with more anterior parts. Nevertheless, for the IFG, the 'semantic' functional contrasts were mostly limited to RWvsPW. Results obtained for the average location, the T value and also the linear regression results predicting reading behavior were all consistent in showing a clearly different pattern for the RWvsPW relative to the other functional contrasts.

Regarding the location coordinates, our results showed that the averages for the RWvsPW were more anteriorly located across both block and event-related fMRI designs. And, we also found a hint of a gradient along the X-axis, as previously reported by Vinckier et al. (2007). Nevertheless, as happened for the pPC, the most interesting results were related to the GMax T values: 1) RWvsFF was part of the group of perceptual functional contrasts; 2) the RWvsPW was the smallest and most anteriorly located contrast, and clearly separated out from all the other contrasts; and, 3) the RWvsCS contrast lay in between the RWvsPW contrast and the rest of the perceptual functional contrasts.

As the results from RWvsPW are well-aligned with previous findings showing activation in the *pars triangularis* (Badre and Wagner, 2002; Wagner et al., 2001), it is worthwhile further discussing the results for the RWvsCS functional contrast. This result is of interest because it shows the

evolution of an activation gradient within the semantic contrasts. In the vOT we had 3 perceptual and three semantic contrasts clearly separated; in the iPS, the RWvsFF contrast started to fall apart; in the AG the RWvsFF contrast was fully part of the perceptual contrast group and the RWvsCS contrast was marginally larger than that for RWvsPW. In the IFG, following the same trend, the RWvsCS contrast was definitively separated out and only the RWvsPW (in fact, the most semantic contrast) remained in the semantic contrast group.

That activation for the RWvsCS contrast lay more posterior than that for RWvsPW, coinciding with the *opercularis*, is consistent with findings from previous studies (Poldrack et al., 1999) and highlights the role of the *pars opercularis* in phonological processing. Therefore, the differentiation between RWvsPW and RWvsCS could be explained as a double contrast: if the RWvsPW contrast leaves only the semantic part of a word, and RWvsCS leaves both the semantics and the phonology, the main component differentiating these two contrasts should be the phonological component.

Finally, we would like to mention the striking similarities between the functional results of the pPC and IFG in terms of their predictions for reading behavior. In both cases we found that: 1) the prediction clusters from the RWvsCB functional contrast were more posteriorly located than the prediction clusters from the RWvsPW contrast, and 2) the prediction clusters from the RWvsCB functional contrasts coincided with the average GMax T locations for the RWvsCB contrast, but the prediction clusters from the RWvsPW functional contrasts were located slightly more

dorsally. In any case, consistent with previous studies, the area associated with RWvsCB was in the *opercularis*, while the area associated with the RWvsPW was in the *triangularis*.

Null effects of the fMRI design (block versus event-related) factor

Similar to what was observed in the vOT, the selection of block versus event-related fMRI designs had no effect on the location or the T values of the functional contrasts. In three analyses out of four, ROIs (i.e., whole pPC, pPC_vOF, pPC_pAF and IFG), the average coordinate locations for block and event-related fMRI designs fell almost one on top of the other systematically for every contrast. We find this result striking, considering that 1) we are selecting the highly variable GMax T value coordinates, and 2) we are averaging independently across the three X, Y, Z coordinates, that had previously been converted to MNI 152 from individual space. Although the values were close enough, the only cortical area where this did not happen for all the contrasts was the whole pPC ROI.

In this regard, our conclusion is that in controlled experimental settings, using the same amount of stimuli and presentation times, no statistically significant effects emerged, and both block and event-related designs behaved similarly. Nevertheless, although the existence of this null effect is important per se, confirming the reliability of the materials and methods here employed, we strongly recommend a further examination of the potential influence of the use of different fMRI designs for localizers in future studies.

Conclusion

The present study revealed that the selection of the localizer and functional contrasts had effects beyond the vOT, in associated reading regions such as the iPS, AG and IFG. Importantly, reading behavior was predicted by the functional activation of a semantic and a perceptual functional contrast in a different cortical location, with these locations mimicking the anterior-posterior segregation that we previously observed within the vOT: more posterior locations were found for perceptual operations and more anterior locations for semantic processing.

Now that we have specifically characterized the vOT, pPC (iPS, AG) and the IFG, in the next chapter we will proceed to link the areas together and to provide an integrative view of the computations carried out by these three reading regions and the WM fiber tracts connecting them.

9 EXPERIMENT 3: Multimodal integration of visual word recognition

In the previous experiments 1) we provided evidence suggesting a functional segregation within the vOT for the semantic *versus* perceptual characteristics of the functional contrasts, 2) we showed that this functional segregation relates to tract endings in the vOT and identified the vOT contrasts that predict individual reading behavior, and 3) we showed that these functional differences extend through the reading network, more precisely, to the pPC (AG and iPS) and the IFG.

The objective of the last experiment of this doctoral dissertation was to provide an integrative view of visual word recognition. To this end, we first characterized the WM tracts that connect these areas of interest and explored the relations between structural and functional results. Next, we created behavior predictive models in the cortical areas with the most significant results, integrating functional time-series and structural MRI information such as CT and qMRI. Finally, we performed a series of hierarchical regression analyses including functional and structural measures to predict reading behavior.

9.1 Methods, materials and experimental procedures

Please refer to Experiment 1 and Experiment 2 for information regarding participants, materials and procedures, MRI acquisition, MRI data processing and ROI definitions. Next, we describe the methods specific for this Experiment: qMRI data acquisition and analysis, a new DWI analysis

to create WM tracts between our functional ROIs, CT, and the corresponding data analysis.

9.1.1 qMRI acquisition and data processing

Data were collected on the same 3T Siemens TRIO whole-body MRI scanner detailed in Experiment 1 and 2, and during the same acquisition session. qMRI measurements were obtained from the protocols set forth in Mezer et al (2013). T1 relaxation times were measured from four T1-flash images with flip angles of 4°, 10°, 20°, 30° (TR=12 ms, TE=2.27 ms) at a scan resolution of 1.0x1.0x1.0 mm^3. For the purposes of removing field inhomogeneities, we collected four additional spin-echo inversion recovery (SEIR) scans with an echo-planar imaging (EPI) read-out, a slab inversion pulse, spectral spatial fat suppression, 2x acceleration factor, and a TR of 3 s. The inversion times were 50, 400, 1200, and 2400 ms, and were collected at a 2x2 mm^2 in-plane resolution and a slice thickness of 4 mm.

All qMRI data were processed using the mrQ software package in MATLAB to produce the MTV maps. The mrQ analysis pipeline corrects for RF coil bias using SEIR-EPI scans, producing accurate proton density (PD) and T1 fits across the brain. Using individual participants' voxels containing CSF within the ventricles, maps of macromolecular tissue volume (MTV) are produced calculating the fraction of a voxel that is non-water (CSF voxels are taken to be nearly 100% water). The full analysis pipeline and its description can be found at (https://github.com/mezera/mrQ).

9.1.2 ROI definition

This final experiment is focused on further integrating previous results. As a starting point for the analysis reported in this chapter, we used the average GMax cortical locations defined in Experiments 1 and 2. In *Figure 129* below the six ROIs based on the average functional contrasts calculated in the previous experiments are shown: two for each main region (i.e. vOT, pPC, IFG). The red ROIs are semantic ROIs and the blue ROIs are perceptual ROIs.

The blue ROI in the vOT corresponds to the average of the three perceptual contrasts (i.e., RWvsPS/CB/SD), and is equivalent to the perVWFA defined in Experiment 1. Similarly, the red ROI in the vOT corresponds to the average of the three semantic contrasts (i.e., RWvsPW/CS/FF). In the pPC, the blue ROI corresponds to the average perceptual contrasts in pPC_vOF and the red ROI to the average semantic contrasts in the pPC_pAF. In the IFG, the blue ROI corresponds to the average perceptual contrasts, including the RWvsFF, and the red ROI to the average semantic contrasts, excluding the RWvsFF. These ROIs were used in two different ways. On the one hand, we selected surface ROIs used for extracting structural information such as CT or MTV. On the other hand, we translated the center coordinate to the individual volume space and used it as the center of a sphere that defined the tracts between the regions.

Figure 29. Location of ROIs in the vOT, pPC and IFG

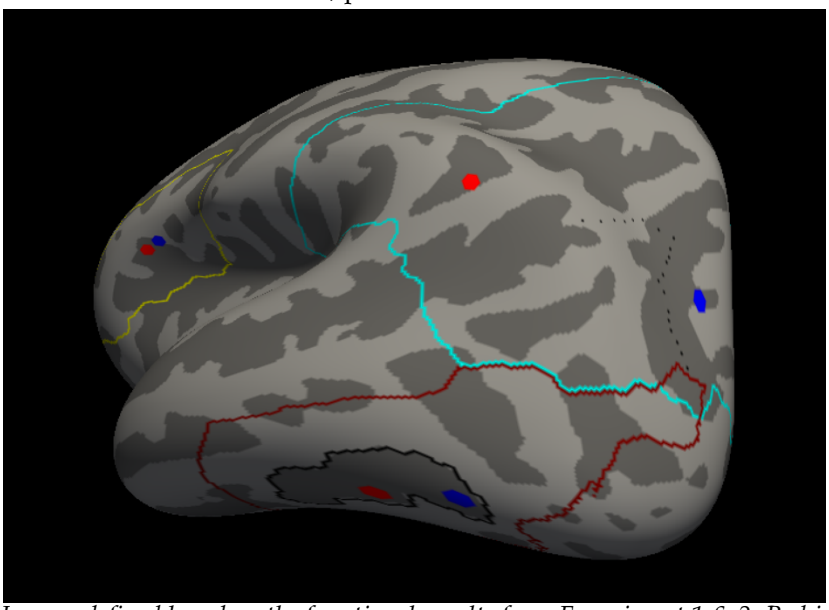

The six ROIs were defined based on the functional results from Experiment 1 & 2. Red is related to the averaged semantic contrasts and blue is related to the averaged perceptual contrasts for vOT, pPC and IFG regions.

The dark red outline corresponding to the vOT was already presented in Experiment 1, and the light blue outline corresponding to the pPC and the yellow outline corresponding to the IFG were already presented in Experiment 2. The black outline inside the vOT delineates the boundary of the lateral occipitotemporal sulcus (lOTS). Finally, the series of aligned black dots represent a path of vertexes of interest that go from ventral iPS to the end of the AG. These vertexes with the vertexes inside the IFG and lOTS ROIs were used in a regression analysis (explained below).

9.1.3 DWI and qMRI Data Analysis

With the objective of exploring the structural connectivity between the 6 semantic/perceptual ROIs, the DWI data was reanalyzed in Experiment 3. Subject motion was initially corrected by co-registering each volume to the average of the non-diffusion weighted *b0* images. Gradient directions were adjusted to account for this co-registration. Using FSL's topup, the

susceptibility induced off-resonance field was estimated, and eddy currents were corrected using FSL's eddy tool (Smith et al., 2004).

Subsequently, we used the MRtrix3.0 tools (Jeurissen et al., 2014). To enable robust quantitative comparisons across subjects, we performed bias-field correction to eliminate low frequency intensity inhomogeneities across the image, followed by a global intensity normalization of the median WM $b = 0$ intensity across all subjects.

Next, we obtained the average single fiber response functions across all subjects, and we used these averaged values for all subjects when estimating the fiber orientation distribution functions for each voxel using the $b = 1000$ and $b = 2500$ measurements. We implemented this analysis with MRtrix3's anatomical multi-tissue constrained spherical deconvolution (CSD; lmax = 4), and Freesurfer to inform the algorithm of the different types of tissues. Whole-brain fiber tracts were estimated with probabilistic tractography (with 2,000,000 fibers) using the iFOD2 algorithm (Tournier et al., 2010), and afterwards the SIFT2 algorithm (Smith et al., 2015) was applied to allow for the quantitative assessment of brain WM connectivity.

Next, we translated the 6 semantic/perceptual functional average coordinates shown in Figure 29 to the individual surface, using Freesurfer's mris_surf2surf program. The surface coordinate was translated to the volume coordinate to be used as the center of a sphere. Using these spheres as ROIs, three pairs of tracts were selected from the whole tractogram, for both semantic and perceptual ROIs: from vOT to

pPC, from vOT to IFG, and from PPC to IFG. The program was instructed to select only those fibers that had cortical endings inside both spheres.

Every fiber of the tract found in this manner had a weight assigned after the SIFT2 processing. We considered the apparent fiber density (AFD) value to be the sum of the weights of all fibers, and this measurement was used as a proxy for the connectivity between two areas. Furthermore, in order to obtain the average MTV values per tract, we obtained the mean MTV values for each fiber, multiplied them by the SIFT2 weight of the fiber, and then added all the individual fiber values and divided them by the total number of fibers.

9.1.4 Cortical thickness

The cortical thickness measurements were calculated using the standard Freesurfer processing pipeline (explained in Experiment 1). In the individual space, we obtained a per-vertex cortical thickness value that afterwards we mapped to the fsaverage space for comparison purposes.

9.1.5 Data analysis

To study the internal consistency of our WM connectivity data, we focused on the Test-Retest experiment (N = 31). We performed intra-class correlations (ICC) with several measurements to test the extent to which the data was reliable over time with a delay of 7-10 days. Afterwards, with data from the 66 subjects in the Main experiment, we examined the contribution of the WM tracts to the correlations of the functional data in different regions. To do so, we first selected 20 vertexes in the pPC, (see Figure 31*a*); second, for both the lateral occipitotemporal sulcus (lOTS)

and IFG ROIs, the T value for the RWvsCB and RWvsPW functional contrasts at every vertex was used to predict the T value of the same contrasts in every one of the 20 pPC vertexes using linear regression. In this step, only the adjusted R square was stored for later use. Third, the same calculations were performed, but in this case, the tract information (the per-WM tract MTV values previously calculated) was included in the linear regression. If the adjusted R square value of the new regression was superior to the stored adjusted R square value, the ordinary R square value was stored; otherwise, a zero was stored. In this way, we could obtain maps in the IFG and the lOTS showing the variance explained between the two regions, but only for those cases where the tracts contributed to explaining variance (see Figure 31*c*).

To check if there were parallelisms between the functional and a structural measurement, we repeated the same analysis as above using only CT values.

Afterwards, to integrate the different behavioral, functional and structural results, we performed a hierarchical regression analysis using different functional and structural indexes as independent variables and reading behavior (expressed as the reaction times to RW and PW in the lexical decision task that participants had performed outside the scanner) as the dependent variables.

9.2 Results

In this section we first report the patterns of WM connectivity between our regions of interest. Second, we show the contribution of these tracts to

the functional correlations between areas. Third, we report the hierarchical regression analysis results examining the contribution of several functional and structural measures in predicting reading behavior.

9.2.1 Patterns of WM connectivity

We examined 6 WM fiber tracts: 3 tracts connecting the semantic ROIs and 3 tracts connecting the perceptual ROIs (see Figure 30). We created WM tract equivalencies for the vOF as the tract that goes from the perVWFA to the iPS, for the pAF as the tract that goes from the semVWFA to the AG, and for the aAF as the tract that goes from the AG to the IFG. The rest of the WM tracts included the whole AF going directly from the semVWFA to the IFG, and the remaining two tracts, the perceptual vOT2IFG and the perceptual pPC2IFG.

Figure 30. WM connectivity pattern between regions for two moments in time

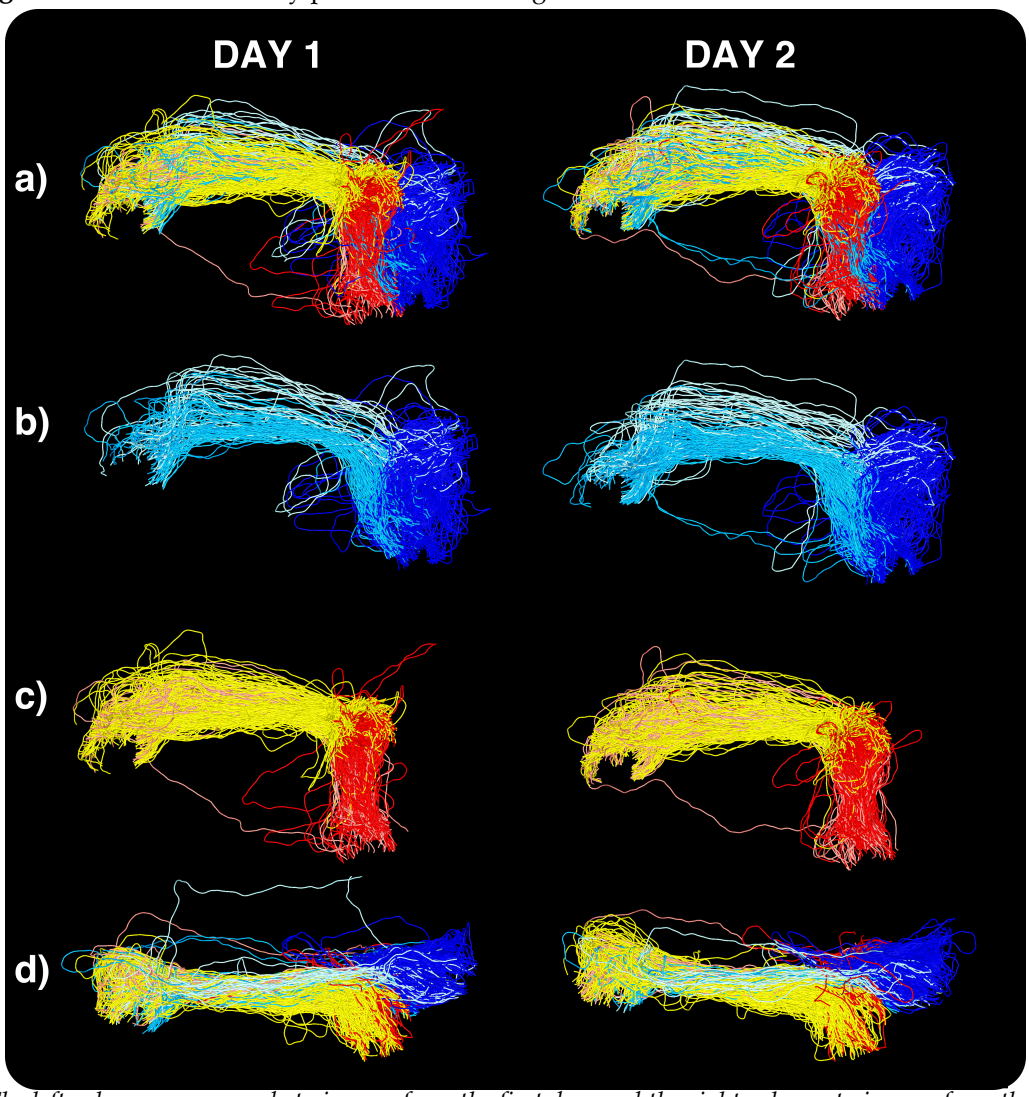

The left column corresponds to images from the first day, and the right column to images from the second day acquisitions for the same subject (S001). There were 7 days between acquisitions. a) The six tracts linking our average functional based ROIs are shown in a lateral sagittal view: red is the vOF and dark blue is vOF, yellow is aAF and light blue is a tract that goes from iPS to IFG (iPS>IFG), pink (almost not visible as it is intermingled with the red and the yellow) is the whole AF with fibers that start in the semVWFA and end in the IFG, and medium blue are the fibers that start in the perVWFA and end in IFG. b) Same image as a) but showing only the three tracts linking the perceptual averages. c) Same image as a) but showing only the three tracts linking the semantic averages. d) Same image as a) but from a dorsal axial view.

As indicated in the *Methods* section, first, to study the consistency of the methods identifying the same 6 tracts over time, we used the Test-Retest data (N=31). We performed an ICC analysis to statistically check for consistency. We found that most of the test-retest correlations were highly significant (ICC $\geq$ 0.73, $p \leq 0.0001$), and that even the two WM tracts with lower values (ICC = 0.38 and 0.65, $p \leq 0.01$) were also statistically

significant. These two WM tracts corresponded to tracts not previously predicted (perceptual vOT2IFG and perceptual pPC2IFG), and their average connectivity was lowest, i.e. few fibers were found per subject. This effect is reflected as well by the number of subjects who did not have a single fiber along these tracts (subjects without fibers are expressed by the number of NAs in Table 5). We will later discuss the meaning of the different values for AFD, as our focus here is on the test-retest analysis.

Table 5. Means and standard deviations of T values per contrast and design

PERCEPTUAL	ICC	*F*	p	*nº NA*	mean AFD	*sd AFD*
vOF	0.87	*15*	< 0.0001	*2*	736.10	*395.84*
vOT2IFG	0.65	*4.8*	< 0.0001	*22*	10.30	*13.37*
pPC2IFG	0.38	*2.2*	0.01	*7*	8.29	*5.20*
SEMANTIC						
pAF	0.73	*6.3*	< 0.0001	*2*	121.54	*96.67*
aAF	0.83	*11*	< 0.0001	*2*	50.27	*43.98*
AF	0.86	*13*	< 0.0001	*6*	16.05	*17.48*

After showing the reliability of the method used to detect the WM fiber tracts between functional ROIs with the test-retest data (N=31), we performed a new analysis, this time using data from the Main experiment (N=66). The objective of this new analysis was twofold: 1) to examine the relationship of the functional activations between the vOT-pPC and IFG-pPC regions, and 2) to integrate these functional activation values with the WM tracts connecting them: if there is an association between the functional activation in these regions, do the measures for the WM tract connecting them (i.e., MTV values) contribute to this association?

For this objective, we used the RWvsPW and RWvsCB contrast T values at every vertex of the lOTS and IFG, to predict the T values of the 20 vertexes selected in the pPC (i.e., as many simple regressions as vertexes were

performed in the lOTS and IFG ROIs). As explained in the *Methods* section, for this functional-to-functional prediction, only the adjusted R square was stored. Afterwards, each tract's MTV value was included in the model. In every vertex of the ROI, if the adjusted R squared of the new model with the tract MTV independent variable improved the adjusted R squared of the simpler functional-to-functional regression, the ordinary R squared of the new model was stored. With this procedure we obtained a R squared map for lOTS and another for the IFG, as can be seen in Figure 31*c*. There, we observed that the association strength between the pPC and the lOTS/IFG varied consistently along a predictable gradient. For the lOTS, the most occipital/visual vertexes of the iPS were associated more strongly with the most posterior vertexes of the lOTS, and the more dorsal vertexes in the iPS were associated with the more anterior vertexes in the lOTS. Once the vertexes reached the AG, no statistically significant associations were found. For the IFG, a similar pattern was observed, with the difference that the association occurred later when moving from vertex to vertex. For the most ventral/visual vertexes of the iPS, there was no association with the IFG. In the more dorsal vertexes of the iPS we found the strongest association, which again, disappeared once the AG was reached.

Figure 31. Functional and structural integration between vOT-pPC-IFG areas

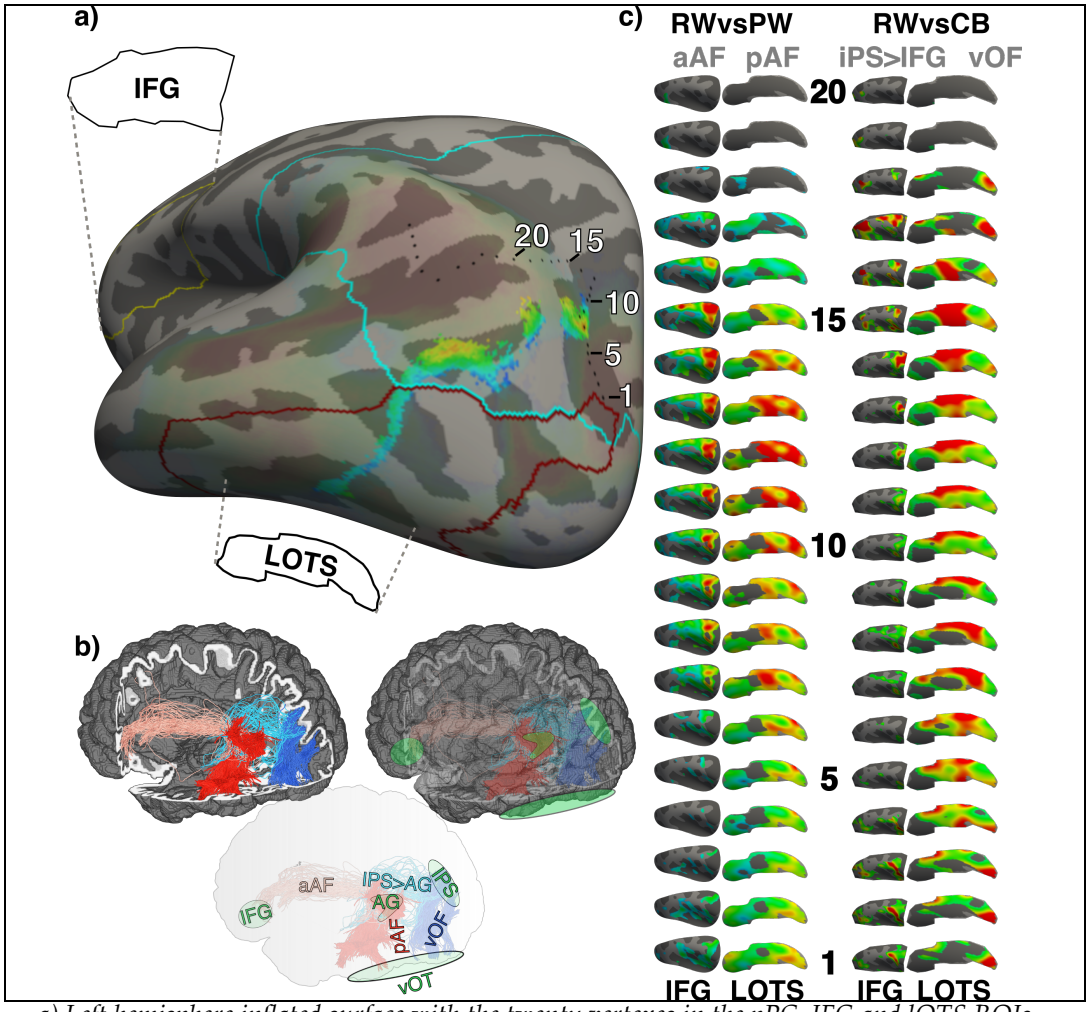

a) Left hemisphere inflated surface with the twenty vertexes in the pPC, IFG and lOTS ROIs. Superimposed with transparency the pAF, iPS and the intersection between the two. For reference, the layout of the vOT mask (dark red), pPC (light blue) and IFG (yellow) have been included. b) Schematics with the main cortical region of interest (vOT, iPS, AG, IFG) and the main tracts of interest (pAF, vOF, aAF). c) Ordinary R squared (the amount of variance explained) when explaining the T value of the selected pPC vertex. Only those points were the WM tract makes a significant contribution (improved Adjusted R squared) show R squared value (i.e. color).

These results revealed that 1) there was a functional-to-functional association between the lOTS/pPC and IFG/pPC, 2) that this relation followed a gradient going along the iPS-AG, and that 3) the WM connectivity between these regions contributed significantly to the observed functional-to-functional associations.

We performed an additional analysis repeating the ROI-to-vertex correlation analyses but using the CT values at every vertex instead. The results were not as consistent as those for the functional values, although

some activation patterns were visible: around vertex 15 for the IFG ROI, and around vertex 10 for the lOTS ROI.

To close this section it is worth noticing that with the methods we reported, we did not find any fibers with cortical endings in the vOT connecting ventrally to the IFG. In contrast, we found that there are passing fibers in parallel to the vOT that start from the occipital cortex and reach the IFG ventrally. We don't report these fibers here as it is beyond the scope of the present study.

9.2.2 Behavioral prediction

Analogous to the previous two experiments, we conclude the analysis of this experiment by predicting the behavioral results. In this third experiment, we used functional and structural indices from the three main different regions of interest (i.e., vOT, pPC and IFG) in hierarchical regression analyses.

To study individual contributions in predicting reading behavior, we added predictors to a regression model hierarchically, following a reasoned strategy: first the T values in the VWFA, followed by the MTV values of the vOF/pAF, then the T values in the pPC, and so on.

It is important to take into account that the functional T values used in these analyses were not the maximum prediction locations of the previous experiments. Instead, they were the averaged ROIs explained above, and obtained by averaging the GMax Ts for every subject. Thus, in this analysis we are interested in integrating the contributions of previously

reported areas in explaining the variance of reading behavior, instead of maximizing predictive power *per se*.

Table 6. Hierarchical regression analyses predicting reading behavior

a) All functional T values, for perceptual and semantic contrasts

Dependent:	RW RT in msec				PW RT in msec			
Independent: T values in ROI	Ordinary R squared	*p*	Adjusted R squared	Improves Model?	Ordinary R squared	*p*	Adjusted R squared	Improves Model?
Perc. vOT	16.20	0.001	14.80		11.87	0.006	10.40	
Sem. vOT	16.22	0.005	13.38	NO	12.11	0.022	9.13	NO
Perc. pPC	19.85	0.005	15.71	**YES**	19.49	0.005	15.33	**YES**
Sem. pPC	22.59	0.005	17.16	**YES**	21.25	0.008	15.72	**YES**
Perc. IFG	25.81	0.004	19.19	**YES**	25.63	0.004	18.99	**YES**
Sem. IFG	26.70	0.007	18.71	NO	25.64	0.010	17.53	NO

b) Perceptual contrast T values and WM tract MTV information

Dependent:	RW RT in msec				PW RT in msec			
Independent:	Ordinary R squared	*p*	Adjusted R squared	Improves Model?	Ordinary R squared	*p*	Adjusted R squared	Improves Model?
T: Perc. vOT	16.20	0.001	14.80		11.87	0.006	10.40	
MTV: vOF	20.08	0.002	17.18	**YES**	18.18	0.004	15.20	**YES**
T: Perc. pPC	21.52	0.004	17.16	NO	22.55	0.003	18.25	**YES**
MTV: pPC>IFG	21.16	0.022	14.45	NO	23.43	0.012	16.91	NO
T: Perc. IFG	26.19	0.013	18.17	**YES**	33.56	0.002	26.34	**YES**
MTV: vOT>IFG	49.74	0.001	40.01	**YES**	58.09	0.000	49.98	**YES**

c) Semantic contrast T values and WM tract MTV information

Dependent:	RW RT in msec				PW RT in msec			
Independent:	Ordinary R squared	*p*	Adjusted R squared	Improves Model?	Ordinary R squared	*p*	Adjusted R squared	Improves Model?
T: Sem. vOT	0.85	0.476	-0.80		1.29	0.379	-0.35	
MTV: pAF	0.87	0.786	-2.73	NO	1.23	0.712	-2.36	NO
T: Sem. pPC	4.84	0.440	-0.45	**YES**	3.92	0.536	-1.42	**YES**
MTV: aAF	6.38	0.479	-0.83	NO	7.39	0.397	0.27	**YES**
T: Sem. IFG	6.47	0.622	-2.70	NO	9.33	0.399	0.44	**YES**
MTV: AF	7.74	0.662	-3.55	NO	11.02	0.429	0.13	NO

The results presented in Table 6 demonstrate an expected pattern based on the results in Experiment 1 and 2. When combining the functional T values in all six ROIs (with RWvsCB in the perceptual ROIs and RWvsPW in the semantic ROIs), about 25% of the reading behavior variance was

explained. Although the contribution from semantic values is almost null (see Table 6*a*), all the models were significant ($p \leq 0.007$). When combining only the perceptual functional T values (RWvsCB) with the MTV values of the tracts interconnecting them, about 50% of the reading behavior variance was explained (see Table 6*b*). Although not all the individual variables contributed to the model, all the models were significant ($p \leq 0.02$). Finally, when the semantic functional T values (RWvsPW) were combined with the MTV values of the tracts interconnecting them, we did not obtain a single significant ($p < 0.05$) model. Thus, the semantic RWvsPW contrast does not explain reading behavior in a significant manner. In contrast, the perceptual RWvsCB contrast does predict reading behavior more consistently.

9.3 Discussion

The objective of this third and last experiment was to integrate the information presented in Experiment 1 and 2 in regard to the vOT, pPC and IFG, in a manner that could help to further our understanding of how the visual word recognition process occurs.

Perceptual and semantic functional contrasts reliably identified main reading tracts

We showed that the cortical areas located by the perceptual and semantic contrasts (perVWFA and semVWFA, iPS and AG, anterior and posterior IFG), can be used to identify the main reading tracts: vOF and AF. This result is remarkable in its own way, since it demonstrated that we could reproduce a technique based on purely anatomical grounds using AFQ (Weiner et al., 2016b; Yeatman et al., 2012b) on our functional results,

following the hypothesis that there are two types of contrasts that will identify two different VWFAs and each VWFA will be related to a different WM tract (i.e., vOF or pAF).

Furthermore, with a test-retest experiment, we showed that the characterization of the WM tracts based on the functional activation was highly reliable over time. Nevertheless, further experiments will be needed in this regard. For instance, the values showed in Experiment 3 were based on a 2,000,000 fiber whole tractogram, but using more fibers (e.g., 10,000,000) might show further connections among the functional areas examined. This will possibly help to reduce the variability of a measurement such as AFD. Also, using cortical areas instead of spheres could substantially help to normalize the connectivity values between areas. When using a sphere we do not have control over the extent that sulci/gyri are selected for each individual subject, and this can influence the amount of fibers identified by the tool. When selecting a cortical ROI, it may be possible to select only values in sulci across all subjects, for example. These are active experimental research questions in the DWI analysis field that could be of great help in an experiment like the present one.

Language areas were associated with a dorsal-to-ventral iPS gradient

We integrated the WM tract information in a regression analysis that focused on the functional associations between different sections within the pPC with the lOTS and with the IFG. We observed a clear gradient, mediated by the WM tracts connecting these areas. On the one hand, functional activations in the more ventral iPS locations were associated

with functional activations in the more posterior lOTS positions, coinciding with the perVWFA. On the other hand, functional activations in the more dorsal iPS locations were associated with functional activations in the more mid-lOTS positions, coinciding with the semVWFA. Interestingly, the functional activations in the dorsal iPS were not associated with functional activations in IFG, but significant associations were found between the functional activations in the more dorsal iPS locations, near the AG, and the functional activations in the IFG.

These results are in accordance with previous reports showing connectivity between the iPS and the lOTS (Kay and Yeatman, 2017) and with our general hypothesis that the perVWFA might be related to visual feature extraction and that only in the semVWFA does word begin to be treated as a language unit.

Although not as conclusively, the correlation analysis using CT values was aligned with those observed for functional values. The CT values provide an indirect measure of cortical development and typically the regions that co-activate together show correlation for their CT values. Nevertheless, usually a larger cohort of subjects is required to find significant results. Similar analyses using other structural morphometric measurements, such as cortical volume, cortical curvature and quantitative MRI measurements (e.g., T1 or MTV) might shed further light on the structural correlations between critical ROIs within the reading network.

Perceptual contrasts predicted reading behavior

Our last analyses and results were related to idea of using functional and structural indexes associated with core regions within the reading network to predict reading behavior, which were separately noted in the previous experiments. Here, we specifically found that the regions located using perceptual functional contrasts provided a better prediction of reading behavior. This is not surprising, considering that when we extracted the functional information from the ROIs created from the GMax T averages, we already saw that the perceptual contrasts lay inside the clusters that predicted reading behavior. We could not generate predictions using the semantic contrasts.

In the next chapter we integrate the findings from the three Experiments in a general discussion highlighting the main ideas and contributions of the present work to our understanding of how visual word recognition is implemented in the human cortex, and the main theoretical accounts supporting our results.

10 GENERAL DISCUSSION

The ability to read is one of the most successful and powerful communication technologies humans have ever developed. Its critical importance in education, culture, business and interpersonal communication is something most of us experience every single day. Nevertheless, similar to other human cognitive processes, we still do not fully understand how our brain implements reading and the main factors that contribute to atypical reading, such as dyslexia.

This doctoral dissertation constitutes a further step towards the neurobiological understanding of the early stages of reading, where visual word recognition takes place. Toward this end, we proposed a set of specific hypothesis regarding the cortical regions and their structural connectivity and three experiments to test them.

Our results revealed 1) that there are two VWFAs within the vOT performing different computations in the visual word recognition process; 2) that the patterns of functional activation in these two VWFAs are related to functional activation in other critical areas within the reading network: pPC and IFG; 3) that these two VWFAs are structurally connected via different WM tracts (vOF, pAF) tp two separate pPC regions: iPS and AG; and 4) that functional and structural information from these vOT, pPC and IFG regions predicts individual differences in reading behavior. These main findings are further discussed next.

There are at least two VWFAs performing different computations

The main group of hypotheses and the first experiment focused on the vOT. A review of the literature suggested that the VWFA, a specific patch of cortex typically associated with visual word recognition, is part of a extended brain area (i.e., the vOT) that typically shows a posterior-to-anterior gradient in its sensitivity to visual words (Price, 2012; Vinckier et al., 2007). The whole vOT is involved in visual word recognition and different cortical areas within the vOT perform different tasks at different time-points (Hirshorn et al., 2016; Xue and Poldrack, 2007). Some studies have even proposed the existence of different VWFAs in anterior, classical and posterior lOTS locations (Vogel et al., 2012; see blue, white and light red ROIs in Figure 32*a*), or in mid and posterior lOTS locations (Stigliani et al., 2015; Weiner et al., 2016a). Nevertheless, due to the fact that different functional contrasts, tools and normalizations were used in almost every study, it is difficult to get a clear sense of the exact locations of these VWFAs and their function in the complete visual word recognition process.

In the present work, using a state-of-the-art multimodal approach, and integrating functional and structural MRI indices, we started characterizing the activation pattern of the RWvsNull contrast. This contrast was used to identify the word selective areas for visual stimuli in the vOT and visual cortex. Results from Experiment 1 revealed that the RWvsNull contrast produced highly significant functional activations along the entire vOT, with a decreasing posterior-to-anterior gradient in T values. Although the functional contrast RWvsNull has been extensively used in previous studies, our results showed that this contrast was not

especially useful for identifying and locating potentially different components or VWFA(s) and, consequently, insufficient in terms of advancing our understanding of the mechanisms supporting the visual word recognition process.

Therefore, with the aim of integrating previous research evidence and to better understand the visual word recognition process, we designed a systematic approach to study the effects of different functional contrasts and fMRI designs at the individual-subject level, including repeated acquisitions across time to further elucidate the robustness and reliability of the findings. We hypothesized that some of the functional contrasts (RWvsPW/CS/FF) that we grouped under the category 'semantic') would have their maximas in more anterior vOT positions than other functional contrasts (RWvsCB/PS/SD) that we grouped under the category 'perceptual'). Our results confirmed these hypotheses as can be seen in Figure 32*a*. Basically, when a word-like stimuli signal (e.g., PW) is subtracted from the RW stimuli signal, the signal that is left is smaller than the signal that is left when subtracting perceptual stimuli (e.g., PS) from RW (see Figure 32*b*). In the former case (i.e., RWvsPW), the lexical and semantic processing of the RW is left, while in the latter case (i.e., RWvsPS) the whole word is left, including its semantics/ phonology/ orthography and word/letter shapes. Considering the gradient of the RWvsNull stimuli from posterior visual cortex to anterior vOT, it was reasonable to expect that the 'perceptual' visual contrast would identify a more posterior word sensitive cortex than the semantic contrasts, as our results systematically confirmed.

Figure 32: Conceptual explanation of differences in semantic and perceptual contrasts

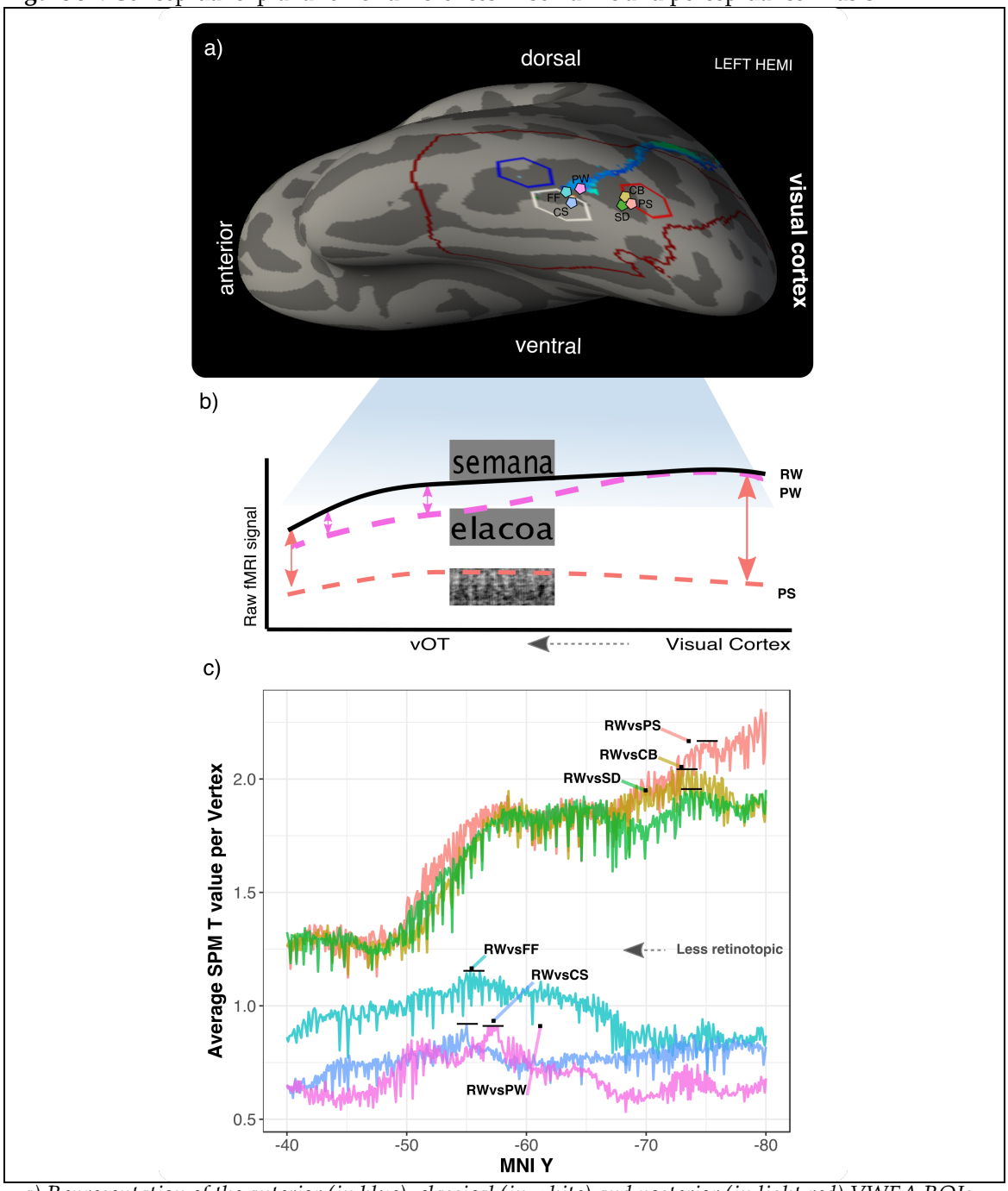

a) Representation of the anterior (in blue), classical (in white) and posterior (in light red) VWFA ROIs (i.e., hexagons) reported in previous research and the specific global maximas found for each of the six contrasts used in the present study (RWvsPW/CS/FF/SD/PS/CB) clustered in two main perVWFA and semVWFA-s locations, roughly separated by the intersection of the cortical endings of the vOF and pAF tracts (blue line). b) Graphical conceptualization of the posterior-anterior raw fMRI signals for RW, PW and PS; where the vertical arrows express the expected contrast value (i.e. RWvsPW and RWvsPS) at the corresponding location of the vOT. c) Data from Experiment 1 showing the differences in specific SPM T values between the six contrasts along the anterior-posterior vOT (i.e., MNI Y-axis). Color-code for the functional contrasts are the same in sections a), b) and c).

The same conceptual idea presented in Figure 32*b* is also represented by data from our study in Figure 32*c*, where average maximum T values for

semantic and perceptual functional contrasts from posterior-to-anterior vOT (i.e., MNI Y coordinates) are shown. The three perceptual contrast (i.e., RWvsCB/SD/PS) T values were significantly higher than those for semantic contrasts (i.e., RWvsPW/CS/FF) along the whole vOT. The perceptual stimuli (CB/PS/SD) removed less signal from the RW signal than the word-like stimuli (PW/CS/FF).

Perceptual contrasts had a global maxima in the posterior lOTS at around MNI Y = -70/-75, but there were also significant local maximas along most of the vOT, i.e.: they follow the same pattern as RWvsNull, with an anterior-to-posterior gradient. This behavior is explained by the fact that we are only subtracting general visual information from the RW signal. On the other hand, semantic contrasts had a maxima in the mid part of the lOTS, at around MNI Y = -57. In this case, as predicted in Figure 32*b*, these semantic contrasts did not show a similar pattern as the RWvsNull contrast, with a signal drop in the posterior lOTS.

We proposed that the cortical region in the posterior lOTS, that can be identified using perceptual contrasts, be called perVWFA. The mid lOTS area that can be identified using semantic contrasts be termed semVWFA. The logic of the name semVWFA can be further extended, as the maxima for the RWvsPW contrast, which only contains the lexico-semantic information, is located here. Activations related to the other five contrasts corresponds to additional information on top of this lexical-semantic information.

Consistent with previous evidence, the perVWFA could be responsible for visual feature extraction, i.e. at this point the word may still be interpreted as an abstract visual image, although language related information processing (orthography, bigram frequency…) may be processed in this area as well. More evidence, however, is required to further understand this posterior-to-anterior gradient and fully support this claim. Once the computations reach the semVWFA, the word and its lexico-semantic-orthographic-phonetic qualities appear to have been computed and fully integrated into the language network. Our own results and evidence from other studies support the following description of the visual word recognition process:

1. The fact that the three perceptual contrasts in perVWFA (see *Figure 32c*) showed a strong activation and that the three semantic contrasts showed a lower activation might support the claim that the main role of the perVWFA is visual feature extraction. According to this view, once the generic visual information is removed in the perceptual contrasts, the abstract word form will remain. If this perVWFA area is dedicated mainly to word- and letter-form feature extraction, it follows that the remaining signal for the semantic contrasts in the perVWFA is reduced (i.e., the region is mainly sensitive to visual word-forms and the semantic contrasts carry no visual word-form information since it has been removed). Further, we observe that the RWvsPW contrast, being PWs the stimuli most similar visually to RWs, has the lowest signal. We assume that the word is fully processed as a language unit in the semVWFA, interfacing with the language network (which

seems to be a gradient going from more visual features to more language-like features). The perceptual contrasts have higher signal than the semantic contrasts in the semVWFA as well; because all the language related information (i.e., visual, semantic, phonological and orthographical) in the RW remains.

2. Our WM connectivity results showed that the perVWFA connects to dorsal occipital areas around the iPS through the vOF. These are areas which are usually engaged in visual and top-down task-related computations (Kay and Yeatman, 2017). On the other hand, the semVWFA connects with the AG region via the pAF, a classical region related to language processing in general, and semantic processes in particular. This correspondence between the functional and structural results, may confirm a division of labor in the computations carried out by these differentiated perVWFA and semVWFA regions.

3. For the three RWvsCB/PS/SD perceptual contrasts, the functional activation of the perVWFA predicted reading behavior in the lexical decision task for CS, PW, and RW. Thus, the perVWFA seems to be critical in performing computations for word-form perception. In contrast, additional consistent activations which extended from the perVWFA to the semVWFA were associated with PW and RW reading behavior. Thus, it seems that that the semVWFA is only relevant when lexico-semantic information is required during reading to distinguish between RWs and PWs.

4. Using a different localizer from the one used in our study, Stigliani et al. (2015) and Weiner et al.'s (2016) studies found bilateral posterior lOTS character sensitive areas that match our left hemisphere perVWFA. However, they only reported a left hemisphere mid lOTS character sensitive area that matches our left hemisphere semVWFA. This previous evidence, albeit indirect, is consistent with the hypothesis that the perVWFA is mainly dedicated to visual feature extraction while the semVWFA is in charge of interfacing with high-level language-related processes and, therefore, only left lateralized.

5. Recent work by Planton et al. (2017) also aligns well with this same idea. In their experiment, participants were only presented with auditory word stimuli. They observed a gradient of activations across lOTS: no activations were found in the posterior part (which corresponds to our perVWFA), but significant activations were found in the mid lOTS (which corresponds to our semVWFA). These results suggest a top-down effect from the auditory language areas that, consequently, only occurs in semVWFA.

All of this evidence suggests that VWFAs play different roles as part of a continuum of recurrent processes that proceed hierarchically along the vOT in a posterior-anterior fashion. Vision and reading studies have suggested that the visual features of an image are extracted hierarchically increasing the level of abstraction, and that the information is combined in more meaningful units along the vOT (Goodale and Milner, 1992; Hong et al., 2016; McCandliss et al., 2003). Therefore, it would be reasonable to

assume that the most posterior part of the vOT is retinotopically organized and it is mainly involved in basic visual feature extraction. More anterior positions along the y-axis seem to deal with more complex/abstract information (Dehaene and Cohen, 2011; Hong et al., 2016; Price and Devlin, 2011). In fact, the first place where eye-movement invariant visual representations can be observed is the vOT (Nishimoto et al., 2017). Some earlier studies have made similar claims that the VWFA still contains retinotopic information and that its activation is sensitive to word presentation position (Rauschecker et al., 2012). However, others have suggested that this effect only occurs in the most posterior parts of the vOT and that it is very soon lost (Hannagan et al., 2015; Hannagan and Grainger, 2013).

In sum, we were able to functionally identify a gradient of activations in the vOT word selective areas that could be segregated into two separate VWFAs (i.e., semVWFA and perVWFA) using contrasts of different types. This result suggests that these two VWFA are responsible for different processes during the continuum of computations occurring in visual word recognition. To further unravel the computations carried out by these two VWFAs within the reading network, we performed a series of other experiments to examine: 1) functional activation in other critical language-related areas in the reading network, including the iPS and the AG in the pPC, and the *pars opercularis* and *triangularis* in the IFG, 2) WM connections between these main three language areas (i.e., vOT, pPC and IFG), and 3) to what extent combining the previous functional and structural MRI indices could further predict reading behavior as

measured by a lexical decision task that participants performed outside of the scanner.

Coherent patterns of activation in related language areas

As predicted in Figure 32*b* and observed in Figure 32*c*, the T values for the semantic contrasts are grouped together and they are significantly lower than the perceptual contrasts found in the vOT. This grouping was also found in the iPS, but it was not as consistent as in the vOT, with activation from the RWvsFF contrast not falling within the semantic group. In the AG, the RWvsFF contrast was fully integrated in the perceptual contrasts; in the semantic group only the RWvsPW/CS contrast remained clustered. Furthermore, in the IFG, only the RWvsPW remained as a separate contrast and RWvsCS was found between the remaining contrasts. Thus, similar to the vOT, there seemed to be a posterior-to-anterior gradient in the pPC. The iPS was fairly sensitive to visual word-forms probably due to the direct connections to the perVWFA through the vOF. In contrast, the AG and IFG appeared to be less sensitive to visual word forms, being more functionally selective for lexico-semantic information.

Figure 33 represents the main areas involved in the process we just described. Although the temporal resolution of the MRI is limited, based on previous evidence it is reasonable to speculate that the visual information might be first processed in the perVWFA with the help of the ventral iPS, with these areas connected via the vOF. Then, the computations might move gradually into the semVWFA and the dorsal iPS/AG connected via the pAF. This possibility is consistent with Greenblatt's (1973) post-mortem study of patients who exhibited reading

disabilities, which indicated that both pAF and vOF are required for reading. Later in the process, information might be carried along the connections between the iPS and the AG and the aAF and other cortico-cortical fibers to the IFG. Although this possible linear sequence of computations is relevant, it is clearly an oversimplification considering that previous studies using techniques with higher temporal resolution (Cornelissen et al., 2009; Marinkovic et al., 2003; Wheat et al., 2010) strongly suggest that these computations are highly recurrent and involve rapid and parallel interactions among these three core reading regions.

Figure 33: Main functional areas and structural connections

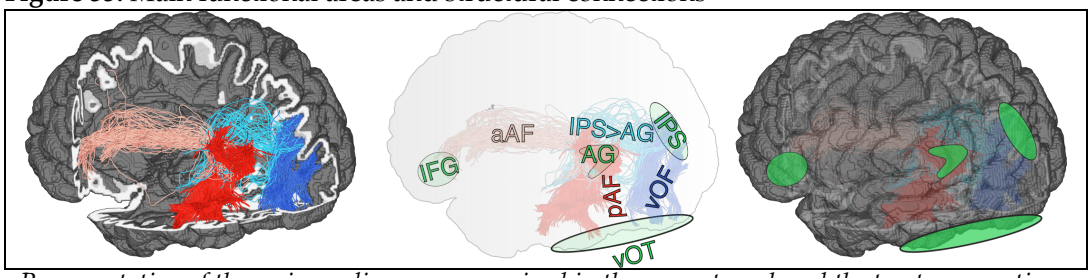

Representation of the main reading areas examined in the present work and the tracts connecting them. The leftmost image shows the main tracts connecting the ROIs. The middle image corresponds to a schematic labeled representation of the ROIs and WM tracts. Finally, the rightmost image also shows the main ROIs (in green) and the connecting tracts superimposed on the grey matter. These three images were obtained from a representative subject.

Coherent patterns of functional activation and WM tracts connecting them

The WM structural connectivity analyses yielded results that were consistent with those observed in the functional analyses for the main language areas of interest (i.e., vOT, pPC, IFG). First, we structurally identified the vOF and pAF tracts in Experiment 1 using the AFQ algorithms (Yeatman et al., 2012b). Second, using spheres around the average functional coordinates for the perceptual and semantic contrasts in the vOT, iPS, AG and IFG, we first functionally identified the vOF and pAF tracts for comparison purposes, and then all the other tracts

connecting the different language regions as well, i.e. aAF, AF, perVWFA-to-IFG and iPS- to-IFG (see Figure 33). Although results for the WM tracts were remarkably consistent in the test-retest analysis, using the methods in Experiment 3 (i.e., 2 million fiber tractograms) we could not find robust structural connections between some of the areas, such as between the iPS and IFG. Third, in Experiment 3 we integrated the functional and structural data. We found that a qMRI measurement (i.e., the MTV information for a tract connecting two of the language ROIs) made a significant contribution to the simple regression analyses for functional activation in the pPC and vOT and the pPC and IFG. Again, these results were consistent with previous findings, and we could observe the contribution of the main tracts and the y-axis functional gradients found along the main language regions (i.e., perVWFA-semVWFA, iPS-AG, *pars opercularis-pars triangularis*).

All the language areas contribute to the prediction of reading behavior

The pattern of functional activation in the language areas predicted reading behavior. We already discussed the vOT results in terms of their contribution to predicting reading behavior in the first section of this general discussion. In addition, in Experiment 2 we also observed that functional activation in pPC and IFG clusters predicted individual differences in reading behavior.

Importantly, hierarchical regression analysis reported in Experiment 3 revealed that the perceptual contrasts and WM tracts explained more variance in the behavioral results than the semantic contrasts did. There could be two explanations for this finding: 1) the average location ROIs

used to obtain the functional values to predict reading behavior in the case of the perceptual contrasts matched the prediction cluster, but this was not the case for the semantic contrasts; 2) as we have seen throughout this work, the perceptual signal is more robust and seems to be involved in the early stages of visual word recognition, and therefore it is not surprising to find stronger associations between these and reading behavior, which was based on reading speed. Nevertheless, the objective of these analyses was not to maximize the prediction of the behavioral measurements, but to understand and to examine in an integrative way the contribution of the studied functional and structural neuroimaging measures.

Conclusion

Based on previous evidence and the current results, we argue for the existence of both semVWFA and perVWFA as two distinct cortical regions within vOT which perform different computations in the visual word recognition process. The patterns of functional activation found in these VWFAs were associated with functional activation in the pPC and IFG. Importantly, the perVWFA and semVWFA were structurally connected via the vOF and the pAF WM tracts to two separate pPC regions: the iPS and AG. Our findings revealed that the three main classical reading regions are linked functionally and also structurally, and that combining functional and structural information from these core reading regions predicted reading behavior.

These results contribute to several theoretical and practical debates. Regarding the main theories, on the one hand, in line with the interactive

account (Price and Devlin, 2011), the semVWFA could take part in a strong top-down process from language areas that would provide semantic information to help recognize a word. On the other hand, the perVWFA may have been trained to detect the most frequent bigrams and could contain prelexical word abstractions, as predicted by the local combination detector model (Dehaene and Cohen, 2011).

The present work represents a critical step in the creation of a highly detailed characterization of the early stages of reading at the individual-subject level and helps to establish a baseline model and parameter range that might serve in future to clarify functional and structural differences between typical and atypical readers.

Future steps:

The analyses performed for these experiments suggest an additional set of relevant possibilities for further work on this rich data set that can further understanding of visual word recognition processes.

1) Time-course analysis: although MRI is not the best tool to examine differences in time courses, in line with previous evidence (Boynton et al., 2012) it might still be possible to find differences in the time courses between the perVWFA and semVWFA, as well as between iPS and AG. Theoretically, we would expect an earlier peak in the activation of the perVWFA and the iPS, possibly related to visual feature extraction, and a later one in the semVWFA and the AG related to semantic processing. Along this vein, future studies integrating functional MRI localizers with EEG/MEG would be of high interest (see Cichy et al. (2014) for a recent

study combining fMRI and MEG to examine spatial and temporal dynamics in object recognition).

2) Right hemisphere: we have not considered the right hemisphere in our three experiments. As found in some recent studies (Stigliani et al., 2015; Weiner et al., 2016a), it would be especially relevant to examine to what extent the perVWFA is bilateral, whereas the semVWFA is left lateralized due to its specific role in language processing.

3) Functional-connectivity analysis: although in Experiment 3 we performed a basic analysis using multiple regression analysis vertex by vertex along the pPC, a functional connectivity analysis using beta-series correlation (Rissman et al., 2004) could provide further information in regard to what extent the iPS and perVWFA are mediated by the vOF, and the AG and semVWFA by the pAF. Also, a functional connectivity analysis at the inter-hemispheric level would be relevant to examine if the left and right perVWFA show tighter coupling than left and right semVWFA.

4) Retinotopy analysis: Although we gathered retinotopic data, these data were not analyzed for the current dissertation. Nevertheless, these data will be analyzed to specifically examine if, in line with findings from Rauschecker et al.'s (2012) study, our perVWFA displays a retinotopic organization, which is not present for the semVWFA.

5) Network analysis: a network analysis of the areas in the reading circuit (as seen in the current work) to investigate how they communicate is also in the pipeline. We propose this analysis for both the resting state and the functional data. Similarly, a path analysis could also help explore in

further detail the specific relationship between the functional and structural indices that predicted reading behavior in the results reported in this doctoral dissertation.

6) Structural pathways within the ventral reading route: Reading models and neuroimaging studies on reading processes have suggested the existence of dorsal and ventral reading networks. The present doctoral dissertation focused on WM tracts strongly related to the dorsal reading network. Further detailed DWI analysis examining the ventral fiber tracts that may connect the vOT with the IFG (e.g., iLF, iFOF) will provide useful information. For instance, there is evidence from MEG studies (Cornelissen et al., 2009; Marinkovic et al., 2003; Wheat et al., 2010) showing early connectivity between the vOT and the IFG that is assumed to be carried out by the ventral reading network. It is hypothesized that these ventral connections involve the ILF innervating the vOT with projections to the temporal pole, and from there connections from the uncinate fasciculus to the IFG (Gil-Robles et al., 2013). However, in the methods and data presented in the present work we did not find vOT fiber endings connecting directly in the IFG, but only passing fibers in the vOT that started in the occipital visual cortex, and arrived ventrally to the IFG, with fibers going parallel to both VWFAs but without innervating either. In this vein, reanalyzing our data including some methodological changes [e.g., a) obtaining a whole tractogram with 10 or 20 million fibers and creating cortical ROIs to be used as starting, end and passing points, and b) generation of fibers directly from seeds, without generating the whole tractogram, might help to further elucidate if these additional tracts

within the ventral network contribute to interactions between the vOT and IFG and reading behavior.

11 BIBLIOGRAPHY

Acheson, D.J., Hagoort, P., 2013. Stimulating the Brain's Language Network: Syntactic Ambiguity Resolution after TMS to the Inferior Frontal Gyrus and Middle Temporal Gyrus. J. Cogn. Neurosci. 25, 1664–1677. doi:10.1162/jocn_a_00430

Amunts, K., Lenzen, M., Friederici, A.D., Schleicher, A., Morosan, P., Palomero-Gallagher, N., Zilles, K., 2010. Broca's region: Novel organizational principles and Multiple Receptor Mapping. PLoS Biol. 8. doi:10.1371/journal.pbio.1000489

Amunts, K., Zilles, K., 2012. Architecture and organizational principles of Broca's region. Trends Cogn. Sci. 16, 418–426. doi:10.1016/j.tics.2012.06.005

Armstrong, B.C., Watson, C.E., Plaut, D.C., 2012. SOS! An algorithm and software for the stochastic optimization of stimuli. Behav. Res. Methods 44, 675–705. doi:10.3758/s13428-011-0182-9

Assaf, Y., Pasternak, O., 2008. Diffusion tensor imaging (DTI)-based white matter mapping in brain research: A review. J. Mol. Neurosci. 34, 51–61. doi:10.1007/s12031-007-0029-0

Badre, D., Wagner, A.D., 2002. Semantic retrieval, mnemonic control, and prefrontal cortex. Behav. Cogn. Neurosci. Rev. 1, 206–218. doi:10.1177/1534582302001003002

Baker, C.I., Liu, J., Wald, L.L., Kwong, K.K., Benner, T., Kanwisher, N., 2007. Visual word processing and experiential origins of functional selectivity in

human extrastriate cortex. Proc. Natl. Acad. Sci. U. S. A. 104, 9087–92. doi:10.1073/pnas.0703300104

Bandettini, P.A., 2012. Twenty years of functional MRI: The science and the stories. Neuroimage 62, 575–588. doi:10.1016/j.neuroimage.2012.04.026

Bar, M., Kassam, K.S., Ghuman, A.S., Boshyan, J., Schmid, A.M., Dale, A.M., Hamalainen, M.S., Marinkovic, K., Schacter, D.L., Rosen, B.R., Halgren, E., 2006. Top-down facilitation of visual recognition. Proc. Natl. Acad. Sci. 103, 449–454. doi:10.1073/pnas.0507062103

Barazany, D., Basser, P.J., Assaf, Y., 2009. In vivo measurement of axon diameter distribution in the corpus callosum of rat brain. Brain 132, 1210–1220. doi:10.1093/brain/awp042

Beaulieu, C., Plewes, C., Paulson, L.A., Roy, D., Snook, L., Concha, L., Phillips, L., 2005. Imaging brain connectivity in children with diverse reading ability. Neuroimage 25, 1266–1271. doi:10.1016/j.neuroimage.2004.12.053

Behrens, T.E.J., Berg, H.J., Jbabdi, S., Rushworth, M.F.S., Woolrich, M.W., 2007. Probabilistic diffusion tractography with multiple fibre orientations: What can we gain? Neuroimage 34, 144–155. doi:10.1016/j.neuroimage.2006.09.018

Ben-Shachar, M., Dougherty, R.F., Deutsch, G.K., Wandell, B.A., 2011. The development of cortical sensitivity to visual word forms. J. Cogn. Neurosci. 23, 2387–2399. doi:10.1162/jocn.2011.21615

Ben-Shachar, M., Dougherty, R.F., Deutsch, G.K., Wandell, B.A., 2007.

Differential sensitivity to words and shapes in ventral occipito-temporal cortex. Cereb. Cortex 17, 1604–1611. doi:10.1093/cercor/bhl071

Binder, J.R., Desai, R.H., 2011. The neurobiology of semantic memory. Trends Cogn. Sci. 15, 527–536. doi:10.1016/j.tics.2011.10.001

Binder, J.R., Desai, R.H., Graves, W.W., Conant, L.L., 2009. Where is the semantic system? A critical review and meta-analysis of 120 functional neuroimaging studies. Cereb. Cortex 19, 2767–96. doi:10.1093/cercor/bhp055

Binder, J.R., Medler, D.A., Westbury, C.F., Liebenthal, E., Buchanan, L., 2006. Tuning of the human left fusiform gyrus to sublexical orthographic structure. Neuroimage 33, 739–748.

Blackburne, L.K., Eddy, M.D., Kalra, P., Yee, D., Sinha, P., Gabrieli, J.D.E., 2014. Neural correlates of letter reversal in children and adults. PLoS One 9, e98386. doi:10.1371/journal.pone.0098386

Borowsky, R., Besner, D., 2006. Parallel distributed processing and lexical-semantic effects in visual word recognition: Are a few stages necessary? Psychol. Rev. 113, 181–193. doi:10.1037/0033-295x.113.1.181

Bouhali, F., Thiebaut de Schotten, M., Pinel, P., Poupon, C., Mangin, J.-F., Dehaene, S., Cohen, L., 2014. Anatomical Connections of the Visual Word Form Area. J. Neurosci. 34, 15402–15414. doi:10.1523/JNEUROSCI.4918-13.2014

Boukrina, O., Hanson, S.J., Hanson, C., 2013. Modeling activation and effective

connectivity of VWFA in same script bilinguals. Hum. Brain Mapp. 0. doi:10.1002/hbm.22348

Boynton, G.M., Engel, S.A., Heeger, D.J., 2012. Linear systems analysis of the fMRI signal. Neuroimage 62, 975–984.

Brem, S., Bach, S., Kucian, K., Guttorm, T.K., Martin, E., Lyytinen, H., Brandeis, D., Richardson, U., 2010. Brain sensitivity to print emerges when children learn letter-speech sound correspondences. Proc. Natl. Acad. Sci. U. S. A. 107, 7939–44. doi:10.1073/pnas.0904402107

Brockway, J.P., 2000. Two functional magnetic resonance imaging f(MRI) tasks that may replace the gold standard, Wada testing, for language lateralization while giving additional localization information. Brain Cogn. 43, 57–9.

Brodmann, K., 1909. Vergleichende Lokalisationslehre der Grosshirnrinde in ihren Prinzipien dargestellt auf Grund des Zellenbaues. Barth, Leipzig.

Bruno, J.L., Zumberge, A., Manis, F.R., Lu, Z.L., Goldman, J.G., 2008. Sensitivity to orthographic familiarity in the occipito-temporal region. Neuroimage 39, 1988–2001. doi:10.1016/j.neuroimage.2007.10.044

Büchel, C., Price, C., Friston, K., 1998. A multimodal language region in the ventral visual pathway. Nature 394, 274–277. doi:10.1038/28389

Buckner, R.L., Bandettini, P.A., O'Craven, K.M., Savoy, R.L., Petersen, S.E., Raichle, M.E., Rosen, B.R., 1996. Detection of cortical activation during averaged single trials of a cognitive task using functional magnetic

resonance imaging. Proc. Natl. Acad. Sci. U. S. A. 93, 14878–83. doi:10.1073/pnas.93.25.14878

Buxton, R.B., Wong, E.C., Frank, L.R., 1998. Dynamics of blood flow and oxygenation changes during brain activation: The balloon model. Magn. Reson. Med. 39, 855–864. doi:10.1002/mrm.1910390602

Caramazza, A., Zurif, E.B., 1976. Dissociation of algorithmic and heuristic processes in language comprehension: Evidence from aphasia. Brain Lang. 3, 572–582. doi:10.1016/0093-934X(76)90048-1

Carreiras, M., Armstrong, B.C., Perea, M., Frost, R., 2014. The what, when, where, and how of visual word recognition. Trends Cogn. Sci. 18, 90–98. doi:10.1016/j.tics.2013.11.005

Carreiras, M., Mechelli, A., Este, A., Price, C.J., 2007. Brain Activation for Lexical Decision and Reading Aloud: Two Sides of the Same Coin? J. Cogn. Neurosci. 19, 433–444. doi:10.1162/jocn.2007.19.3.433

Caspers, S., Eickhoff, S.B., Geyer, S., Scheperjans, F., Mohlberg, H., Zilles, K., Amunts, K., 2008. The human inferior parietal lobule in stereotaxic space. Brain Struct. Funct. 212, 481–495. doi:10.1007/s00429-008-0195-z

Caspers, S., Geyer, S., Schleicher, A., Mohlberg, H., Amunts, K., Zilles, K., 2006. The human inferior parietal cortex: Cytoarchitectonic parcellation and interindividual variability. Neuroimage 33, 430–448. doi:10.1016/j.neuroimage.2006.06.054

Caspers, S., Schleicher, A., Bacha-Trams, M., Palomero-Gallagher, N., Amunts,

K., Zilles, K., 2013. Organization of the human inferior parietal lobule based on receptor architectonics. Cereb. Cortex 23, 615–628. doi:10.1093/cercor/bhs048

Changizi, M. a, Shimojo, S., 2005. Character complexity and redundancy in writing systems over human history. Proc. Biol. Sci. 272, 267–75. doi:10.1098/rspb.2004.2942

Changizi, M., Zhang, Q., Ye, H., Shimojo, S., 2006. The structures of letters and symbols throughout human history are selected to match those found in objects in natural scenes. Am. Nat. 167, E117–E139. doi:10.1086/502806

Church, J. a, Balota, D. a, Petersen, S.E., Schlaggar, B.L., 2011. Manipulation of length and lexicality localizes the functional neuroanatomy of phonological processing in adult readers. J. Cogn. Neurosci. 23, 1475–1493. doi:10.1162/jocn.2010.21515

Cichy, R.M., Pantazis, D., Oliva, A., 2014. Resolving human object recognition in space and time. Nat. Neurosci. 17, 455–62. doi:10.1038/nn.3635

Clascá, F., Porrero, C., Galazo, M.J., Rubio-Garrido, P., Evangelio, M., 2016. Anatomy and Development of Multispecific Thalamocortical Axons, in: Axons and Brain Architecture. Elsevier, pp. 69–92. doi:10.1016/B978-0-12-801393-9.00004-9

Cohen, L., Dehaene, S., 2004. Specialization within the ventral stream: The case for the visual word form area. Neuroimage 22, 466–476. doi:10.1016/j.neuroimage.2003.12.049

Cohen, L., Dehaene, S., Naccache, L., Lehéricy, S., Dehaene-Lambertz, G., Hénaff, M. a, Michel, F., 2000. The visual word form area: spatial and temporal characterization of an initial stage of reading in normal subjects and posterior split-brain patients. Brain 123, 291–307.

Cohen, L., Dehaene, S., Vinckier, F., Jobert, A., Montavont, A., 2008. Reading normal and degraded words: Contribution of the dorsal and ventral visual pathways. Neuroimage 40, 353–366. doi:10.1016/j.neuroimage.2007.11.036

Cohen, L., Jobert, A., Le Bihan, D., Dehaene, S., 2004. Distinct unimodal and multimodal regions for word processing in the left temporal cortex. Neuroimage 23, 1256–1270. doi:10.1016/j.neuroimage.2004.07.052

Cohen, L., Lehéricy, S., Chochon, F., Lemer, C., Rivaud, S., Dehaene, S., 2002. Language-specific tuning of visual cortex? Functional properties of the Visual Word Form Area. Brain 125, 1054–69.

Coltheart, M., Rastle, K., Perry, C., Langdon, R., Ziegler, J.C., 2001. DRC: a dual route cascaded model of visual word recognition and reading aloud. Psychol. Rev. 108, 204–56. doi:10.1037/0033-295X.108.1.204

Cornelissen, P.L., Kringelbach, M.L., Ellis, A.W., Whitney, C., Holliday, I.E., Hansen, P.C., 2009. Activation of the left inferior frontal gyrus in the first 200 ms of reading: Evidence from Magnetoencephalography (MEG). PLoS One 4, 1–13. doi:10.1371/journal.pone.0005359

D'Esposito, M., Postle, B.R., Ballard, D., Lease, J., 1999. Maintenance versus manipulation of information held in working memory: an event-related

fMRI study. Brain Cogn. 41, 66–86. doi:10.1006/brcg.1999.1096

Dale, A.M., 1999. Optimal experimental design for event-related fMRI, in: Human Brain Mapping. pp. 109–114. doi:10.1002/(SICI)1097-0193(1999)8:2/3<109::AID-HBM7>3.0.CO;2-W

Dale, A.M., Buckner, R.L., 1997. Selective averaging of rapidly presented individual trials using fMRI. Hum. Brain Mapp. 5, 329–340. doi:10.1002/(SICI)1097-0193(1997)5:5<329::AID-HBM1>3.0.CO;2-5

De Santis, S., Drakesmith, M., Bells, S., Assaf, Y., Jones, D.K., 2014. Why diffusion tensor MRI does well only some of the time: Variance and covariance of white matter tissue microstructure attributes in the living human brain. Neuroimage 89, 35–44. doi:10.1016/j.neuroimage.2013.12.003

Dehaene, S., Cohen, L., 2011. The unique role of the visual word form area in reading. Trends Cogn. Sci. 15, 254–62. doi:10.1016/j.tics.2011.04.003

Dehaene, S., Cohen, L., Sigman, M., Vinckier, F., 2005. The neural code for written words: a proposal. Trends Cogn. Sci. 9, 335–41. doi:10.1016/j.tics.2005.05.004

Dehaene, S., Dehaene-Lambertz, G., 2016. Is the brain prewired for letters? Nat. Neurosci. 19, 1192. doi:10.1038/nn.4369

Dehaene, S., Le Clec'H, G., Poline, J.-B., Le Bihan, D., Cohen, L., 2002. The visual word form area: a prelexical representation of visual words in the fusiform gyrus. Neuroreport 13, 321–325. doi:10.1097/00001756-200203040-00015

Dehaene, S., Nakamura, K., Jobert, A., Kuroki, C., Ogawa, S., Cohen, L., 2010. Why do children make mirror errors in reading? Neural correlates of mirror invariance in the visual word form area. Neuroimage 49, 1837–1848. doi:10.1016/j.neuroimage.2009.09.024

Dejerine, J., 1891. Sur un cas de cecite verbale avec agraphie. C.R. Soc. Biol. 43, 197–201.

Dejerine, J.J., 1892. Contribution a l'étude anatomo-pathologique et clinique des différentes variétés de cécité verbale. Mémoires la Société Biol. 4, 61–90.

Dell'Acqua, F., Simmons, A., Williams, S.C.R., Catani, M., 2013. Can spherical deconvolution provide more information than fiber orientations? Hindrance modulated orientational anisotropy, a true-tract specific index to characterize white matter diffusion. Hum. Brain Mapp. 34, 2464–2483. doi:10.1002/hbm.22080

Depue, B.E., Banich, M.T., 2012. Increased inhibition and enhancement of memory retrieval are associated with reduced hippocampal volume. Hippocampus 22, 651–5. doi:10.1002/hipo.20952

Devlin, J.T., Jamison, H.L., Gonnerman, L.M., Matthews, P.M., 2006. The role of the posterior fusiform gyrus in reading. J. Cogn. Neurosci. 18, 911–922. doi:10.1162/jocn.2006.18.6.911

Donald, M.W., 1991. Origins of the modern mind: Three stages in the evolution of culture and cognition. Harvard University Press, Cambridge, MA.

Draganski, B., Gaser, C., Busch, V., Schuierer, G., Bogdahn, U., May, A., 2004.

Neuroplasticity: Changes in grey matter induced by training. Nature 427, 311–312. doi:10.1038/427311a

Duchon, A., Perea, M., Sebastián, N., Martí, M.A., Carreiras, M., 2013. EsPal: one-stop shopping for Spanish word properties. Behav. Res. Methods 45, 1246–58. doi:10.3758/s13428-013-0326-1

Duncan, K.J., Pattamadilok, C., Knierim, I., Devlin, J.T., 2009. Consistency and variability in functional localisers. Neuroimage 46, 1018–1026. doi:10.1016/j.neuroimage.2009.03.014

Eklund, A., Nichols, T.E., Knutsson, H., 2016. Cluster failure: Why fMRI inferences for spatial extent have inflated false-positive rates. Proc. Natl. Acad. Sci. U. S. A. 113, 7900–5. doi:10.1073/pnas.1602413113

Fan, Q., Anderson, A.W., Davis, N., Cutting, L.E., 2014. Structural connectivity patterns associated with the putative visual word form area and childrens reading ability. Brain Res. 1586, 118–129. doi:10.1016/j.brainres.2014.08.050

Fedorenko, E., Hsieh, P.-J., Nieto-Castañón, A., Whitfield-Gabrieli, S., Kanwisher, N., 2010. New method for fMRI investigations of language: defining ROIs functionally in individual subjects. J. Neurophysiol. 104, 1177–1194. doi:10.1152/jn.00032.2010

Fields, R.D., 2009. The Other Brain: From Dementia to Schizophrenia, How New Discoveries about the Brain Are Revolutionizing Medicine and Science. Simon & Schuster, New York.

Finkelstein, D., McCleery, A., 2013. An introduction to book history. Routledge.

Fischl, B., 2004. Automatically Parcellating the Human Cerebral Cortex. Cereb. Cortex 14, 11–22. doi:10.1093/cercor/bhg087

Fischl, B., Dale, A.M., 2000. Measuring the thickness of the human cerebral cortex from magnetic resonance images. Proc. Natl. Acad. Sci. U. S. A. 97, 11050–5. doi:10.1073/pnas.200033797

Friederici, A.D., 2012. The cortical language circuit: from auditory perception to sentence comprehension. Trends Cogn. Sci. 16, 262–8. doi:10.1016/j.tics.2012.04.001

Friederici, A.D., 2011. The brain basis of language processing: from structure to function. Physiol. Rev. 91, 1357–92. doi:10.1152/physrev.00006.2011

Friman, O., Farneback, G., Westin, C.-F., 2006. A Bayesian approach for stochastic white matter tractography. IEEE Trans. Med. Imaging 25, 965–978. doi:10.1109/TMI.2006.877093

Friston, K.J., Holmes, A.P., Poline, J.-B., Grasby, P.J., Williams, S.C.R., Frackowiak, R.S.J., Turner, R., 1995. Analysis of fMRI Time-Series Revisited. Neuroimage 2, 45–53. doi:10.1006/nimg.1995.1007

Friston, K.J., Zarahn, E., Josephs, O., Henson, R.N., Dale, a M., 1999. Stochastic designs in event-related fMRI. Neuroimage 10, 607–619. doi:10.1006/nimg.1999.0498

Geschwind, N., 1970. The organization of language and the brain. Science (80-.). 170, 940–944. doi:10.1126/science.170.3961.940

Gil-Robles, S., Carvallo, A., Jimenez, M. del M., Caicoya, A.G., Martinez, R., Ruiz-Ocaña, C., Duffau, H., 2013. Double dissociation between visual recognition and picture naming: a study of the visual language connectivity using tractography and brain stimulation. Neurosurgery 72, 678–686.

Glezer, L.S., Eden, G.F., Jiang, X., Luetje, M.M., Napoliello, E.M., Kim, J., Riesenhuber, M., 2016. Uncovering phonological and orthographic selectivity across the reading network using fMRI-RA. Neuroimage 138, 248–256. doi:10.1016/j.neuroimage.2016.05.072

Glezer, L.S., Jiang, X., Riesenhuber, M., 2009. Evidence for highly selective neuronal tuning to whole words in the "visual word form area". Neuron 62, 199–204. doi:10.1016/j.neuron.2009.03.017

Glezer, L.S., Kim, J., Rule, J., Jiang, X., Riesenhuber, M., 2015. Adding Words to the Brain's Visual Dictionary: Novel Word Learning Selectively Sharpens Orthographic Representations in the VWFA. J. Neurosci. 35, 4965–4972. doi:10.1523/JNEUROSCI.4031-14.2015

Glezer, L.S., Riesenhuber, M., 2013. Individual variability in location impacts orthographic selectivity in the "visual word form area". J. Neurosci. 33, 11221–6. doi:10.1523/JNEUROSCI.5002-12.2013

Gomez, J., Barnett, M.A., Natu, V., Mezer, A., Palomero-Gallagher, N., Weiner, K.S., Amunts, K., Zilles, K., Grill-Spector, K., 2017. Microstructural proliferation in human cortex is coupled with the development of face processing. Science (80-.). 355, 68–71. doi:10.1126/science.aag0311

Goodale, M.A., Milner, A.D., 1992. Separate visual pathways for perception and action. Trends Neurosci. 15, 20–25.

Graves, W.W., Desai, R., Humphries, C., Seidenberg, M.S., Binder, J.R., 2010. Neural systems for reading aloud: a multiparametric approach. Cereb. Cortex 20, 1799–815. doi:10.1093/cercor/bhp245

Greenblatt, S.H., 1973. Alexia without agraphia or hemianopsia. Anatomical analysis of an autopsied case. Brain 96, 307–316.

Greve, D.N., Haegen, L. Van Der, Cai, Q., Stufflebeam, S., Sabuncu, M.R., Fischl, B., Brysbaert, M., 2013. A Surface-based Analysis of Language Lateralization and Cortical Asymmetry. J. Cogn. Neurosci. 25, 1477–1492. doi:10.1162/jocn_a_00405

Grill-Spector, K., Knouf, N., Kanwisher, N., 2004. The fusiform face area subserves face perception, not generic within-category identification. Nat. Neurosci. 7, 555–562. doi:10.1038/nn1224

Hagoort, P., 2013. MUC (memory, unification, control) and beyond. Front. Psychol. 4, 1–13. doi:10.3389/fpsyg.2013.00416

Hagoort, P., 2005. On Broca, brain, and binding: a new framework. Trends Cogn. Sci. 9, 416–23. doi:10.1016/j.tics.2005.07.004

Hannagan, T., Amedi, A., Cohen, L., Dehaene-Lambertz, G., Dehaene, S., 2015. Origins of the specialization for letters and numbers in ventral occipitotemporal cortex. Trends Cogn. Sci. 19, 374–382. doi:10.1016/j.tics.2015.05.006

Hannagan, T., Grainger, J., 2013. The Lazy Visual Word Form Area: Computational Insights into Location-Sensitivity. PLoS Comput. Biol. 9, e1003250. doi:10.1371/journal.pcbi.1003250

Hickok, G., Poeppel, D., 2007. The cortical organization of speech processing. Nat. Rev. Neurosci. 8, 393–402.

Hirshorn, E.A., Li, Y., Ward, M.J., Richardson, R.M., Fiez, J.A., Ghuman, A.S., 2016. Decoding and disrupting left midfusiform gyrus activity during word reading. Proc. Natl. Acad. Sci. 201604126. doi:10.1073/pnas.1604126113

Hong, H., Yamins, D.L.K., Majaj, N.J., DiCarlo, J.J., 2016. Explicit information for category-orthogonal object properties increases along the ventral stream. Nat. Neurosci. doi:10.1038/nn.4247

Huang, S.Y., Nummenmaa, A., Witzel, T., Duval, T., Cohen-Adad, J., Wald, L.L., McNab, J.A., 2015. The impact of gradient strength on in vivo diffusion MRI estimates of axon diameter, NeuroImage. doi:10.1016/j.neuroimage.2014.12.008

Ishibashi, T., Dakin, K.A., Stevens, B., Lee, P.R., Kozlov, S. V., Stewart, C.L., Fields, R.D., 2006. Astrocytes promote myelination in response to electrical impulses. Neuron 49, 823–832. doi:10.1016/j.neuron.2006.02.006

Jackowski, M., Kao, C.Y., Qiu, M., Constable, R.T., Staib, L.H., 2004. Estimation of Anatomical Connectivity by Anisotropic Front Propagation and Diffusion Tensor Imaging. Springer Berlin Heidelberg, pp. 663–670.

doi:10.1007/978-3-540-30136-3_81

James, K.H., James, T.W., Jobard, G., Wong, A.C.N., Gauthier, I., 2005. Letter processing in the visual system: different activation patterns for single letters and strings. Cogn. Affect. Behav. Neurosci. 5, 452–466. doi:10.3758/CABN.5.4.452

Jeurissen, B., Leemans, A., Tournier, J.-D., Jones, D.K., Sijbers, J., 2013. Investigating the prevalence of complex fiber configurations in white matter tissue with diffusion magnetic resonance imaging. Hum. Brain Mapp. 34, 2747–2766. doi:10.1002/hbm.22099

Jeurissen, B., Tournier, J.D., Dhollander, T., Connelly, A., Sijbers, J., 2014. Multi-tissue constrained spherical deconvolution for improved analysis of multi-shell diffusion MRI data. Neuroimage 103, 411–426. doi:10.1016/j.neuroimage.2014.07.061

Jobard, G., Crivello, F., Tzourio-Mazoyer, N., 2003. Evaluation of the dual route theory of reading: a metanalysis of 35 neuroimaging studies. Neuroimage 20, 693–712. doi:10.1016/S1053-8119(03)00343-4

Jones, D.K., Griffin, L.D., Alexander, D.C., Catani, M., Horsfield, M.A., Howard, R., Williams, S.C.R., 2002. Spatial Normalization and Averaging of Diffusion Tensor MRI Data Sets. Neuroimage 17, 592–617. doi:10.1006/nimg.2002.1148

Jones, D.K., Knösche, T.R., Turner, R., 2013. White matter integrity, fiber count, and other fallacies: The do's and don'ts of diffusion MRI. Neuroimage.

doi:10.1016/j.neuroimage.2012.06.081

Jones, D.K., Pierpaoli, C., 2005. Confidence mapping in diffusion tensor magnetic resonance imaging tractography using a bootstrap approach. Magn. Reson. Med. 53, 1143–1149. doi:10.1002/mrm.20466

Julian, J.B., Fedorenko, E., Webster, J., Kanwisher, N., 2012. An algorithmic method for functionally defining regions of interest in the ventral visual pathway. Neuroimage 60, 2357–2364. doi:10.1016/j.neuroimage.2012.02.055

Kanwisher, N., 2010. Functional specificity in the human brain: a window into the functional architecture of the mind. Proc. Natl. Acad. Sci. U. S. A. 107, 11163–11170. doi:10.1073/pnas.1005062107

Kaufman, A.S., Kaufman, N.L., 1993. A review: Kaufman Brief Intelligence Test. Percept. Mot. Skills 77, 703.

Kay, K.N., Yeatman, J.D., 2017. Bottom-up and top-down computations in high-level visual cortex. Elife 10.7554/eL.

Kemmotsu, N., Girard, H.M., Kucukboyaci, N.E., McEvoy, L.K., Hagler, D.J., Dale, A.M., Halgren, E., McDonald, C.R., 2012. Age-related changes in the neurophysiology of language in adults: relationship to regional cortical thinning and white matter microstructure. J. Neurosci. 32, 12204–13. doi:10.1523/JNEUROSCI.0136-12.2012

Keuleers, E., Brysbaert, M., 2010. Wuggy: a multilingual pseudoword generator. Behav. Res. Methods 42, 627–633. doi:10.3758/BRM.42.3.627

Klingberg, T., Hedehus, M., Temple, E., Salz, T., Gabrieli, J.D.., Moseley, M.E., Poldrack, R.A., 2000. Microstructure of Temporo-Parietal White Matter as a Basis for Reading Ability. Neuron 25, 493–500. doi:10.1016/S0896-6273(00)80911-3

Konen, C.S., Kastner, S., 2008. Representation of eye movements and stimulus motion in topographically organized areas of human posterior parietal cortex. J. Neurosci. 28, 8361–8375. doi:10.1523/JNEUROSCI.1930-08.2008

Kriegeskorte, N., 2015. Deep Neural Networks: A New Framework for Modeling Biological Vision and Brain Information Processing. Annu. Rev. Vis. Sci. 1, 417–446. doi:10.1146/annurev-vision-082114-035447

Kronbichler, M., Bergmann, J.R.V.J.J.R.V.J., Hutzler, F., Staffen, W., Mair, A., Ladurner, G., Wimmer, H., 2007. Taxi vs. taksi: on orthographic word recognition in the left ventral occipitotemporal cortex. J. Cogn. Neurosci. 19, 1584–1594. doi:10.1162/jocn.2007.19.10.1584

Kronbichler, M., Hutzler, F., Wimmer, H., Mair, A., Staffen, W., Ladurner, G., 2004. The visual word form area and the frequency with which words are encountered: evidence from a parametric fMRI study. Neuroimage 21, 946–53. doi:10.1016/j.neuroimage.2003.10.021

Kucyi, A., Moayedi, M., Weissman-Fogel, I., Hodaie, M., Davis, K.D., 2012. Hemispheric asymmetry in white matter connectivity of the temporoparietal junction with the insula and prefrontal cortex. PLoS One 7. doi:10.1371/journal.pone.0035589

Lau, E.F., Phillips, C., Poeppel, D., 2008. A cortical network for semantics: (de)constructing the N400. Nat. Rev. Neurosci. 9, 920–33. doi:10.1038/nrn2532

Lauritzen, T.Z., Esposito, M.D., Heeger, D.J., Silver, M. a, Wills, H., Jr, H.H.W., 2009. Top–down flow of visual spatial attention signals from parietal to occipital cortex. J. Vis. 9, 1–14. doi:10.1167/9.13.18.Introduction

Lazar, M., Lee, J.H., Alexander, A.L., 2005. Axial asymmetry of water diffusion in brain white matter. Magn. Reson. Med. 54, 860–867. doi:10.1002/mrm.20653

Lazar, M., Weinstein, D.M., Tsuruda, J.S., Hasan, K.M., Arfanakis, K., Meyerand, M.E., Badie, B., Rowley, H.A., Haughton, V., Field, A., Alexander, A.L., 2003. White matter tractography using diffusion tensor deflection. Hum. Brain Mapp. 18, 306–321. doi:10.1002/hbm.10102

Lebel, C., Gee, M., Camicioli, R., Wieler, M., Martin, W., Beaulieu, C., 2012. Diffusion tensor imaging of white matter tract evolution over the lifespan. Neuroimage 60, 340–52. doi:10.1016/j.neuroimage.2011.11.094

Lebel, C., Walker, L., Leemans, a, Phillips, L., Beaulieu, C., 2008. Microstructural maturation of the human brain from childhood to adulthood. Neuroimage 40, 1044–55. doi:10.1016/j.neuroimage.2007.12.053

Lerma-Usabiaga, G., Iglesias, J.E., Insausti, R., Greve, D.N., Paz-Alonso, P.M., 2016. Automated segmentation of the human hippocampus along its longitudinal axis. Hum. Brain Mapp. doi:10.1002/hbm.23245

Longcamp, M., Hlushchuk, Y., Hari, R., 2011. What differs in visual recognition of handwritten vs. printed letters? An fMRI study. Hum. Brain Mapp. 32, 1250–9. doi:10.1002/hbm.21105

Maier-Hein, K., Neher, P., Houde, J.-C., Cote, M.-A., Garyfallidis, E., Zhong, J., Chamberland, M., Yeh, F.-C., Lin, Y.C., Ji, Q., Reddick, W.E., Glass, J.O., Chen, D.Q., Feng, Y., Gao, C., Wu, Y., Ma, J., Renjie, H., Li, Q., Westin, C.-F., Deslauriers-Gauthier, S., Gonzalez, J.O.O., Paquette, M., St-Jean, S., Girard, G., Rheault, F., Sidhu, J., Tax, C.M.W., Guo, F., Mesri, H.Y., David, S., Froeling, M., Heemskerk, A.M., Leemans, A., Bore, A., Pinsard, B., Bedetti, C., Desrosiers, M., Brambati, S., Doyon, J., Sarica, A., Vasta, R., Cerasa, A., Quattrone, A., Yeatman, J., Khan, A.R., Hodges, W., Alexander, S., Romascano, D., Barakovic, M., Auria, A., Esteban, O., Lemkaddem, A., Thiran, J.-P., Cetingul, H.E., Odry, B.L., Mailhe, B., Nadar, M., Pizzagalli, F., Prasad, G., Villalon-Reina, J., Galvis, J., Thompson, P., Requejo, F., Laguna, P., Lacerda, L., Barrett, R., Dell'Acqua, F., Catani, M., Petit, L., Caruyer, E., Daducci, A., Dyrby, T., Holland-Letz, T., Hilgetag, C., Stieltjes, B., Descoteaux, M., 2016. Tractography-based connectomes are dominated by false-positive connections. bioRxiv 1–23. doi:http://dx.doi.org/10.1101/084137

Mano, Q.R., Humphries, C., Desai, R.H., Seidenberg, M.S., Osmon, D.C., Stengel, B.C., Binder, J.R., 2013. The role of left occipitotemporal cortex in reading: reconciling stimulus, task, and lexicality effects. Cereb. Cortex 23, 988–1001. doi:10.1093/cercor/bhs093

Marinkovic, K., Dhond, R.P., Dale, A.M., Glessner, M., Carr, V., Halgren, E.,

2003. Spatiotemporal dynamics of modality-specific and supramodal word processing. Neuron 38, 487–497. doi:10.1016/S0896-6273(03)00197-1

Mazaika, P., Hoeft, F., Glover, G.H., Reiss, A.L., 2009. "Methods and Software for fMRI Analysis for Clinical Subjects", in: Human Brain Mapping.

McCandliss, B.D., Cohen, L., Dehaene, S., 2003. The visual word form area: expertise for reading in the fusiform gyrus. Trends Cogn. Sci. 7, 293–299. doi:10.1016/S1364-6613(03)00134-7

Mechelli, A., Crinion, J.T., Long, S., Friston, K.J., Ralph, M.A.L., Patterson, K., McClelland, J.L., Price, C.J., 2005. Dissociating Reading Processes on the Basis of Neuronal Interactions. J. Cogn. Neurosci. 17, 1753–1765. doi:10.1162/089892905774589190

Mechelli, A., Gorno-Tempini, M.L., Price, C.J., 2003. Neuroimaging Studies of Word and Pseudoword Reading: Consistencies, Inconsistencies, and Limitations. J. Cogn. Neurosci. 15, 260–271. doi:10.1162/089892903321208196

Melonakos, J., Gao, Y., Tannenbaum, A., 2007. Tissue tracking: applications for brain MRI classification, in: Pluim, J.P.W., Reinhardt, J.M. (Eds.), . p. 651218. doi:10.1117/12.710063

Menenti, L., Segaert, K., Hagoort, P., 2012. The neuronal infrastructure of speaking. Brain Lang. 122, 71–80. doi:10.1016/j.bandl.2012.04.012

Mezer, A., Yeatman, J.D., Stikov, N., Kay, K.N., Cho, N.-J., Dougherty, R.F., Perry, M.L., Parvizi, J., Hua, L.H., Butts-Pauly, K., Wandell, B.A., 2013.

Quantifying the local tissue volume and composition in individual brains with magnetic resonance imaging. Nat. Med. doi:10.1038/nm.3390

Mori, S., Barker, P.B., 1999. Diffusion magnetic resonance imaging: Its principle and applications. Anat. Rec. 257, 102–109. doi:10.1002/(SICI)1097-0185(19990615)257:3<102::AID-AR7>3.0.CO;2-6

Murtagh, F., 1985. Multidimensional clustering algorithms, in: Compstat Lectures. Physika Verlag, Vienna.

Nestor, A., Behrmann, M., Plaut, D.C., 2013. The neural basis of visual word form processing: A multivariate investigation. Cereb. Cortex 23, 1673–1684. doi:10.1093/cercor/bhs158

Nishimoto, S., Huth, A.G., Bilenko, N.Y., Gallant, J.L., 2017. Eye movement-invariant representations in the human visual system. J. Vis. 17, 1–10. doi:10.1167/17.1.11.doi

Ogawa, S., Lee, T.M., Kay, A.R., Tank, D.W., 1990. Brain magnetic resonance imaging with contrast dependent on blood oxygenation. Proc. Natl. Acad. Sci. U. S. A. 87, 9868–72. doi:10.1073/pnas.87.24.9868

Oliver, M., Carreiras, M., Paz-Alonso, P.M., 2016. Functional Dynamics of Dorsal and Ventral Reading Networks in Bilinguals. Cereb. Cortex 1–13. doi:10.1093/cercor/bhw310

Olulade, O.A., Flowers, D.L., Napoliello, E.M., Eden, G.F., 2015. Dyslexic children lack word selectivity gradients in occipito-temporal and inferior frontal cortex. NeuroImage Clin. 7, 742–754. doi:10.1016/j.nicl.2015.02.013

Pammer, K., Hansen, P.C., Kringelbach, M.L., Holliday, I., Barnes, G., Hillebrand, A., Singh, K.D., Cornelissen, P.L., 2004. Visual word recognition: The first half second. Neuroimage 22, 1819–1825. doi:10.1016/j.neuroimage.2004.05.004

Paolicelli, R.C., Bolasco, G., Pagani, F., Maggi, L., Scianni, M., Panzanelli, P., Giustetto, M., Alves Ferreira, T., Guiducci, E., Dumas, L., Ragozzino, D., Gross, C.T., 2011. Synaptic Pruning by Microglia Is Necessary forNormal Brain Development. Science (80-.). 333, 1456–1458. doi:10.1126/science.1202529

Pegado, F., Nakamura, K., Cohen, L., Dehaene, S., 2011. Breaking the symmetry: Mirror discrimination for single letters but not for pictures in the Visual Word Form Area. Neuroimage 55, 742–749. doi:10.1016/j.neuroimage.2010.11.043

Perea, G., Sur, M., Araque, A., 2014. Neuron-glia networks: integral gear of brain function. Front. Cell. Neurosci. 8, 378. doi:10.3389/fncel.2014.00378

Perea, M., Urkia, M., Davis, C.J., Agirre, A., Laseka, E., Carreiras, M., 2006. E-Hitz: a word frequency list and a program for deriving psycholinguistic statistics in an agglutinative language (Basque). Behav. Res. Methods 38, 610–5.

Pestilli, F., Yeatman, J.D., Rokem, A., Kay, K.N., Wandell, B.A., 2014. Evaluation and statistical inference for human connectomes. Nat. Methods 1–9. doi:10.1038/nmeth.3098

Pichon, E., Westin, C.-F., Tannenbaum, A.R., 2005. A Hamilton-Jacobi-Bellman Approach to High Angular Resolution Diffusion Tractography. Springer Berlin Heidelberg, pp. 180–187. doi:10.1007/11566465_23

Pierpaoli, C., Barnett, A., Pajevic, S., Chen, R., Penix, L.R., Virta, A., Basser, P., 2001. Water diffusion changes in Wallerian degeneration and their dependence on white matter architecture. Neuroimage 13, 1174–85. doi:10.1006/nimg.2001.0765

Planton, S., Chanoine, V., Sein, J., Anton, J.-L., Nazarian, B., Pallier, C., Pattamadilok, C., 2017. Involvement of the visuo-orthographic system during spoken sentence processing, in: Cognitive Neuroscience Society, 24th Annual Meeting. p. 62.

Poeppel, D., Emmorey, K., Hickok, G., Pylkkänen, L., 2012. Towards a new neurobiology of language. J. Neurosci. 32, 14125–31. doi:10.1523/JNEUROSCI.3244-12.2012

Poldrack, R.A., 2011. The future of fMRI in cognitive neuroscience. Neuroimage. doi:10.1016/j.neuroimage.2011.08.007

Poldrack, R.A., 2007. Region of interest analysis for fMRI. Soc. Cogn. Affect. Neurosci. 2, 67–70. doi:10.1093/scan/nsm006

Poldrack, R.A., Wagner, A.D., Prull, M.W., Desmond, J.E., Glover, G.H., Gabrieli, J.D., 1999. Functional specialization for semantic and phonological processing in the left inferior prefrontal cortex. Neuroimage 10, 15–35. doi:10.1006/nimg.1999.0441

Price, C.J., 2012. A review and synthesis of the first 20 years of PET and fMRI studies of heard speech, spoken language and reading. Neuroimage 62, 816–847. doi:10.1016/j.neuroimage.2012.04.062

Price, C.J., Devlin, J.T., 2011. The interactive account of ventral occipitotemporal contributions to reading. Trends Cogn. Sci. 15, 246–53. doi:10.1016/j.tics.2011.04.001

Price, C.J., Devlin, J.T., 2003. The myth of the visual word form area. Neuroimage 19, 473–481. doi:10.1016/S1053-8119(03)00084-3

Pugh, K.R., Mencl, W.E., Jenner, A.R., Katz, L., Frost, S.J., Lee, J.R., Shaywitz, S.E., Shaywitz, B.A., 2001. Neurobiological studies of reading and reading disability. J. Commun. Disord. 34, 479–492. doi:10.1016/S0021-9924(01)00060-0

Purcell, J.J., Jiang, X., Eden, G.F., 2017. Shared Neuronal Representations for Spelling and Reading. Neuroimage 147, 554–567. doi:10.1016/j.neuroimage.2016.12.054

Purger, D., Gibson, E.M., Monje, M., 2016. Myelin plasticity in the central nervous system. Neuropharmacology 110, 563–573. doi:10.1016/j.neuropharm.2015.08.001

Pylkkänen, L., McElree, B., 2007. An MEG study of silent meaning. J. Cogn. Neurosci. 19, 1905–21. doi:10.1162/jocn.2007.19.11.1905

Raffelt, D., Tournier, J.-D., Rose, S., Ridgway, G.R., Henderson, R., Crozier, S., Salvado, O., Connelly, A., 2012. Apparent Fibre Density: A novel measure

for the analysis of diffusion-weighted magnetic resonance images. Neuroimage 59, 3976–3994. doi:10.1016/j.neuroimage.2011.10.045

Raichle, M.E., 2009. A brief history of human brain mapping. Trends Neurosci. 32, 118–26. doi:10.1016/j.tins.2008.11.001

Rauschecker, A.M., Bowen, R.F., Parvizi, J., Wandell, B.A., 2012. Position sensitivity in the visual word form area. Proc. Natl. Acad. Sci. U. S. A. 109, E1568-77. doi:10.1073/pnas.1121304109

Richardson, F.M., Seghier, M.L., Leff, A.P., Thomas, M.S.C., Price, C.J., 2011. Multiple routes from occipital to temporal cortices during reading. J. Neurosci. 31, 8239–47. doi:10.1523/JNEUROSCI.6519-10.2011

Rissman, J., Gazzaley, A., D'Esposito, M., 2004. Measuring functional connectivity during distinct stages of a cognitive task. Neuroimage 23, 752–763. doi:10.1016/j.neuroimage.2004.06.035

Robinson, A., 2009. Writing and script: a very short introduction. OUP, Oxford.

Rombouts, S.A., Barkhof, F., Hoogenraad, F.G., Sprenger, M., Valk, J., Scheltens, P., 1997. Test-retest analysis with functional MR of the activated area in the human visual cortex. AJNR. Am. J. Neuroradiol. 18, 1317–1322. doi:10.1097/00041327-199906000-00012

Rosenbloom, M., Sullivan, E. V, Pfefferbaum, A., 2003. Using magnetic resonance imaging and diffusion tensor imaging to assess brain damage in alcoholics. Alcohol Res. Heal. 27, 146–52.

Rueckl, J.G., Paz-Alonso, P.M., Molfese, P.J., Kuo, W.-J., Bick, A., Frost, S.J., Hancock, R., Wu, D.H., Mencl, W.E., Duñabeitia, J.A., Lee, J.-R., Oliver, M., Zevin, J.D., Hoeft, F., Carreiras, M., Tzeng, O.J.L., Pugh, K.R., Frost, R., 2015. Universal brain signature of proficient reading: Evidence from four contrasting languages. Proc. Natl. Acad. Sci. U. S. A. 112, 15510–5. doi:10.1073/pnas.1509321112

Rushton, W.A.H., 1951. A theory of the effects of fibre size in medullated nerve. J. Physiol. 115, 101–122.

Rutherford, A., 2016. A Brief History of Everyone who Ever Lived: The Stories in Our Genes. Hachette UK.

Saalmann, Y.B., Pigarev, I.N., Vidyasagar, T.R., 2007. Neural Mechanisms of Visual Attention: How Top-Down Feedback Highlights Relevant Locations. Science (80-.). 316, 1612–5.

Sandak, R., Mencl, W.E., Frost, S.J., Pugh, K.R., 2004. The Neurobiological Basis of Skilled and Impaired Reading: Recent Findings and New Directions. Sci. Stud. Read. 8, 273–292.

Sandrone, S., Bacigaluppi, M., Galloni, M.R., Cappa, S.F., Moro, A., Catani, M., Filippi, M., Monti, M.M., Perani, D., Martino, G., 2013. Weighing brain activity with the balance : Angelo Mosso ' s original manuscripts come to light. doi:10.1093/brain/awt091

Saur, D., Kreher, B.W., Schnell, S., Kümmerer, D., Kellmeyer, P., Vry, M.-S., Umarova, R., Musso, M., Glauche, V., Abel, S., Huber, W., Rijntjes, M.,

Hennig, J., Weiller, C., 2008. Ventral and dorsal pathways for language. Proc. Natl. Acad. Sci. U. S. A. 105, 18035–40. doi:10.1073/pnas.0805234105

Saxe, R., Brett, M., Kanwisher, N., 2006. Divide and conquer: A defense of functional localizers. Neuroimage 30, 1088–1096. doi:10.1016/j.neuroimage.2005.12.062

Saygin, Z.M., Osher, D.E., Norton, E.S., Youssoufian, D.A., Beach, S.D., Feather, J., Gaab, N., Gabrieli, J.D.E., Kanwisher, N., 2016. Connectivity precedes function in the development of the visual word form area. Nat. Neurosci. 19, 1250–1255. doi:10.1038/nn.4354

Schacter, D.L., Buckner, R.L., Koutstaal, W., Dale, A.M., Rosen, B.R., 1997. Late onset of anterior prefrontal activity during true and false recognition: an event-related fMRI study. Neuroimage 6, 259–269. doi:10.1006/nimg.1997.0305

Schlaggar, B.L., McCandliss, B.D., 2007. Development of neural systems for reading. Annu. Rev. Neurosci. 30, 475–503. doi:10.1146/annurev.neuro.28.061604.135645

Schoenemann, T., 2009. Evolution of Brain and Language. Lang. Learn. 59: Suppl., 162–186.

Schurz, M., Sturm, D., Richlan, F., Kronbichler, M., Ladurner, G., Wimmer, H., 2010. A dual-route perspective on brain activation in response to visual words: evidence for a length by lexicality interaction in the visual word form area (VWFA). Neuroimage 49, 2649–61.

doi:10.1016/j.neuroimage.2009.10.082

Schuster, S., Hawelka, S., Hutzler, F., Kronbichler, M., Richlan, F., 2016. Words in Context: The Effects of Length, Frequency, and Predictability on Brain Responses during Natural Reading. Cereb. Cortex 26, 3889–3904. doi:10.1093/cercor/bhw184

Schwartz, S.J., Lilienfeld, S.O., Meca, A., Sauvigné, K.C., 2016a. Psychology and neuroscience: How close are we to an integrative perspective? Reply to Staats (2016) and Tryon (2016). Am. Psychol. 71, 898–899. doi:10.1037/amp0000119

Schwartz, S.J., Lilienfeld, S.O., Meca, A., Sauvigné, K.C., 2016b. The role of neuroscience within psychology: A call for inclusiveness over exclusiveness. Am. Psychol. 71, 52–70. doi:10.1037/a0039678

Seghier, M.L., 2013. The angular gyrus: multiple functions and multiple subdivisions. Neurosci. 19, 43–61. doi:10.1177/1073858412440596

Seghier, M.L., Fagan, E., Price, C.J., 2010. Functional subdivisions in the left angular gyrus where the semantic system meets and diverges from the default network. J. Neurosci. 30, 16809–17. doi:10.1523/JNEUROSCI.3377-10.2010

Seghier, M.L., Price, C.J., 2013. Dissociating frontal regions that co-lateralize with different ventral occipitotemporal regions during word processing. Brain Lang. 126, 133–140. doi:10.1016/j.bandl.2013.04.003

Seidenberg, M.S., 2012. Connectionist models of reading. Oxford Handb.

Psycholinguist. 235–250. doi:10.1093/oxfordhb/9780198568971.013.0014

Seidenberg, M.S., Plaut, D.C., 2006. Progress in Understanding Word Reading : Data Fitting Versus Theory Building Address for correspondence. From Inkmarks to Ideas Curr. Issues Lex. Process. 25–49. doi:10.4324/9780203841211

Shaw, P., Greenstein, D., Lerch, J.P., Clasen, L., Lenroot, R., Gogtay, N., Evans, A., Rapoport, J., Giedd, J., 2006. Intellectual ability and cortical development in children and adolescents. Nature 440, 676–9. doi:10.1038/nature04513

Shaw, P., Kabani, N.J., Lerch, J.P., Eckstrand, K., Lenroot, R., Gogtay, N., Greenstein, D., Clasen, L., Evans, A., Rapoport, J.L., Giedd, J.N., Wise, S.P., 2008. Neurodevelopmental trajectories of the human cerebral cortex. J. Neurosci. 28, 3586–94. doi:10.1523/JNEUROSCI.5309-07.2008

Shepherd, G.M., 1991. Foundations of the neuron doctrine. Oxford University Press.

Silvanto, J., Muggleton, N., Lavie, N., Walsh, V., 2009. The Perceptual and Functional Consequences of Parietal Top-Down Modulation on the Visual Cortex 10–13. doi:10.1093/cercor/bhn091

Simons, J.S., Koutstaal, W., Prince, S., Wagner, A.D., Schacter, D.L., 2003. Neural mechanisms of visual object priming: Evidence for perceptual and semantic distinctions in fusiform cortex. Neuroimage 19, 613–626. doi:10.1016/S1053-8119(03)00096-X

Smith, R.E., Tournier, J.D., Calamante, F., Connelly, A., 2015. SIFT2: Enabling dense quantitative assessment of brain white matter connectivity using streamlines tractography. Neuroimage 119, 338–351. doi:10.1016/j.neuroimage.2015.06.092

Smith, R.E., Tournier, J.D., Calamante, F., Connelly, A., 2013. SIFT: Spherical-deconvolution informed filtering of tractograms. Neuroimage 67, 298–312. doi:10.1016/j.neuroimage.2012.11.049

Smith, S.M., Jenkinson, M., Woolrich, M.W., Beckmann, C.F., Behrens, T.E.J., Johansen-Berg, H., Bannister, P.R., De Luca, M., Drobnjak, I., Flitney, D.E., Niazy, R.K., Saunders, J., Vickers, J., Zhang, Y., De Stefano, N., Brady, J.M., Matthews, P.M., 2004. Advances in functional and structural MR image analysis and implementation as FSL. Neuroimage 23. doi:10.1016/j.neuroimage.2004.07.051

Sowell, E., Peterson, B., Thompson, P., Welcome, S., Henkenius, A., Toga, A., 2003. Mapping cortical change across the human life span. Nat. Neurosci. 6, 309–315. doi:10.1038/nn1008

Staats, A.W., 2016. Neurological exclusiveness or unified science inclusiveness: Comment on Schwartz et al. (2016). Am. Psychol. 71, 894–895. doi:10.1037/amp0000032

Sterling, N.W., Wang, M., Zhang, L., Lee, E.-Y., Du, G., Lewis, M.M., Styner, M., Huang, X., 2016. Stage-dependent loss of cortical gyrification as Parkinson disease "unfolds". Neurology 86, 1143–51. doi:10.1212/WNL.0000000000002492

Stigliani, A., Weiner, K.S., Grill-Spector, K., 2015. Temporal Processing Capacity in High-Level Visual Cortex Is Domain Specific. J. Neurosci. 35, 12412–12424. doi:10.1523/JNEUROSCI.4822-14.2015

Stikov, N., Perry, L.M., Mezer, A., Rykhlevskaia, E., Wandell, B.A., Pauly, J.M., Dougherty, R.F., 2011. Bound pool fractions complement diffusion measures to describe white matter micro and macrostructure. Neuroimage 54, 1112–1121. doi:10.1016/j.neuroimage.2010.08.068

Szwed, M., Dehaene, S., Kleinschmidt, A., Eger, E., Valabrègue, R., Amadon, A., Cohen, L., 2011. Specialization for written words over objects in the visual cortex. Neuroimage 56, 330–344. doi:10.1016/j.neuroimage.2011.01.073

Tagamets, M. a, Novick, J.M., Chalmers, M.L., Friedman, R.B., 2000. A parametric approach to orthographic processing in the brain: an fMRI study. J. Cogn. Neurosci. 12, 281–297. doi:10.1162/089892900562101

Takemura, H., Caiafa, C.F., Wandell, B.A., Pestilli, F., 2016. Ensemble Tractography. PLoS Comput. Biol. 12, 1–22. doi:10.1371/journal.pcbi.1004692

Talairach, J., Tournoux, P., 1988. Co-planar stereotaxic atlas of the human brain: 3-dimensional proportional system: an approach to cerebral imaging, Neuropsychologia. doi:10.1111/mono.12083

Tamnes, C.K., Ostby, Y., Fjell, A.M., Westlye, L.T., Due-Tønnessen, P., Walhovd, K.B., 2010. Brain maturation in adolescence and young adulthood: regional age-related changes in cortical thickness and white

matter volume and microstructure. Cereb. Cortex 20, 534–48. doi:10.1093/cercor/bhp118

Tarkiainen, A., Helenius, P., Hansen, P.C., Cornelissen, P.L., Salmelin, R., 1999. Dynamics of letter string perception in the human occipitotemporal cortex. Brain 122, 2119–2131. doi:10.1093/brain/122.11.2119

Tarkiainen, a, Cornelissen, P.L., Salmelin, R., 2002. Dynamics of visual feature analysis and object-level processing in face versus letter-string perception. Brain 125, 1125–36. doi:10.1093/brain/awf112

Thesen, T., McDonald, C.R., Carlson, C., Doyle, W., Cash, S., Sherfey, J., Felsovalyi, O., Girard, H., Barr, W., Devinsky, O., Kuzniecky, R., Halgren, E., 2012. Sequential then interactive processing of letters and words in the left fusiform gyrus. Nat. Commun. 3, 1284. doi:10.1038/ncomms2220

Thiebaut de Schotten, M., Cohen, L., Amemiya, E., Braga, L.W., Dehaene, S., 2012. Learning to Read Improves the Structure of the Arcuate Fasciculus. Cereb. Cortex. doi:10.1093/cercor/bhs383

Tofts, P. (Ed.), 2003. Quantitative MRI of the Brain. John Wiley & Sons, Ltd, Chichester, UK. doi:10.1002/0470869526

Tomasi, D., Volkow, N.D., 2011. Association between Functional Connectivity Hubs and Brain Networks. Cereb. Cortex 2, 2003–2013. doi:10.1093/cercor/bhq268

Tournier, J.-D., Calamante, F., Connelly, A., 2010. Improved probabilistic streamlines tractography by 2 nd order integration over fibre orientation

distributions, in: ISMRM. p. 1670.

Tournier, J.-D., Mori, S., Leemans, A., 2011. Diffusion tensor imaging and beyond. Magn. Reson. Med. 65, 1532–56. doi:10.1002/mrm.22924

Tryon, W.W., 2016. Integrating psychology and neuroscience: Comment on Schwartz et al. (2016). Am. Psychol. 71, 896–897. doi:10.1037/amp0000031

Twomey, T., Kawabata Duncan, K.J., Price, C.J., Devlin, J.T., 2011. Top-down modulation of ventral occipito-temporal responses during visual word recognition. Neuroimage 55, 1242–1251. doi:10.1016/j.neuroimage.2011.01.001

Uddén, J., Bahlmann, J., 2012. A rostro-caudal gradient of structured sequence processing in the left inferior frontal gyrus. Philos. Trans. R. Soc. Lond. B. Biol. Sci. 367, 2023–32. doi:10.1098/rstb.2012.0009

Uddin, L.Q., Supekar, K., Amin, H., Rykhlevskaia, E., Nguyen, D.A., Greicius, M.D., Menon, V., 2010. Dissociable connectivity within human angular gyrus and intraparietal sulcus: Evidence from functional and structural connectivity. Cereb. Cortex 20, 2636–2646. doi:10.1093/cercor/bhq011

van der Mark, S., Klaver, P., Bucher, K., Maurer, U., Schulz, E., Brem, S., Martin, E., Brandeis, D., 2011. The left occipitotemporal system in reading: Disruption of focal fMRI connectivity to left inferior frontal and inferior parietal language areas in children with dyslexia. Neuroimage 54, 2426–2436. doi:10.1016/j.neuroimage.2010.10.002

Vartiainen, J., Parviainen, T., Salmelin, R., 2009. Spatiotemporal convergence of

semantic processing in reading and speech perception. J. Neurosci. 29, 9271–9280. doi:10.1523/JNEUROSCI.5860-08.2009

Vinckier, F., Dehaene, S., Jobert, A., Dubus, J.P., Sigman, M., Cohen, L., 2007. Hierarchical coding of letter strings in the ventral stream: dissecting the inner organization of the visual word-form system. Neuron 55, 143–56. doi:10.1016/j.neuron.2007.05.031

Vogel, A.C., Miezin, F.M., Petersen, S.E., Schlaggar, B.L., 2012a. The putative visual word form area is functionally connected to the dorsal attention network. Cereb. Cortex 22, 537–549. doi:10.1093/cercor/bhr100

Vogel, A.C., Petersen, S.E., Schlaggar, B.L., 2012b. The left occipitotemporal cortex does not show preferential activity for words. Cereb. Cortex 22, 2715–2732. doi:10.1093/cercor/bhr295

Vogt, O., 1910. Die myeloarchitektonische Felderung des menschlichen Stirnhirns. J. für Psychol. und Neurol. 15, 221–232.

von Economo, K., Koskinas, G., 1925. Die Cytoarchitektonik der Hirnrinde des erwachsenen Menschen. Springer, Wien.

Wagner, A.D., Paré-Blagoev, E.J., Clark, J., Poldrack, R.A., 2001. Recovering meaning: Left prefrontal cortex guides controlled semantic retrieval. Neuron 31, 329–338. doi:10.1016/S0896-6273(01)00359-2

Wandell, B.A., 2016. Clarifying Human White Matter. Annu. Rev. Neurosci. 39, annurev-neuro-070815-013815. doi:10.1146/annurev-neuro-070815-013815

Wandell, B.A., Rauschecker, A.M., Yeatman, J.D., 2012. Learning to see words. Annu. Rev. Psychol. 63, 31–53. doi:10.1146/annurev-psych-120710-100434

Wandell, B.A., Yeatman, J.D., 2013. Biological development of reading circuits. Curr. Opin. Neurobiol. 23, 261–8. doi:10.1016/j.conb.2012.12.005

Wang, L., Mruczek, R.E.B., Arcaro, M.J., Kastner, S., 2015. Probabilistic maps of visual topography in human cortex. Cereb. Cortex 25, 3911–3931. doi:10.1093/cercor/bhu277

Wang, X., Caramazza, A., Peelen, M. V, Han, Z., Bi, Y., 2014. Reading Without Speech Sounds: VWFA and its Connectivity in the Congenitally Deaf. Cereb. Cortex 25, 2426. doi:10.1093/cercor/bhu044

Weiner, K.S., Barnett, M.A., Lorenz, S., Caspers, J., Stigliani, A., Amunts, K., Zilles, K., Fischl, B., Grill-spector, K., 2016a. The Cytoarchitecture of Domain-specific Regions in Human High-level Visual Cortex. Cereb. Cortex 1–16. doi:10.1093/gbe/evw245

Weiner, K.S., Grill-Spector, K., 2012. The improbable simplicity of the fusiform face area. Trends Cogn. Sci. 16, 251–254. doi:10.1016/j.tics.2012.03.003

Weiner, K.S., Yeatman, J.D., Wandell, B.A., 2016b. The posterior arcuate fasciculus and the vertical occipital fasciculus. Cortex. doi:10.1016/j.cortex.2016.03.012

Wendelken, C., O'Hare, E.D., Whitaker, K.J., Ferrer, E., Bunge, S. a, 2011. Increased functional selectivity over development in rostrolateral prefrontal cortex. J. Neurosci. 31, 17260–8. doi:10.1523/JNEUROSCI.1193-

10.2011

Wheat, K.L., Cornelissen, P.L., Frost, S.J., Hansen, P.C., 2010. During visual word recognition, phonology is accessed within 100 ms and may be mediated by a speech production code: evidence from magnetoencephalography. J Neurosci 30, 5229–33. doi:10.1523/JNEUROSCI.4448-09.2010

Woodhead, Z.V.J., Barnes, G.R., Penny, W., Moran, R., Teki, S., Price, C.J., Leff, A.P., 2014. Reading front to back: MEG evidence for early feedback effects during word recognition. Cereb. Cortex 24, 817–825. doi:10.1093/cercor/bhs365

Woodhead, Z.V.J., Brownsett, S.L.E., Dhanjal, N.S., Beckmann, C., Wise, R.J.S., 2011. The visual word form system in context. J. Neurosci. 31, 193–9. doi:10.1523/JNEUROSCI.2705-10.2011

Woollams, A.M., Silani, G., Okada, K., Patterson, K., Price, C.J., 2011. Word or word-like? Dissociating orthographic typicality from lexicality in the left occipito-temporal cortex. J. Cogn. Neurosci. 23, 992–1002. doi:10.1162/jocn.2010.21502

Wright, N.D., Mechelli, A., Noppeney, U., Veltman, D.J., Rombouts, S.A.R.B., Glensman, J., Haynes, J.D., Price, C.J., 2008. Selective activation around the left occipito-temporal sulcus for words relative to pictures: Individual variability or false positives? Hum. Brain Mapp. 29, 986–1000. doi:10.1002/hbm.20443

Xue, G., Chen, C., Jin, Z., Dong, Q., 2006. Language experience shapes fusiform activation when processing a logographic artificial language: An fMRI training study. Neuroimage 31, 1315–1326. doi:10.1016/j.neuroimage.2005.11.055

Xue, G., Poldrack, R.A., 2007. The neural substrates of visual perceptual learning of words: implications for the visual word form area hypothesis. J. Cogn. Neurosci. 19, 1643–1655. doi:10.1162/jocn.2007.19.10.1643

Yarkoni, T., Balota, D., Yap, M., 2008. Moving beyond Coltheart's N: a new measure of orthographic similarity. Psychon. Bull. Rev. 15, 971–979. doi:10.3758/PBR.15.5.971

Yeatman, J.D., Dougherty, R.F., Ben-Shachar, M., Wandell, B.A., 2012a. Development of white matter and reading skills. Proc. Natl. Acad. Sci. U. S. A. 109, E3045-53. doi:10.1073/pnas.1206792109

Yeatman, J.D., Dougherty, R.F., Myall, N.J., Wandell, B.A., Feldman, H.M., 2012b. Tract profiles of white matter properties: automating fiber-tract quantification. PLoS One 7, e49790. doi:10.1371/journal.pone.0049790

Yeatman, J.D., Rauschecker, A.M., Wandell, B.A., 2013. Anatomy of the visual word form area: adjacent cortical circuits and long-range white matter connections. Brain Lang. 125, 146–55. doi:10.1016/j.bandl.2012.04.010

Yeatman, J.D., Wandell, B.A., Mezer, Aviv, A., 2014a. Maturation and degeneration of human white matter. Nat. Commun. 5, 1–12. doi:10.1038/ncomms5932

Yeatman, J.D., Weiner, K.S., Pestilli, F., Rokem, A., Mezer, A., Wandell, B.A., 2014b. The vertical occipital fasciculus : A century of controversy resolved by in vivo measurements. Proc. Natl. Acad. Sci. U. S. A. 111, E5214–E5223. doi:10.1073/pnas.1418503111

Yendiki, A., Panneck, P., Srinivasan, P., Stevens, A., Zöllei, L., Augustinack, J., Wang, R., Salat, D., Ehrlich, S., Behrens, T.E.J., Jbabdi, S., Gollub, R., Fischl, B., 2011. Automated probabilistic reconstruction of white-matter pathways in health and disease using an atlas of the underlying anatomy. Front. Neuroinform. 5, 23. doi:10.3389/fninf.2011.00023

Zhou, W., Wang, X., Xia, Z., Bi, Y., Li, P., Shu, H., 2016. Neural Mechanisms of Dorsal and Ventral Visual Regions during Text Reading. Front. Psychol. 7, 1–10. doi:10.3389/fpsyg.2016.01399